Autopilot for a Personal Watercraft

Jonas Voigt

Abdulah Alkaysi

LUND
UNIVERSITY

Department of Automatic Control

MSc Thesis
TFRT-6103
ISSN 0280-5316

Department of Automatic Control
Lund University
Box 118
SE-221 00 LUND
Sweden

Printed in Sweden by Tryckeriet i E-huset
Lund 2020

Abstract

The objective in this thesis is to develop an autopilot for a personal watercraft (PWC) – popularly known as a jetski – that is capable of maneuvering in calm and rough waters alike. Maneuvering a PWC in calm waters is usually easy. It gets more challenging in rough waters, where environmental disturbances that can significantly destabilize the craft are present.

In this project, two control strategies are developed; one with the sole focus of positioning and one with regard to environmental disturbances. The positioning controller can be thought of as an autopilot in calm conditions, i.e., no significant disturbances are present. It is divided into a PI-controller that handles thrust and a PID-controller that handles steering. These are tuned through a series of simulations on our PWC-model.

To deal with the disturbances, simple models of these were constructed with the intention of crafting a control algorithm through simulations. However, after studying footage of PWC and other smaller craft in rough waters, it became clear that the sea-state is too unpredictable to rely on control algorithms devised from our simple and idealized wave-model. To obtain strategies that work in real life applications, strategies that are used by experienced (human) riders are brought up. Thus, depending on the direction of the waves, the PWC moves towards its desired position in a certain specific way. Whilst these strategies do not guarantee stability, they are deemed to give the PWC a viable chance of moving towards its desired position without capsizing in rough waters.

Acknowledgements

The authors would like to thank the supervisor Anders Robertsson at the *Department of Automatic Control* at Lund University for supervising the project.

We would also like to thank Anders J Johanson at the *Department of Electrical and Information Technology* at Lund University for supervising as well as being our contact to the Swedish Sea Rescue Society (SSRS) and for suggesting the project.

Table of Content

Glossary

CB Center of Buoyancy.

CG Center of Gravity.

DoF Degrees of Freedom.

PID Proportional-Integral-Derivative controller.

PWC Personal watercraft, commonly known as jetski.

RR RescueRunner, personal watercraft used by SSRS for sea rescue operations.

SSRS Swedish Sea Rescue Society.

1 Introduction

1.1 Background

The Swedish Sea Rescue Society (SSRS) is a voluntary organization focused on saving lives at sea. The SSRS mans 72 rescue stations along Sweden's coasts and larger lakes, with 2300 voluntary members on call with 15 minutes response time to leave the docks. They participate at approximately 80 percent of all sea rescue operations in Sweden.

In the year 2015, a total of 1275 call-outs where made for sea rescue. Another 800 call-outs for sea ambulance and other rescue services and another 3000 in preemptive call-out show the large need of SSRS [1].

Although larger vessels are normally used when moving in open sea, when performing rescue operations, smaller and nimbler craft are often preferred as they are quicker and more efficient at grabbing people from the water. One such craft is the RescueRunner (RR), which is a PWC developed by the company *Safe at Sea* in cooperation with SSRS specifically for such search and rescue operations [2].

Driving a PWC (such as an RescueRunner) can be tiring, especially in rougher waters. As SSRS has no methods of towing it, it has to be driven manually to the site, which can exhaust the driver. To solve this, a virtual leash is established between the lead boat and the RescueRunner. In other words, the RescueRunner should follow the lead boat autonomously to the rescue site. In previous works [3, 4, 5], this has been attempted in calm conditions to a certain capacity. However, many rescue operations take place in conditions that are not necessarily calm, in which environmental disturbances can be significant. In general, PWC perform well in shallow waters and their relative calmness, but struggle in deeper waters where the sea state is more unpredictable and chaotic.

This project aims at developing and analysing autopilots and control methods that are not only viable for calm waters, but also to conditions where disturbances from currents, wind and waves are present.

1.2 Purpose

The project aims to add to the progress of automating the control of a PWC, such that it can maneuver in calm and rough waters alike.

1.3 Problem Description

The objective of this thesis is to build an autopilot for the PWC that is viable not only in calm and shallow waters, but also in rougher conditions. To obtain an answer to this problem, it is divided into the following subproblems:

- Modelling of the PWC.

- Modelling of the environmental disturbances (winds, waves, currents).
- Control strategy for positioning of the PWC.
- Control strategy for dealing with the environmental disturbances.

The report is structured in that order.

1.4 Previous Work

A number of projects centered around unmanned control of the RR have been conducted at *Chalmers University of Technology* throughout the last decade, in cooperation with SSRS. Two of these [3, 4] are similar to our project, but unlike this project environmental disturbances were not taken into consideration. Data are borrowed from these two projects during the modelling process.

Chalmers does not have an RR of their own. Instead, a *Yamaha Waverunner VX Cruiser HO* is used as a proxy. In 2019, one of the projects equipped the Waverunner with hardware that facilitates remote control [5]. Our thesis was meant to be built on that work. The idea was also to conclude the project by travelling to Chalmers in order to test the autopilot on their equipped Waverunner. However, the intended cooperation with SSRS and Chalmers could unfortunately not be done.

1.5 Delimitations

As mentioned above, the equipment relevant to autonomous control have already been installed in previous work. Thus, this project does not concern itself with hardware. In addition, no modification to the design of the craft will be suggested.

In this project, we will limit ourselves to low speeds (< 6 m/s or 12 knots). This is done for the following reasons:

1. A PWC, like all planing craft, behave vastly differently at high velocities (planing mode) than in lower. It would be far more challenging to obtain a model at that range of speed.
2. The higher the velocity, the larger the risks are to capsize in rough waters.

1.6 Basic System Description

A PWC is propelled by a jet-engine. This means that thrust is generated by sucking water in through the intake grate and ejecting it at a high velocity through the nozzle. A PWC turns by angling the nozzle (and thus the water jet), which creates a rotational moment. Steering can thus only occur if throttle is applied. To brake (or reverse), a metal plate is placed behind the nozzle which reflects the water jet to the other side such that it counteracts the forward motion.

2 Modeling

The foundation of every control project is an accurate model of the system of interest. This makes it possible to develop a controller safely and inexpensively through simulations, without needing around the clock access to the actual craft. In this chapter, motions of the PWC under environmental loads (wind, waves, current) moving in 6 DoFs will be modelled and represented in the matrix-vector setting given by [6]

$$M\dot{\nu} + C(\nu)\nu + D(\nu)\nu + g(\eta) = \tau \tag{1}$$

The parameters of the equation are discussed in detail in this chapter.

2.1 Kinematics

In every control study, the manner in which the motion of the body is represented/described is of critical importance. In this rigid-body model, the motion of the PWC is fully described by six independent DoFs. This means the position/velocity/forces are each completely specified by six states. To obtain values related to the DoFs, appropriate geographical reference frames are chosen [7].

2.1.1 Reference Frames

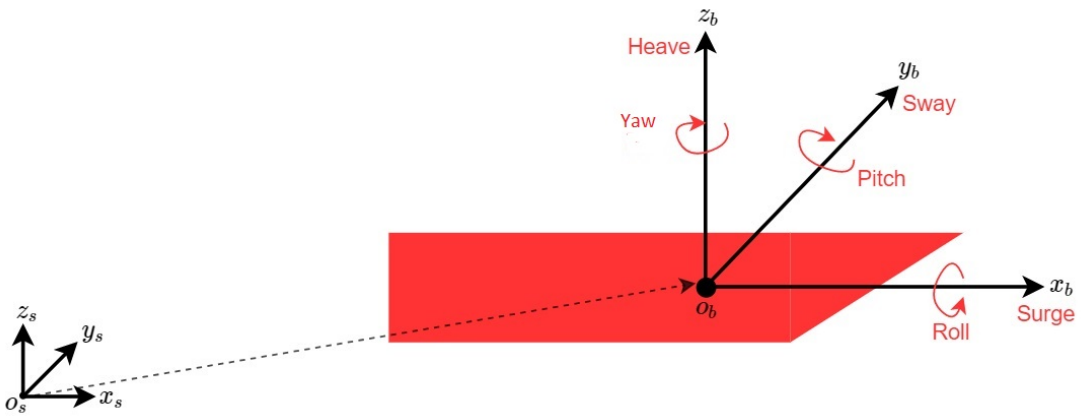

Figure 1: The inertial reference frame $\{s\}$ (left) and the body-fixed frame $\{b\}$ (right).

To represent the position and orientation of the PWC, the PWC is represented by a body-fixed frame $\{b\}$ that moves in an inertial frame $\{s\}$ that is fixed in space. The x_b-axis of $\{b\}$ is aligned along the longitudinal axis of the PWC, the y_b-axis along the transverse axis, and the z_b-axis along the vertical axis.

The position of the PWC is thus the position of the body-fixed frame origin o_b relative to the inertial frame $\{s\}$, expressed in $\{s\}$-coordinates.

$$p_{b/s}^{s} = \begin{bmatrix} x \\ y \\ z \end{bmatrix} \tag{2}$$

Correspondingly, the orientation of the craft is given by the direction of the $\{b\}$-axes relative to their counterparts in the inertial frame $\{s\}$. This is called attitude and is denoted by Euler angles:

$$\Theta_{nb} = \begin{bmatrix} \phi \\ \theta \\ \psi \end{bmatrix} \tag{3}$$

The angles are referred to as roll (ϕ), pitch(θ) and yaw (ψ).

Generally, the inertial frame is assumed to be the Earth-centered Earth-fixed (ECEF) reference frame. However, since the PWC will be operating in a limited area, i.e., almost constant latitude and longitude, flat Earth navigation is assumed. This implies that the NED (North-East-Down) frame $\{n\}$ can be considered inertial and is therefore used extensively in this project. Therefore, the position vector can be denoted in $\{n\}$-format:

$$p_{b/n}^{n} = \begin{bmatrix} N \\ E \\ D \end{bmatrix} \tag{4}$$

The velocities are preferably expressed in the $\{b\}$-frame, such that:

$$\text{Linear velocity: } v_{b/n}^{b} = \begin{bmatrix} u \\ v \\ w \end{bmatrix} \qquad \text{Angular velocity: } \omega_{b/n}^{b} = \begin{bmatrix} p \\ q \\ r \end{bmatrix} \tag{5}$$

The vectors above can be combined into:

$$\text{Position and orientation: } \eta = \begin{bmatrix} p_{b/n}^{n} \\ \Theta_{nb} \end{bmatrix} \tag{6}$$

$$\text{Linear and angular velocity: } \nu = \begin{bmatrix} v_{b/n}^{b} \\ \omega_{nb} \end{bmatrix} \tag{7}$$

$$\text{Forces and moments: } \tau = \begin{bmatrix} f_{b}^{b} \\ m_{b}^{b} \end{bmatrix} \tag{8}$$

2.1.2 Degrees of Freedoms

Degrees of Freedom				
	Movement	Position/angle in $\{n\}$	Linear/angular velocity in $\{b\}$	Force/Moment in $\{b\}$
Surge	Translational motion along x-axis	x	u	X
Sway	Translational motion along y-axis	y	v	Y
Heave	Translational motion along z-axis	z	w	Z
Roll	Angular motion about x-axis	ϕ	p	K
Pitch	Angular motion about y-axis	θ	q	M
Yaw	Angular motion about z-axis	ψ	r	N

Table 1: The DoFs.

The motion of the PWC will be completely specified by three independent linear components and three independent angular components, i.e., 6 DoFs all together. The degrees of freedom are given in Table 1.

2.2 Transformation

In kinematics, it is important to be able to transform vectors from one reference frame to another. An important transformation is the velocity-vector from $\{b\}$-frame to $\{n\}$-frame. This is accomplished by multiplying the vector with a ***transformation matrix***:

$$J_{\Theta}(\Theta_{nb}) = \begin{bmatrix} R_b^n(\Theta_{nb}) & 0_{3x3} \\ 0_{3x3} & T_{\Theta}(\Theta_{nb}) \end{bmatrix} \tag{9}$$

$\mathbf{R_b^n(\Theta_{nb})}$ is the ***rotation matrix***:

$$R(\Theta_{nb}) = \begin{bmatrix} \cos\psi\cos\theta & -\sin\psi\cos\phi + \cos\psi\sin\theta\sin\phi & \sin\psi\sin\phi + \cos\psi\cos\phi\sin\theta \\ \sin\psi\cos\theta & \cos\psi\cos\phi + \sin\phi\sin\theta\sin\psi & -\cos\psi\sin\phi + \sin\theta\sin\psi\cos\phi \\ -\sin\theta & \cos\theta\sin\phi & \cos\theta\cos\phi \end{bmatrix} \tag{10}$$

It transforms the *linear velocity vector* $\mathbf{v_{b/n}^b}$ from $\{b\}$-frame to $\{n\}$:

$$\dot{p}_{b/n}^{n} = R_{b}^{n}(\Theta_{nb})v_{b/n}^{b} \tag{11}$$

Similarly, $\mathbf{T_\Theta(\Theta_{nb})}$ transforms the *angular velocity vector* $\omega_{\mathbf{b/n}}^{\mathbf{b}}$ from $\{b\}$-frame to $\{n\}$:

$$T_\Theta(\Theta_{nb}) = \begin{bmatrix} 1 & \sin\phi\tan\theta & \cos\phi\tan\theta \\ 0 & \cos\phi & -\sin\phi \\ 0 & \sin\phi/\cos\theta & \cos\phi/\cos\theta \end{bmatrix} \tag{12}$$

$$\dot{\Theta}_{nb} = T_\Theta(\Theta_{nb})\omega_{b/n}^{b} \tag{13}$$

With the transformation matrix in mind, the 6 DOF's kinematic equations can be expressed as:

$$\dot{\eta} = J_\Theta(\Theta_{nb}) \begin{bmatrix} \dot{p}_{b/n}^{n} \\ \dot{\Theta}_{nb} \end{bmatrix} = \begin{bmatrix} R_{b}^{n}(\Theta_{nb}) & 0_{3x3} \\ 0_{3x3} & T_\Theta(\Theta_{nb}) \end{bmatrix} \begin{bmatrix} v_{b/n}^{b} \\ \omega_{nb} \end{bmatrix} \tag{14}$$

2.3 Rigid-Body Kinetics

The most vital building blocks in this model are the rigid-body motion of equations. These equations are primarily derived from the *Newton-Euler formulations*, that is *Newton's 2nd law* and *Euler's laws of motion.* Translational and rotational equations with respect to the body-fixed frame $\{b\}$ are constructed and ultimately expressed in a matrix-vector setting, as discussed by Fossen [8]

$$M_{RB}\dot{\nu} + C_{RB}(\nu)\nu = \tau_{RB} \tag{15}$$

where:

$$\nu = \begin{bmatrix} u \\ v \\ w \\ p \\ q \\ r \end{bmatrix} = \text{velocity vector expressed in } \{b\}, \tag{16}$$

$$\tau_{RB} = \begin{bmatrix} X \\ Y \\ Z \\ K \\ M \\ N \end{bmatrix} = \text{external forces and moments vector.} \tag{17}$$

2.3.1 Rigid-Body Mass Matrix

The rigid-body mass matrix is given by:

$$M_{RB} = \begin{bmatrix} mI_{3x3} & -mS(r_g^b) \\ mS(r_g^b) & I_b \end{bmatrix} \tag{18}$$

in which m is the mass of the PWC, S is the skew-symmetric matrix operator, r_g^b is the location of center of gravity CG with respect to the origin o_b, and I_b the inertia matrix about the origin o_b. Since the center of gravity CG is assumed to coincide with origin o_b ($r_g^b = 0$), this will result in:

$$M_{RB} = \begin{bmatrix} mI_{3x3} & 0 \\ 0 & I_b \end{bmatrix} \tag{19}$$

All physical values used to define the PWC is found in Table 2 below.

Parameter	Notation	Value	Unit
LOA (Length over all)	L	3.35	m
Radius (approx shape)	r	0.75	m
Width/2	b	0.75	m
Draught	a	0.3	m
Water Density	ρ	1014	kg/m^3
Gravity	g	9.81	m/s^2
Dry Weight	m	348	kg

Table 2: PWC Parameters

The inertia was found using an approximate model seen in Fig. 2. The axis of rotation is assumed to remain at the center of the half circle while the mass is still concentrated in lower part.

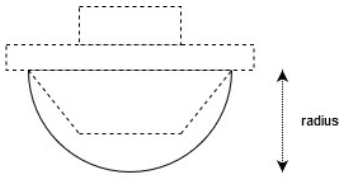

Figure 2: Model used for estimating inertia tensor of the PWC. The dashed area indicates the rough outline of the PWC where the solid half circle is the estimation. The PWC is considered symmetrical over its length.

By approximating the shape to be that of a half-cylinder, the inertia is

$$I_{xx} = \frac{1}{2} \cdot \frac{1}{2} m r^2 \tag{20}$$

$$I_{yy} = \frac{1}{2} \cdot \frac{1}{12} m (3r^2 + L^2) \tag{21}$$

$$I_{zz} = \frac{1}{2} \cdot \frac{1}{12} m (3r^2 + L^2) \tag{22}$$

The remainder of the elements $I_{xy} = I_{xz} = I_{yx} = I_{yz} = I_{zx} = I_{zy} = 0$.

The inertia matrix results in:

$$I_b = \begin{bmatrix} I_{xx} & 0 & 0 \\ 0 & I_{yy} & 0 \\ 0 & 0 & I_{zz} \end{bmatrix} = \begin{bmatrix} 48.94 & 0 & 0 \\ 0 & 187.20 & 0 \\ 0 & 0 & 187.20 \end{bmatrix} \tag{23}$$

giving the expression of M_{RB} as

$$M_{RB} = \begin{bmatrix} m & 0 & 0 & 0 & 0 & 0 \\ 0 & m & 0 & 0 & 0 & 0 \\ 0 & 0 & m & 0 & 0 & 0 \\ 0 & 0 & 0 & I_{xx} & 0 & 0 \\ 0 & 0 & 0 & 0 & I_{yy} & 0 \\ 0 & 0 & 0 & 0 & 0 & I_{zz} \end{bmatrix} \tag{24}$$

2.3.2 Rigid-Body Coriolis-Centripetal Matrix

This matrix contains the terms in the equation of motion that are associated with the rotation of the body-fixed frame $\{b\}$ about the inertial frame $\{n\}$, such as the Coriolis term $\omega^b_{b/n} \times v^b_{b/n}$ and the centripetal term $\omega^b_{b/n} \times (\omega^b_{b/n} \times v^b_{b/n})$. It is given by [8] as:

$$C_{RB}(\nu) = \begin{bmatrix} mS(v_2) & -mS(v_2)S(r^b_g)) \\ mS(r^b_g)S(v_2) & -S(I_b v_2) \end{bmatrix} \tag{25}$$

where:

$$v_1 = \begin{bmatrix} u \\ v \\ w \end{bmatrix} \qquad v_2 = \begin{bmatrix} p \\ q \\ r \end{bmatrix} \tag{26}$$

Since the center of gravity CG is assumed to coincide with origin o_b, $r^b_g = 0$. Thus:

$$C_{RB}(\nu) = \begin{bmatrix} mS(v_2) & 0 \\ 0 & -S(I_b v_2) \end{bmatrix} =$$

$$\begin{bmatrix} 0 & -mr & mq & 0 & 0 & 0 \\ mr & 0 & -mp & 0 & 0 & 0 \\ -mq & mp & 0 & 0 & 0 & 0 \\ 0 & 0 & 0 & 0 & -I_{xz}p - I_{yz}q + I_{zz}r & I_{xy}p - I_{yy}q + I_{yz}r \\ 0 & 0 & 0 & I_{xz}p + I_{yz}q - I_{zz}r & 0 & I_{xx}p - I_{xy}q - I_{xz}r \\ 0 & 0 & 0 & -I_{xy}p + I_{yy}q - I_{yz}r & -I_{xx}p + I_{xy}q + I_{xz}r & 0 \end{bmatrix} \tag{27}$$

2.4 Hydrostatics

Since the PWC is floating on water, hydrostatics is of interest. Most importantly, the craft will be subjected to gravitational and buoyancy forces. These restoring forces can be compared to the spring forces in a mass-spring-damper system. They will help to shape the motion of the PWC in rolling, pitching and heaving. In this section, a vector g(η) with the restoring forces and moments is derived in accordance with [9].

2.4.1 Restoring Forces

The floating PWC is influenced by an gravitational force acting on the center of gravity CG that pulls down the craft, and a buoyancy at the center of buoyancy CB that pushes upwards.

$$\textbf{Gravitational force: } W = mg \tag{28}$$

$$\textbf{Buoyancy: } f_b = \rho g \Delta \tag{29}$$

where m is the mass, ρ is the density of the displaced medium (water), g is the gravitational acceleration, and Δ is the displaced water volume.

At equilibrium, the gravitational force equals the buoyancy.

$$mg = \rho g \Delta \tag{30}$$

In addition, the center of gravity CG and the center of buoyancy CB must be located on the same centerline in order to cancel moment resulting from these forces.

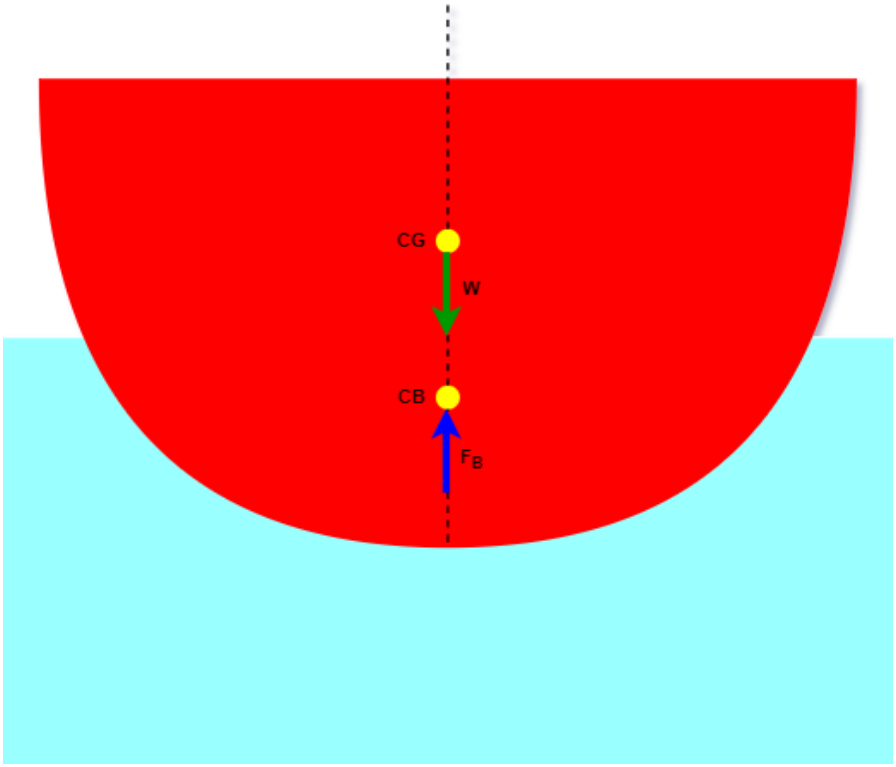

Figure 3: Restoring forces in heave-direction.

Among other factors, the buoyancy is affected by the displacement in heave $\Delta(z)$, since it corresponds to a change in the volume displacement $\delta\Delta(z)$. This means that the equilibrium is disturbed, resulting in a force Z due to the change of buoyancy:

$$Z = mg - \rho g(\Delta + \delta\Delta(z)) = -\delta\Delta(z) \tag{31}$$

The change in volume displacement is calculated through:

$$\delta\Delta(z) = \int_0^z A_{wp}(\zeta)d\zeta \tag{32}$$

where $A_{wp}(\zeta)$ is the water plane area of the PWC. To simplify, the PWC is assumed to be box-shaped, resulting in $A_{wp}(\zeta) = A_{wp}(0)$. The change in displacement of volume can thus be written as:

$$\delta\Delta(z) = A_{wp}(0)z \qquad Z = -\rho g A_{wp}(0)z \tag{33}$$

The restoring forces, expressed in body-fixed frame $\{b\}$ are thus:

$$\delta f_r^b = R_b^n(\Theta_{nb})^{-1} \begin{bmatrix} 0 \\ 0 \\ Z \end{bmatrix} = -\rho g A_{wp} z \begin{bmatrix} -\sin\theta \\ \cos\theta \sin\phi \\ \cos\theta \cos\phi \end{bmatrix} \tag{34}$$

In order to calculate restoring moments, metacentric stability needs to be understood.

2.4.2 Metacenter

When the PWC is tilted from its equilibrium position, the stability of its equilibrium will depend on the location of its metacenter.

If the PWC is tilted to the side, the displaced volume of water Δ will be larger on one side of the body. The center of buoyancy is thus shifted from the centerline to somewhere on the tilted side of the body CB', which means that the buoyancy force will be larger on one side than the other. This will create a lever r_r^b between the buoyancy and gravitational force $f_r^n = [0; 0; \rho g \Delta]$, which manifests as a coupled moment $\mathbf{m_r^b}$ and makes the body rotate.

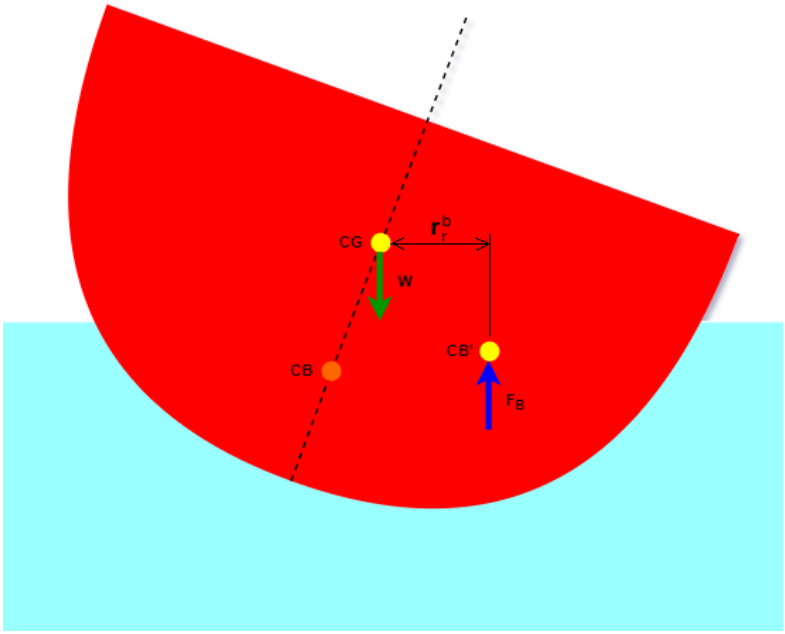

Figure 4: Viewed from behind. There is a lever between the gravity and buoyancy, which will create a moment. This is roll-case, but the same thing occurs in pitch.

This change can be described by the **metacenter**, which is the intersection between the centerline of the PWC and the vertical line through the new center of buoyancy CB' of the tilted body.

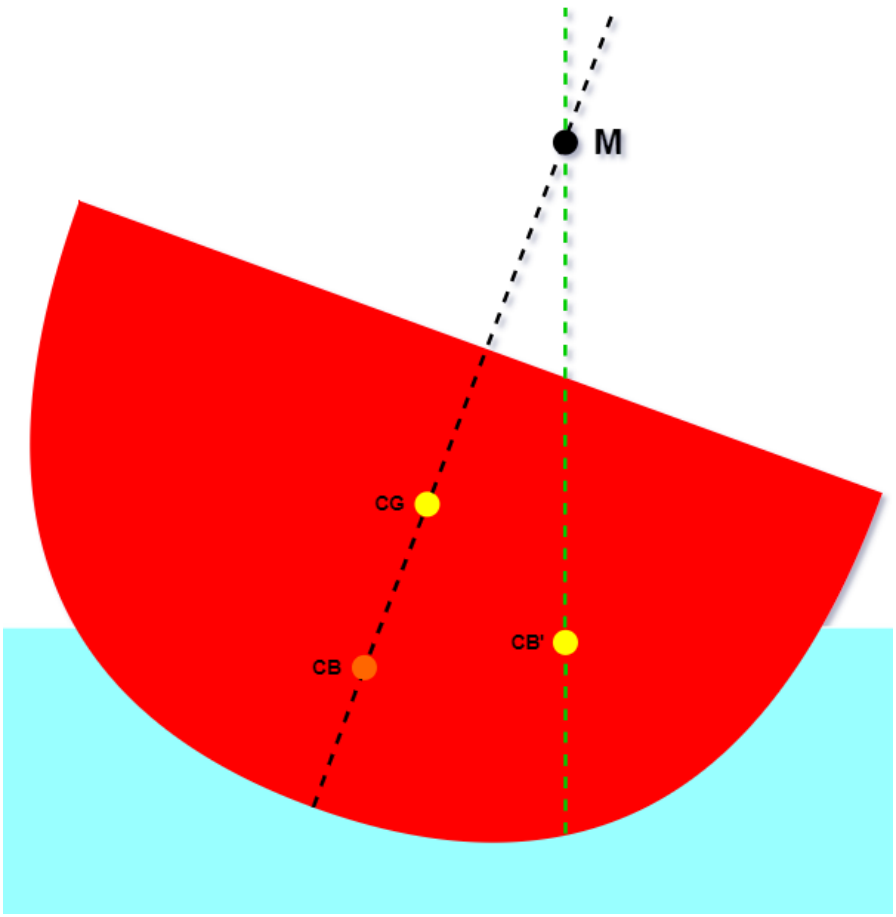

Figure 5: Viewed from the back. The metacenter is the point of intersection between the centerline of the PWC (black) and the centerline of the new center of buoyancy CB' (green).

The metacenter M helps us to obtain the moment levers in pitch and roll.

$$r_r^b = \begin{bmatrix} -\overline{GM}_L \sin\theta \\ \overline{GM}_T \sin\phi \\ 0 \end{bmatrix} \tag{35}$$

where the constants $\overline{GM}_L$ and $\overline{GM}_L$ are the metacentric heights, in longitudinal and transverse distances respectively.

The moment due to the new location of CB' can thus be calculated in pitch and roll respectively:

$$m_r^b = r_r^b \times f_r^b = r_r^b \times R_b^n(\Theta_{nb})^{-1} f_r^n = -\rho g \Delta \begin{bmatrix} \overline{GM}_T \sin\phi\cos\theta\cos\phi \\ \overline{GM}_L \sin\theta\cos\theta\cos\phi \\ (-\overline{GM}_L\cos\theta + \overline{GM}_T)\sin\phi\sin\theta \end{bmatrix} \tag{36}$$

The restoring forces δf_r^b and restoring moments m_r^b are combined into:

$$\mathbf{g}(\eta) = -\begin{bmatrix} \delta f_r^b \\ m_r^b \end{bmatrix} = \begin{bmatrix} -\rho g A_{wp} z \sin\theta \\ \rho g A_{wp} z \cos\theta \sin\phi \\ \rho g A_{wp} z \cos\theta \cos\phi \\ \rho g \Delta \overline{GM}_T \sin\phi \cos\theta \cos\phi \\ \rho g \Delta \overline{GM}_L \sin\theta \cos\theta \cos\phi \\ \rho g \Delta (-\overline{GM}_L \cos\theta + \overline{GM}_T) \sin\phi \sin\theta \end{bmatrix} \tag{37}$$

Motions in heave z, roll ϕ and pitch θ are assumed to be small, which can be approximated with the linear vector:

$$\mathbf{g}(\eta) = \begin{bmatrix} 0 \\ 0 \\ \rho g A_{wp} z \\ \rho g \Delta \overline{GM}_T \phi \\ \rho g \Delta \overline{GM}_L \theta \\ 0 \end{bmatrix} \tag{38}$$

The distance between the center of gravity to the metacenter $\overline{GM}$ can be calculated through

$$\overline{GM} = \overline{BM} - \overline{BG}, \tag{39}$$

where B is the original buoyancy center (CB in Figure 3). For small angular displacements, $\overline{BM}$ can be found as

$$\overline{BM} = \frac{I}{\Delta}, \tag{40}$$

where I is the moment of area about A_{wp} (plane area of the PWC at water-surface) in x- and y-direction respectively, and Δ the displacement of water by the PWC.

If the vessel is approximated to be square-shaped (only in the cast of restoring forces) such that $A_{wp} = 2b \cdot L$, the moment of area can be bounded individually as

$$I_L = \iint_{A_{wp}} x^2 dA < \frac{1}{12} L^3 (2b) \tag{41}$$

$$I_T = \iint_{A_{wp}} y^2 dA < \frac{1}{12} (2b)^3 L \tag{42}$$

where the bounded value can be used as a first estimation.

Using the physical values for the PWC the final value for the metacentric height is given by

$$GM_T = \frac{I_T}{\Delta} - BG = \frac{1.01}{1.68} - 0 = 0.625\,m \tag{43}$$

$$GM_L = \frac{I_L}{\Delta} - BG = \frac{5.83}{1.68} - 0 = 3.47\,m \tag{44}$$

where $BG = 0$ with the assumption that the center of gravity is the same as the center of buoyancy.

2.5 Hydrodynamics

Since the PWC is surrounded and partly submerged in water, hydrodynamics need to be taken into consideration. Each movement of the craft corresponds to a displacement of fluid. The inertia of the surrounding fluid is thus the major contributing factor to the resulting hydrodynamic force, which can be written as:

$$\tau_{hyd} = -M_A\dot{\nu} - C_A(\nu)\nu - D(\nu)\nu \tag{45}$$

where M_A is the added mass inertia matrix with the surrounding fluid inertia, $C_A(\nu)$ the corresponding Coriolis and centripetal matrix of the added mass matrix, and $D(\nu)$ the damping matrix and ν the velocity vector in body frame as given in Eq. (16). These matrices will extensively be constructed in the same manner as in earlier projects [3, 4].

As the motion of the PWC increases, the speed difference between the craft and the water results in an upward pressure. This pressure is known as hydrodynamic lift force and will at sufficiently high velocities vertically displace the craft to the point where the wetted area is significantly reduced, allowing it to travel at high speeds (planing). However, this project constrains itself to lower velocities.

Since the hydrodynamics for small high-speed craft are not well understood, broad assumptions and simplifications are made.

2.5.1 Hydrodynamic System Inertia Matricies

The added mass matrix M_A and its corresponding Coriolis-Centrepetal matrix C_A are defined in [10]. The added mass matrix $\mathbf{M_A}$ is given by:

$$M_A = -\begin{bmatrix} X_{\dot{u}} & X_{\dot{v}} & X_{\dot{w}} & X_{\dot{p}} & X_{\dot{q}} & X_{\dot{r}} \\ Y_{\dot{u}} & Y_{\dot{v}} & Y_{\dot{w}} & Y_{\dot{p}} & Y_{\dot{q}} & Y_{\dot{r}} \\ Z_{\dot{u}} & Z_{\dot{v}} & Z_{\dot{w}} & Z_{\dot{p}} & Z_{\dot{q}} & Z_{\dot{r}} \\ K_{\dot{u}} & K_{\dot{v}} & K_{\dot{w}} & K_{\dot{p}} & K_{\dot{q}} & K_{\dot{r}} \\ M_{\dot{u}} & M_{\dot{v}} & M_{\dot{w}} & M_{\dot{p}} & M_{\dot{q}} & M_{\dot{r}} \\ N_{\dot{u}} & N_{\dot{v}} & N_{\dot{w}} & N_{\dot{p}} & N_{\dot{q}} & N_{\dot{r}} \end{bmatrix} \tag{46}$$

Two assumptions are made in line with earlier projects [3]:

1. Since the PWC is symmetric in the xz-plane, M_A is assumed to be symmetric.
2. Non-diagonal terms are assumed to be negligible compared to the terms that are diagonal. For instance, this means that during surge the term corresponding to surge-direction $X_{\dot{u}}$ will be far larger than the other terms.

These two assumptions simplify the matrix into:

$$M_A = -\begin{bmatrix} X_{\dot{u}} & 0 & 0 & 0 & 0 & 0 \\ 0 & Y_{\dot{v}} & 0 & 0 & 0 & 0 \\ 0 & 0 & Z_{\dot{w}} & 0 & 0 & 0 \\ 0 & 0 & 0 & K_{\dot{p}} & 0 & 0 \\ 0 & 0 & 0 & 0 & M_{\dot{q}} & 0 \\ 0 & 0 & 0 & 0 & 0 & N_{\dot{r}} \end{bmatrix} \tag{47}$$

To construct the matrices above, the values of $X_{\dot{u}}$, $Y_{\dot{v}}$, $Z_{\dot{w}}$, $K_{\dot{p}}$, $M_{\dot{q}}$, and $N_{\dot{r}}$ need to be estimated. This is done with the so called **strip theory**, which is a method that divides the submerged part of the PWC into a finite number of strips, for which a two-dimensional hydrodynamic coefficient is calculated for each strip. These coefficients for each strip are then summed across the length of the body, resulting in the three-dimensional coefficients [11].

In an earlier project [3], strip theory was used to estimate the added mass matrix as defined by the parameters a which is the submerged depth of the PWC and b is half the width of the submerged part (Table 2). The PWC was modelled for the geometry given in Fig. 2, but for more details, see [3].

$$M_A = \begin{bmatrix} \frac{m}{20} & 0 & 0 & 0 & 0 & 0 \\ 0 & \frac{L\pi\rho a^2}{2} & 0 & 0 & 0 & 0 \\ 0 & 0 & \frac{L\pi\rho b^2}{2} & 0 & 0 & 0 \\ 0 & 0 & 0 & \frac{1}{16}(b^2-a^2)^2 L\pi\rho & 0 & 0 \\ 0 & 0 & 0 & 0 & \frac{ma^3}{30} + \frac{L^3\pi\rho b^2}{24} & 0 \\ 0 & 0 & 0 & 0 & 0 & \frac{mb^3}{30} + \frac{L^3\pi\rho a^2}{24} \end{bmatrix} \tag{48}$$

The corresponding Coriolis-Centripetal matrix $\mathbf{C_A}(\nu)$ is derived from M_A [10]:

$$C_A(v) = \begin{bmatrix} 0_{3x3} & -S(A_{11}v_1 + A_{12}v_2) \\ -S(A_{11}v_1 + A_{12}v_2) & -S(A_{21}v_1 + A_{22}v_2) \end{bmatrix} \tag{49}$$

where:

$$M_A = \begin{bmatrix} A_{11} & A_{12} \\ A_{21} & A_{22} \end{bmatrix} \qquad \nu = \begin{bmatrix} v_1 \\ v_2 \end{bmatrix} = \begin{bmatrix} u \\ v \\ w \\ p \\ q \\ r \end{bmatrix} \tag{50}$$

where $A_{11} = diag(X_{\dot{u}}, Y_{\dot{v}}, Z_{\dot{w}})$ and $A_{22} = diag(K_{\dot{p}}, M_{\dot{q}}, N_{\dot{r}})$, such that:

$$C_A(\nu) = \begin{bmatrix} 0 & 0 & 0 & 0 & -Z_{\dot{w}}w & Y_{\dot{v}}v \\ 0 & 0 & 0 & Z_{\dot{w}}w & 0 & -X_{\dot{u}}u \\ 0 & 0 & 0 & -Y_{\dot{v}}v & X_{\dot{u}}u & 0 \\ 0 & -Z_{\dot{w}}w & Y_{\dot{v}}v & 0 & -N_{\dot{r}}r & M_{\dot{q}}q \\ Z_{\dot{w}}w & 0 & -X_{\dot{u}}u & N_{\dot{r}}r & 0 & -K_{\dot{p}}p \\ -Y_{\dot{v}}v & X_{\dot{u}}u & 0 & -M_{\dot{q}}q & K_{\dot{p}}p & 0 \end{bmatrix} \tag{51}$$

2.5.2 Damping

The damping $\mathbf{D}(\nu)$ is a hydrodynamic force that represents the resistance to movement of a body in fluid. The damping force grows with velocity of the craft and with the surface area in contact with the fluid. The damping parameters in the matrix below can be roughly derived from experimental data. A set of experiments (in Appendix B) were drawn up and planned to be performed at one of SSRS's stations, but never materialized. Instead, the parameters had to be estimated from a set of studies.

The damping in surge- and yaw-motion were the most important as these DoFs are controllable. Each degree of freedom was modelled with a damping as:

$$D(v) = \begin{bmatrix} D_u & 0 & 0 & 0 & 0 & 0 \\ 0 & D_v & 0 & 0 & 0 & 0 \\ 0 & 0 & D_w & 0 & 0 & 0 \\ 0 & 0 & 0 & D_\phi & 0 & 0 \\ 0 & 0 & 0 & 0 & D_\theta & 0 \\ 0 & 0 & 0 & 0 & 0 & D_\psi \end{bmatrix} \tag{52}$$

The damping in surge was modelled by [4] as:

$$D_u = c_u \cdot \frac{\rho}{2} u^2 \cdot a_l \tag{53}$$

where c_u is a resistance coefficient depending on the vessel, a_l is the lateral area of the vessel submerged in water and as it is dependent on the velocity it is modeled as $a_l = a/(1 + abs(u))$. The PWC has the surge velocity u and ρ is the density of water.

The damping in yaw was also estimated in [4], but it was not possible to merge those results with this project. Instead, the coefficient was derived from another study [12]. This study had estimations based on Nomoto models (first-order systems) of the dynamics between steer angle and heading angle for certain surge velocities.

Our nonlinear model was matched with the linear models for velocities 2.5, 4 and 6 m/s (5, 8 and 12 knots). For these surge velocities, the value $c_\phi = -704$ gave sufficiently accurate matches using the damping model in Eq. (54).

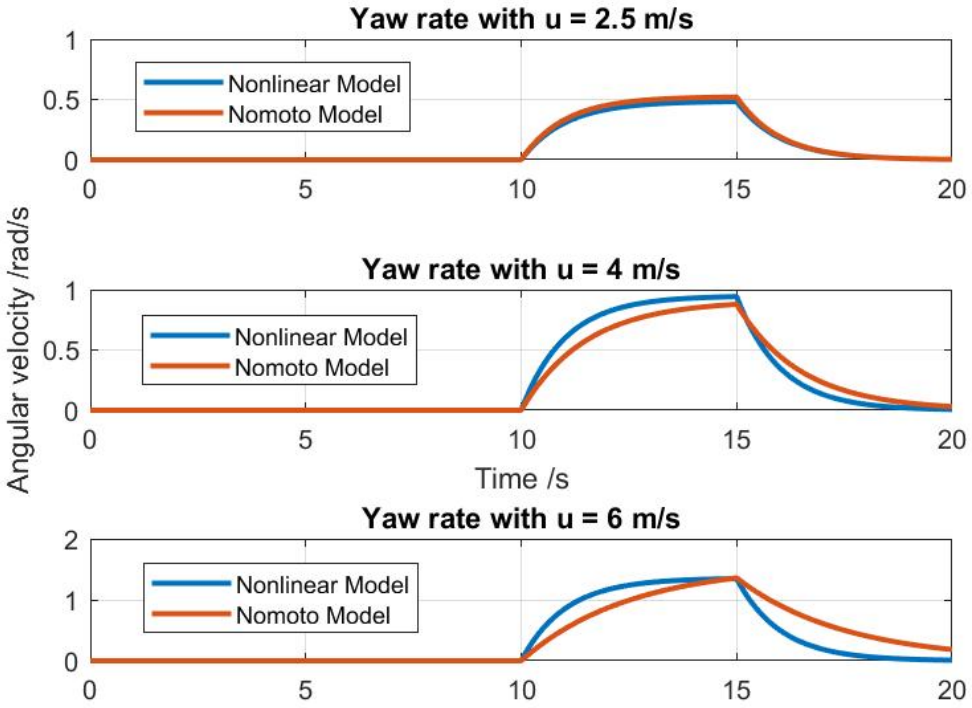

Figure 6: Estimations of c_ϕ by matching the first-order system from [12] with our nonlinear model.

$$D_\psi = c_\psi \cdot \frac{\rho}{2}\dot{\psi} \tag{54}$$

For the remaining states (sway, heave, roll and pitch) pure guesses were made of the damping parameter as to complete the model and avoiding strange behavior with states that keep moving indefinitely. These all used the same squared damping with the resistance parameters c_{sway}, c_{heave}, c_{roll} and c_{pitch}. The final set of parameters used in the damping models for surge and yaw are given in Table 6 below.

Constant	Value	Unit
c_u	-440	
c_ψ	-704	
a_l	1	m^2
ρ	1.0025	kg/L
c_{roll}	-400	
c_{pitch}	-400	
c_{sway}	-400	
c_{heave}	-400	

Table 3: Damping parameters. Note that the water density is measured in kg/L.

2.6 Thrust Model

In [4], the throttle input to the PWC was measured in the range $0 - 100\%$. This resulted in a thrust according to Eq. (55-56).

$$T = 150 \cdot \rho \cdot q \cdot (v_2 - v_1) \tag{55}$$

where v_2 is the velocity of the water from the jet, v_1 the velocity of the PWC, ρ the density of water, and $q = A_o \cdot v_2$ is the flow of water out from the jet. The factor 150 is a scaling factor.

$$v_2 = \sqrt{\frac{2 \cdot (p_1 - p_2)}{\rho}} \tag{56}$$

where p_2 is the normal water pressure and p_1 is the pressure of the water from the jet. This pressure was estimated as $p_1 = (p_2 \cdot (1 + 9 \cdot u))$.

The input signals – throttle and steer – result in 6 forces depending on the placement of the nozzle with regards to the center of gravity CG.

$$\begin{aligned} X &= T \cdot \cos(s) \\ Y &= T \cdot \sin(s) \\ Z &= 0 \\ K &= l_\phi \cdot T \\ M &= l_\theta \cdot T \\ N &= l_\psi \cdot T \cdot \sin(s) \end{aligned}$$

where l_ϕ is the leverarm for roll, l_θ the leverarm for pitch, l_ψ the leverarm for yaw and s the steering angle.

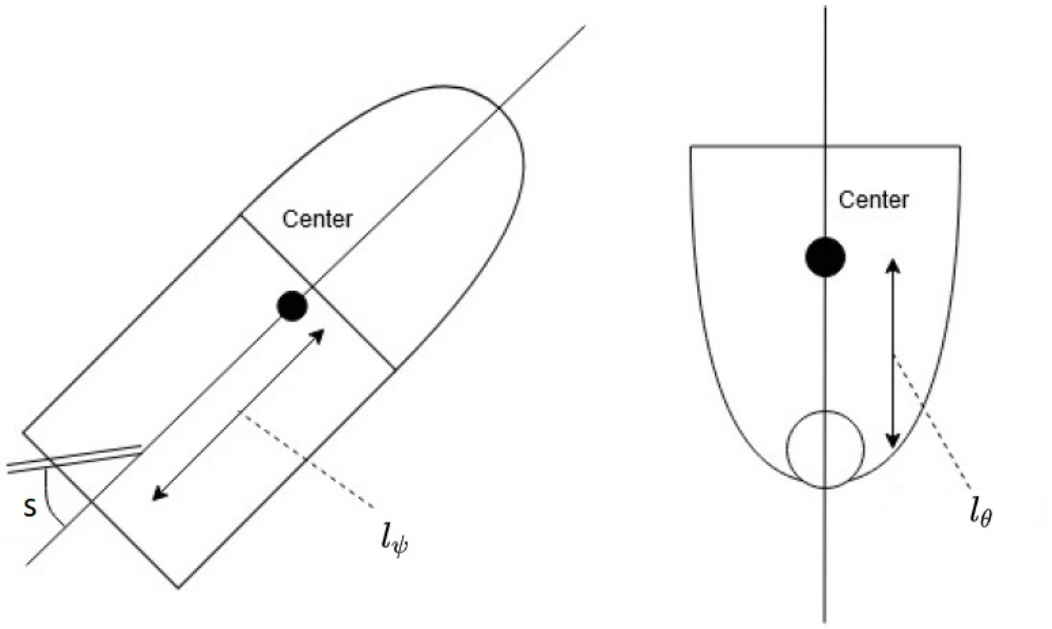

Figure 7: Thrust allocation overview, where center is CG.

The levers for pitch l_θ and roll l_ϕ were kept to zero as they were both expected to be small, but also to simplify the simulations later on. For the turning motion half the length of the PWC was used, $l_\psi = L/2$.

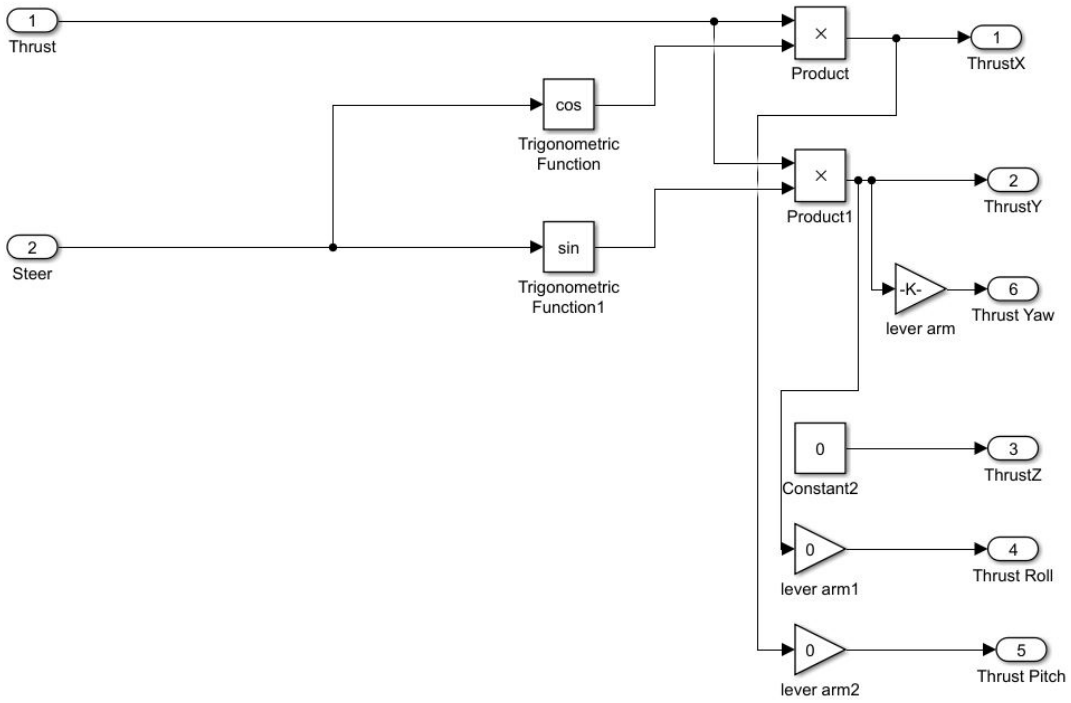

Figure 8: Thrust allocation

2.7 Final Form

The dynamics of the system are given in the matrix-vector form:

$$M\dot{\nu} + C(\nu)\nu + D(\nu)\nu + g(\eta) = \tau \tag{57}$$

The mass matrix of the system is given by $M = M_{RB} + M_A$, with the components:

$$M_{RB} = \begin{bmatrix} m & 0 & 0 & 0 & 0 & 0 \\ 0 & m & 0 & 0 & 0 & 0 \\ 0 & 0 & m & 0 & 0 & 0 \\ 0 & 0 & 0 & I_{xx} & 0 & 0 \\ 0 & 0 & 0 & 0 & I_{yy} & 0 \\ 0 & 0 & 0 & 0 & 0 & I_{zz} \end{bmatrix} \tag{58}$$

$$M_A = \begin{bmatrix} \frac{m}{20} & 0 & 0 & 0 & 0 & 0 \\ 0 & \frac{L\pi\rho a^2}{2} & 0 & 0 & 0 & 0 \\ 0 & 0 & \frac{L\pi\rho b^2}{2} & 0 & 0 & 0 \\ 0 & 0 & 0 & \frac{1}{16}(b^2-a^2)^2 L\pi\rho & 0 & 0 \\ 0 & 0 & 0 & 0 & \frac{ma^3}{30} + \frac{L^3\pi\rho b^2}{24} & 0 \\ 0 & 0 & 0 & 0 & 0 & \frac{mb^3}{30} + \frac{L^3\pi\rho a^2}{24} \end{bmatrix} \tag{59}$$

Table 2 contains the parameter-values.

The Coriolis-centrepetal matrix of the system is given by $C = C_{RB} + C_A$, with the components:

$$C_{RB} = \begin{bmatrix} mS(v_2) & 0) \\ 0 & -S(I_0 v_2) \end{bmatrix} \tag{60}$$

$$C_A = \begin{bmatrix} 0_{3x3} & -S(A_{11}v_1)) \\ -S(A_{11}v_1) & -S(A_{22}v_2) \end{bmatrix} \tag{61}$$

where $A_{11} = diag(X_{\dot{u}}, Y_{\dot{v}}, Z_{\dot{w}})$ and $A_{22} = diag(K_{\dot{p}}, M_{\dot{q}}, N_{\dot{r}})$.

The damping matrix $D(\nu)$ is made up by the components:

$$D_u = c_u \cdot \frac{\rho}{2} u^2 \cdot a_l \tag{62}$$

$$D_\psi = c_\psi \cdot \frac{\rho}{2} \dot{\psi} \tag{63}$$

The damping parameters are given in Table 6.

The restoring forces $g(\eta)$ vector is given by:

$$g(\eta) = \begin{bmatrix} 0 \\ 0 \\ \rho g A_{wp}(0) z \\ \rho g \overline{\nabla G M_T} \phi \\ \rho g \overline{\nabla G M_L} \theta \\ 0 \end{bmatrix} \tag{64}$$

where:

$$GM_T = 0.625m \tag{65}$$

$$GM_L = 3.47m \tag{66}$$

The basic foundation of the model (using M and C) was done using the Marine System Simulator (MSS) Toolbox [13], which provides resources that facilitates rapid implementation of models given in the matrix-vector form seen in Eq. (57). In this case, the MSS Toolbox requires pre-calculation of the M_{RB} and M_A, but derives C_{RB} and C_A on its own.

3 Environmental Disturbances

Since the PWC will be subjected to disturbances from the environment, models are needed for winds, waves and ocean currents.

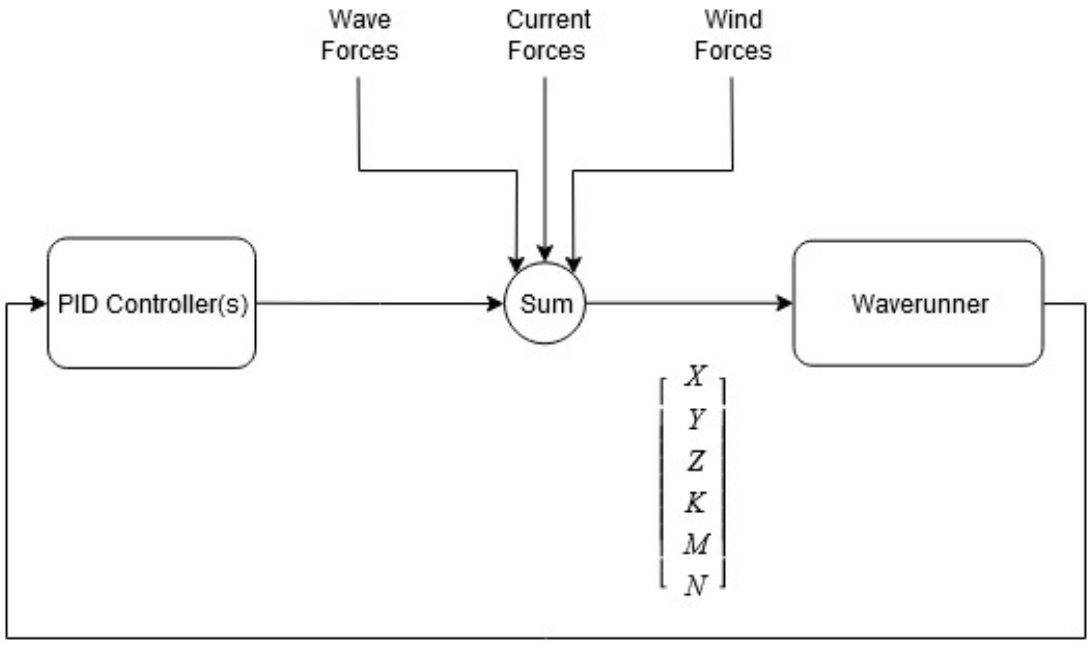

Figure 9: Disturbances affecting the PWC

3.1 Wind Load

When the PWC is moving with a forward speed, the wind forces and moments can be calculated according to [14] as

$$\tau_{\mathbf{wind}} = \begin{bmatrix} X_{\text{wind}} \\ Y_{\text{wind}} \\ Z_{\text{wind}} \\ K_{\text{wind}} \\ M_{\text{wind}} \\ N_{\text{wind}} \end{bmatrix} = \frac{1}{2}\rho_a V_{r\omega}^2 \begin{bmatrix} C_X(\gamma_{r\omega})A_{F\omega} \\ C_Y(\gamma_{r\omega})A_{L\omega} \\ C_Z(\gamma_{r\omega})A_{F\omega} \\ C_K(\gamma_{r\omega})A_{L\omega}H_{L\omega} \\ C_M(\gamma_{r\omega})A_{F\omega}H_{F\omega} \\ C_N(\gamma_{r\omega})A_{L\omega}L_{oa} \end{bmatrix} \tag{67}$$

where:

ρ – density of air,

$V_{r\omega}$ – relative wind speed,

$\gamma_{r\omega}$ – angle of attack,

$A_{F\omega}$ – projected area of the front,

$A_{L\omega}$ – projected area of the side,

$H_{F\omega}$ – height of the centroid of $A_{F\omega}$ (above the water line),

$H_{L\omega}$ – height of the centroid of $A_{L\omega}$ (above the water line),

$C_X, C_Y, C_Z, C_K, C_M, C_N$ – non-dimensional wind coefficients

The wind coefficients varies with different vessels, size and geometry of the craft and are obtained experimentally using scale models. Whilst no experimental data has been obtained for PWC, data is available for speed boats in the MSS Toolbox [13]. By making the assumption that a PWC is just a tiny speed boat, wind coefficients can be derived [14, 13].

3.2 Waves

Waves are generated when energy is transferred from the wind to the surface of the water. The size, direction and period of the waves depends on:

- Speed of the wind
- Direction of the wind
- Duration of the wind
- Uninterrupted distance the winds acts on [15]

The winds results in a irregular sea-state with a broad **spectrum** of waves in terms of sizes and periods [16]. However, a sea-state can generally be characterized by:

- **Significant wave height** H_s, which is the mean height of the one-third largest waves.
- **Average wave period** T_1.

The size of the waves (amplitude) determines the magnitude of the wave-forces [16]. The wave-induced forces can be separated into:

- **1st order wave-induced forces -** wave-frequency motion, i.e., oscillations around zero-mean.
- **2nd order wave-induced forces -** wave drift forces, i.e., nonzero component that varies slowly (no oscillations).

Wave forces thus contain oscillatory component that is associated with pitching, rolling and heaving, as well as a drifting component that primarily contributes to surge, sway and yaw. These two components are calculated through **Force Response Amplitude Operators (RAO)**, that combine knowledge of the geometry of the craft and wave amplitudes to give force components τ_{wave1} and τ_{wave2} acting on the PWC. By extending the Force ROA with a component related to the

dynamics of the PWC, a **Motion ROA** is obtained that gives the disturbance in position and orientation by the waves [16].

The calculations in these methods require extensive understanding of the geometry of the craft as well as powerful and expensive hydrodynamic software-tools, which was not available to this thesis. An alternative when working with waves is assuming that they have an idealised sinusoidal shape [17].

$$\zeta(x,t) = \zeta_a \sin\left(\frac{2\pi x}{\lambda_v} - \frac{2\pi t}{T}\right) \tag{68}$$

where

ζ_a = wave amplitude,

x = horizontal distance,

t = time,

λ_v = wave length.

The expression can be simplified by introducing two new terms, *radian wave number* $k = 2\pi/\lambda_v$ and *radian wave frequency* $\omega = 2\pi/T$, which results in:

$$\zeta(x,t) = \zeta_a \sin(kx - \omega t) \tag{69}$$

The resulting forces and moments due to the waves are given by:

$$f_{waves} = \begin{bmatrix} 0 \\ 0 \\ -C_{\text{heave}}\rho g A_{\text{wp}}\zeta_a \sin\omega_e t \\ -C_{\text{roll}} \sin(\beta_v - \psi)\rho g A_{\text{wp}} B\zeta_a^2 k_e \cos\omega_e t \\ C_{\text{pitch}} \cos(\beta_v - \psi)\rho g A_{\text{wp}} L\zeta_a^2 k_e \cos\omega_e t \\ 0 \end{bmatrix} \tag{70}$$

where:

$C_{\text{heave}}, C_{\text{roll}}, C_{\text{pitch}}$ = wave coefficients,

A_{wp} = water plane area,

β_v = wave direction,

ψ = heading angle (yaw),

B = beam/width of the craft,

L = length of the craft.

$\omega_e = \omega\left(1 - \frac{V_b}{V_v}\cos(\beta_v - \psi)\right)$ = relative frequency

3.3 Simplified Wave Model

The models of wave-response presented above are usually derived for watercraft significantly larger than a PWC, i.e., with a **wave-length to ship-length ratio** less than or close to unity. If the wavelength is significantly larger than the craft, as in this case, the wave appears flat from the perspective of the craft [17]. The wave-response for small and high-speed (planing) watercraft are thus vastly different and unfortunately not well studied, since they simply were not intended for rough waters.

From watching footage of smaller watercraft driving in conditions with significant waves, the sudden increase of buoyancy from the waves appeared to largely manifest itself as an upward-pushing pulse. This resulted in the idea of modelling the waves as periodic upward pointing force vectors, with a large vertical component and lesser horizontal one. The force will act on the point of contact during a very short time relative to the wave-period (as in a tenth of it).

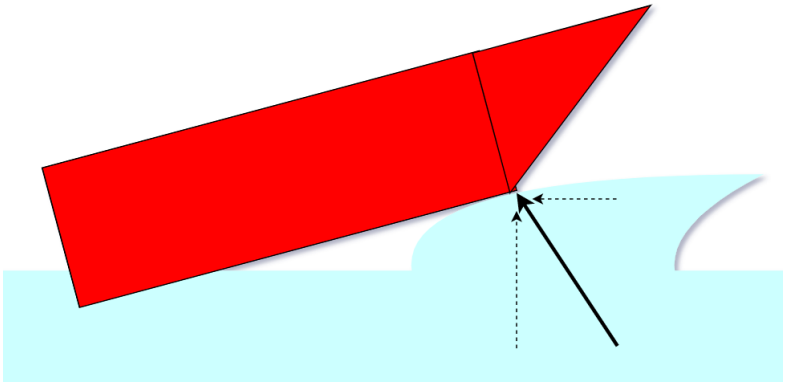

Figure 10: Viewed from the side. The wave is modelled as a force vector, with a vertical component that is dominant and a lesser horizontal component.

The force from the wave is implemented as a pulse acting briefly during the start of every period, as illustrated in Fig. 11 below:

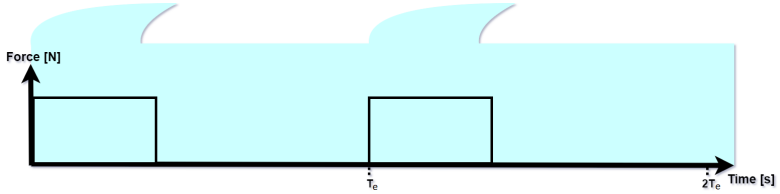

Figure 11: The force F is implemented as a pulse acting for a fraction of every encounter period T_e.

This wave-model is a function of:

- **Angle of Attack** (AoA), i.e., the direction from which the wave hits the craft, denoted as γ.

- **Encounter frequency** ω_e between wave and craft, i.e., how often they meet.
- **Relative velocity** V_r between the craft and waves, since it affects the magnitude of the collision (force) between the craft and wave.

The encounter frequency ω_e as well as the relative velocity V_r are primarily functions of the **wave-period** T, **surge velocity of the craft** u and **AoA** γ [16]:

$$\omega_e(u, T, \gamma) = \left| \omega_0 - \frac{\omega_0^2}{g} u \cos\gamma \right|, \tag{71}$$

where $\omega_0 = 1/T$. If the waves are hitting the craft on the bow (head-on), i.e., they are moving towards each other, the encounter frequency will be greater than the wave-frequency ω_0.

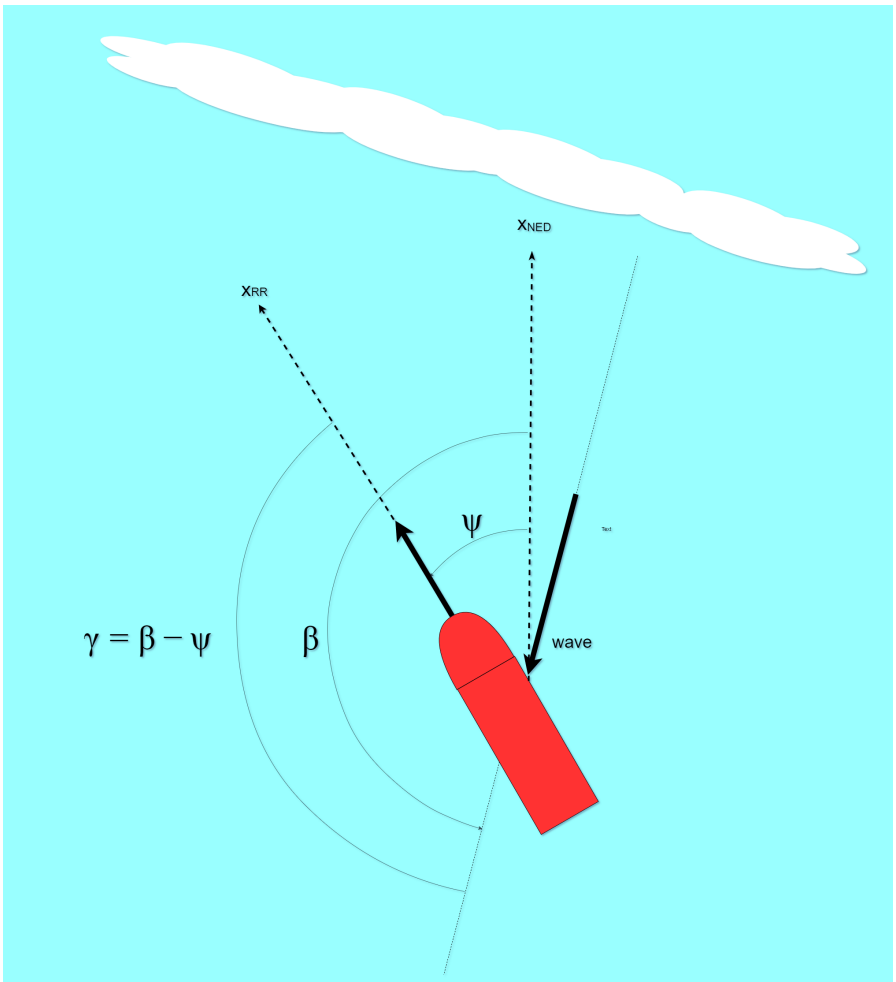

Figure 12: Viewed from above. The waves (white) are hitting the craft (red) at a certain angle of attack. The heading ψ and wave-angle are measured from the inertial frame's x_{NED}-axis

The wave incidence on the craft (AoA) determines the nature of the resulting dis-

placement and movement. Since the wave is modelled as a predominately vertical pointing force, the area of the craft that meets the wave crest will experience a movement upwards. Therefore, if the wave hits from the front, the bow will be pushed upwards, resulting in a positive pitch angle θ. Accordingly if the wave hits from behind, the stern will be pushed upwards and the bow downwards, giving a negative pitch angle.

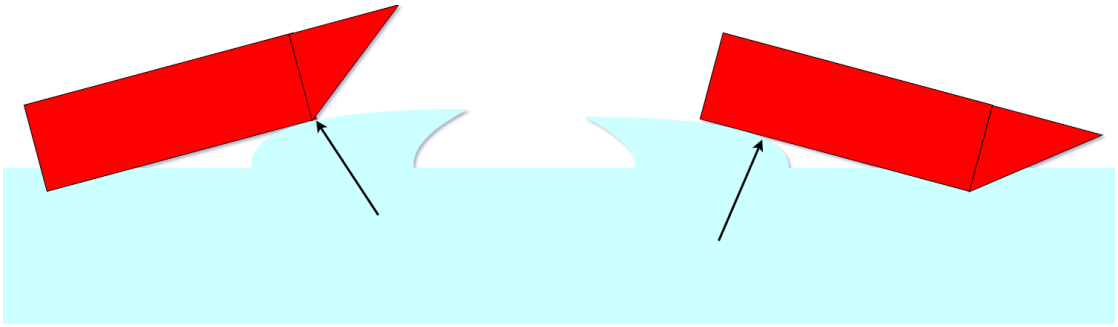

Figure 13: Viewed from the side. The motion when the wave hits from the front (left) and the wave hits from the behind (right)

Similarly if the wave hits the right side (beam), it rolls to the left. If it hits the left, it rolls to the right.

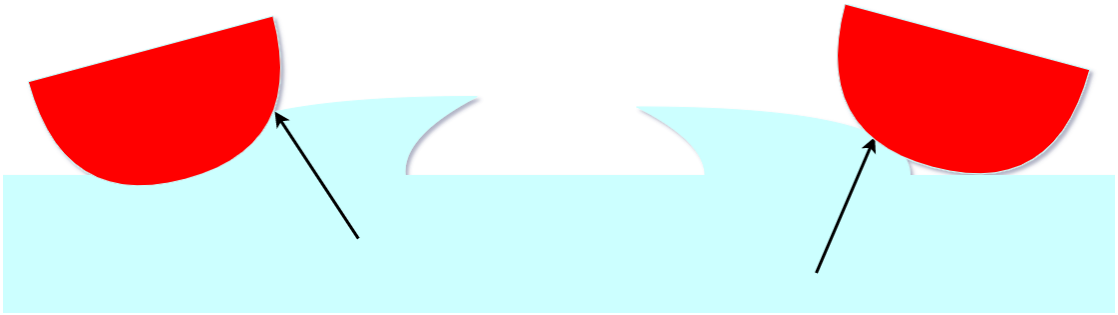

Figure 14: Viewed from the back. The motion when the wave hits from the right (left) and the wave hits the the left (right)

Another important factor is the point of contact of the wave-force on the craft, since it determines the lever from CG to the force. If the bow is raised in a head-on encounter with the wave, the point of contact will be closer to CG and result in a smaller moment. However, since the jet-powered PWC is not capable of trimming its bow and since it will be operating below planing-speed in this project, the bow will mostly be level. From here, it is assumed that the length of the lever is 0.5 m everywhere.

For this model to be implemented in a simulation, it is critical to keep track of the position of the craft relative to the waves, in order to know when the waves hit the craft. Since the encounter period $T_e = 1/\omega_e$ between the craft and waves is known, this can be done by keeping track of the time t, such that:

$$r = \frac{t \mod T_e}{T_e} \tag{72}$$

in which $r = 0$ when it hits the wave (i.e., a force-pulse is sent out) and r=0.99 when it is just about to hit the next wave. The main challenge with this approach is that the encounter period T_e can change, since it is a function of the heading ψ and surge u according to Eq. (71).

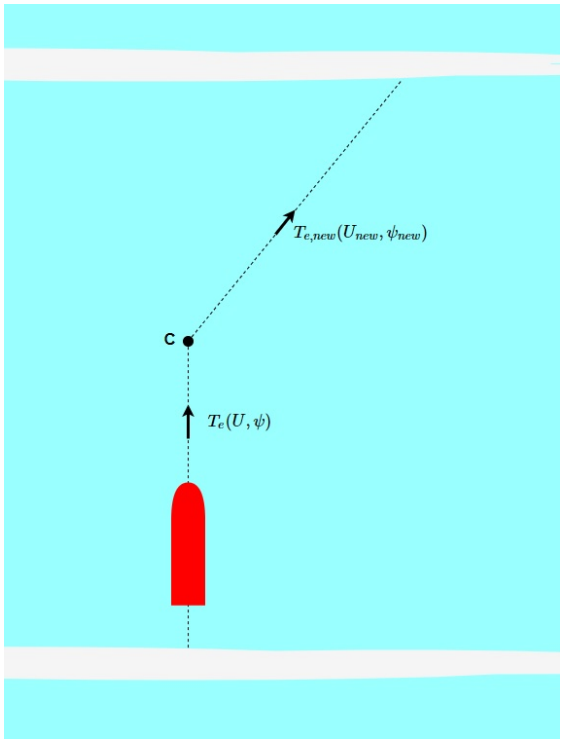

Figure 15: The encounter period T_e changes at point C. Viewed from the above.

When the encounter period is changed at point C, it stores its relative position $r_c = r$ as well as the time-stamp $t_c = t$ of the moment the change occurs. To account for the change in encounter period, Eq. (72) turns into:

$$r = \frac{(t - t_c) + r_c T_{e,new} \mod T_{e,new}}{T_{e,new}} \tag{73}$$

such that at time $t = t_c$, the PWC is still at relative position $r = r_c$.

If the PWC changes speed and/or heading once again, the same equation is used to derive the relative position corresponding the new encounter period.

3.4 Currents

To account for ocean currents and moments, Eq. (57) can simply be modified to use the relative velocities between the ocean currents and the PWC [18].

$$\nu_r = \nu - \nu_c \tag{74}$$

where $\nu_c = \begin{bmatrix} u_c & v_c & 0 & 0 & 0 & 0 \end{bmatrix}$.

The model for simulation can then be altered to

$$M\dot{v}_r + C(v_r)v_r + D(v_r)v_r + g(\eta) = \tau \tag{75}$$

Currents can also be seen as regular input disturbances, just as wave and wind, as seen in Fig. 9. These forces were approximated as acting on only surge, sway and yaw. These forces were suggested by [19] as

$$X = \frac{1}{2}\rho A_{Fc} C_X V_{rc}^2 \tag{76}$$

$$Y = \frac{1}{2}\rho A_{Lc} C_Y V_{rc}^2 \tag{77}$$

$$N = \frac{1}{2}\rho A_{Fc} L_{oa} C_N V_{rc}^2 \tag{78}$$

where ρ is the water density, A_{Fc} is the frontal current area, A_{Lc} lateral current area and L_{oa} is the length of the PWC. The constants C_X, C_Y and C_N are scaling factors depending on the angle of attack. V_{rc} is the current velocity relative to the PWC velocity.

The frontal and lateral areas are again modeled as a rectangle $A_{Fc} = a \cdot B$, $A_{Lc} = L_{oa} \cdot a$. The scaling factors, $\mathrm{C}_{X,Y and N}$, were modelled based on data from an oil tanker. It is in no way ideal, but these scaling parameters give the general idea of how the current force scales with the AoA. These parameters are [19]:

$$C_X = \frac{0.9}{180}\gamma - 0.45 \tag{79}$$

$$C_Y = 0.6 \cdot \sin(\gamma) \cdot \mathrm{abs}(\sin(\gamma)) \tag{80}$$

$$C_N = 0.05 \cdot \sin(2\gamma) \tag{81}$$

As a total overview of the environmental forces used for simulations (and some components being simply discarded for simplicity)

- Current (alt 1) - Constant and affects only surge and sway
  $v_c = \begin{bmatrix} v_x & v_y & 0 & 0 & 0 & 0 \end{bmatrix}$ [m/s]
- Current (alt 2) - Constant and affects surge, sway and yaw
  $\tau_c = \begin{bmatrix} X_c & Y_c & 0 & 0 & 0 & N_c \end{bmatrix}$ [N]
- Waves - Periodic affecting roll, pitch, heave and surge.
  $\tau_{waves} = \begin{bmatrix} X_{waves} & 0 & Z_{waves} & K_{waves} & M_{waves} & 0 \end{bmatrix}$ [N]
- Wind - Constant affecting all states but the heave motion
  $\tau_{wind} = \begin{bmatrix} X_{wind} & Y_{wind} & 0 & K_{wind} & M_{wind} & N_{wind} \end{bmatrix}$ [N]

3.5 Environmental Data

This chapter shows data from weather buoys regarding the values of disturbances; periods, velocities and angle of attack.

The SMHI (Swedish Meterological and Hydrological Institute) provides measurements from several locations around Sweden. SMHI collects data from multiple locations. One such buoy, is the VINGABS just outside Gothenburg. Data sampled for three consecutive days has been used to find approximate values for parameters such as wave period, AoA, wave height and ocean current velocity [20].

3.5.1 Wave data

The data for wave angle (in the global frame), height and period are seen in Figs. 16-18. These values do tend to remain constant over periods of time but as the measurements do not show a better resolution (time aspect) it is hard to say whether using models of constant disturbance parameters (AoA, wave period, amplitude) is an adequate model.

If the parameters do not remain constant, or has large variances, it might be hard to continuously estimate and use the estimations for predictions.

These examples do still show suitable values of wave heights from 0 to 4.0 meters and wave periods of 2 seconds to 10 seconds. Note that these values were marked as unverified by SMHI and certain irregular points might be faulty measurements (such as the zero measurement at hour seven). For simulations, the waves have been modeled using only periodic force with a guessed value which was assumed to be accurate enough. Suitable values for the simulations further on is a period in the interval of $0 - 10$ seconds.

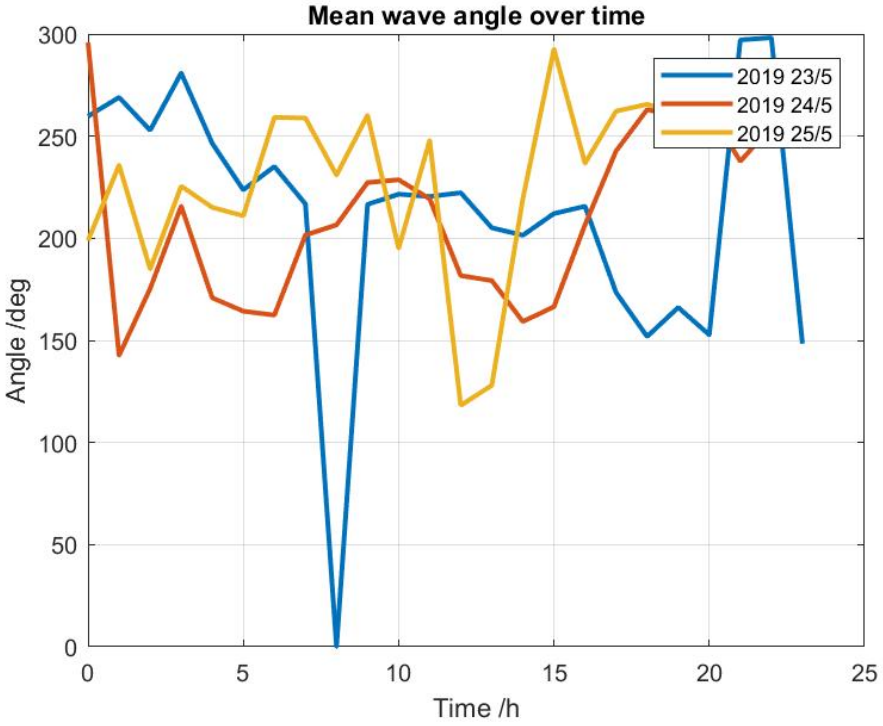

Figure 16: Mean AoA over 30 minutes interval from 3 days [20].

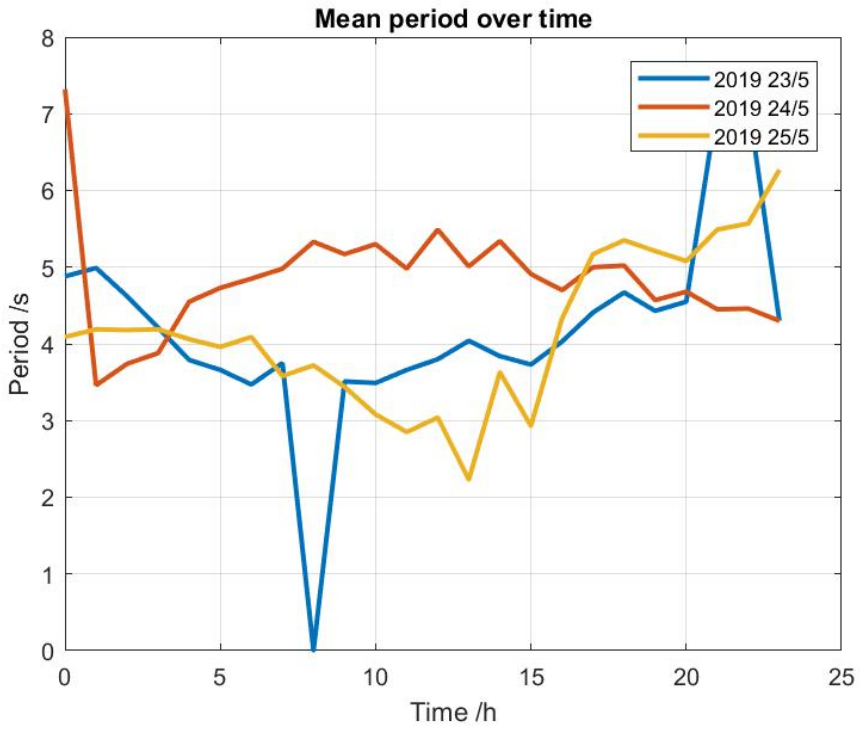

Figure 17: Mean wave period over 30 minutes from 3 days [20].

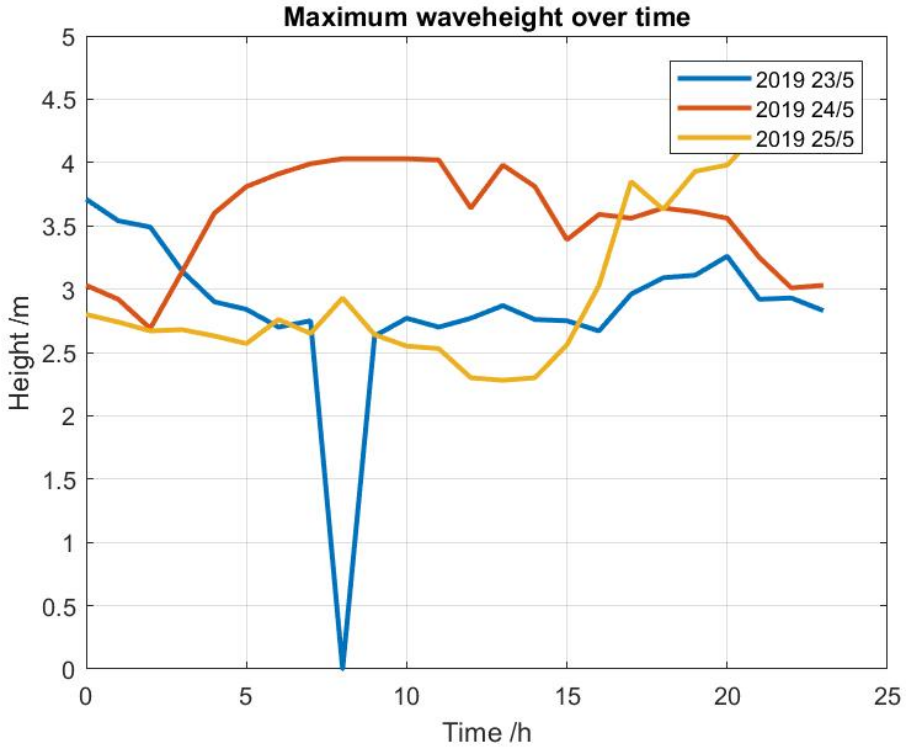

Figure 18: Maximum wave height over three days [20].

3.5.2 Current Data

The current data is seen in Figs. 19-20. The current's impact on the PWC is implemented using relative velocity as described in the current section of modeling. The current's angle does not change greatly over time and neither over sufficiently large areas. Therefore the angle is defined as constant in the global frame and the only parameter which must be selected suitably is the current velocity $v_c = \begin{bmatrix} v_x & v_y & 0 & 0 & 0 & 0 \end{bmatrix}$. The alternative, modelling the current as an input disturbance would also require approximate values of current velocity.

Again, as the values are not updated more than once an hour it is impossible to say anything about how the current changes in between. However the general idea is that current only changes slowly, both in velocity and in angle. The data do suggest velocities in the interval of 0 to 1.0 m/s (0 to 1 knot).

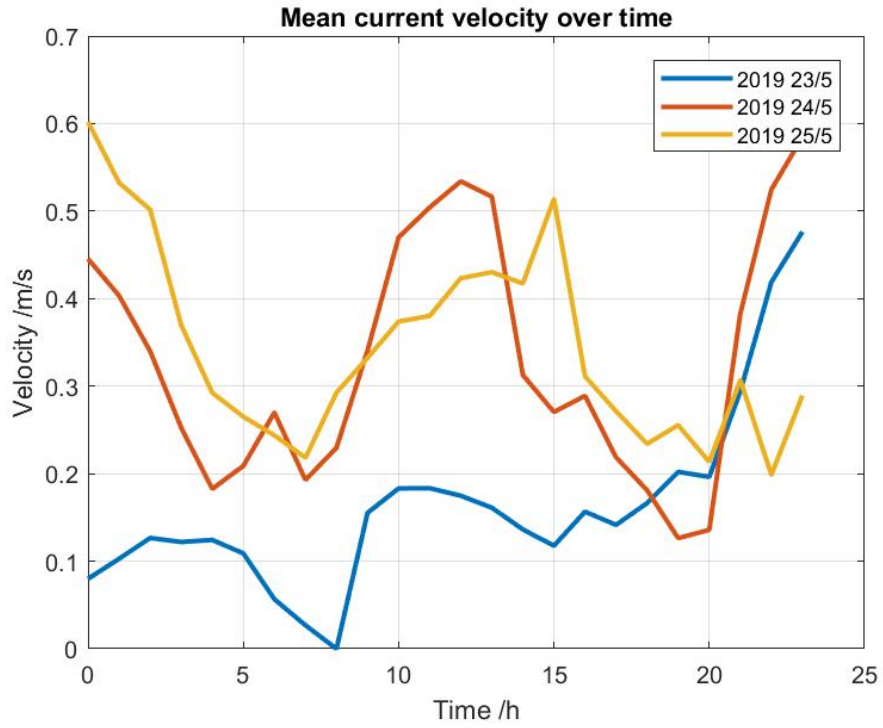

Figure 19: Mean value of the current velocity estimations from the buoy VINGABS [20].

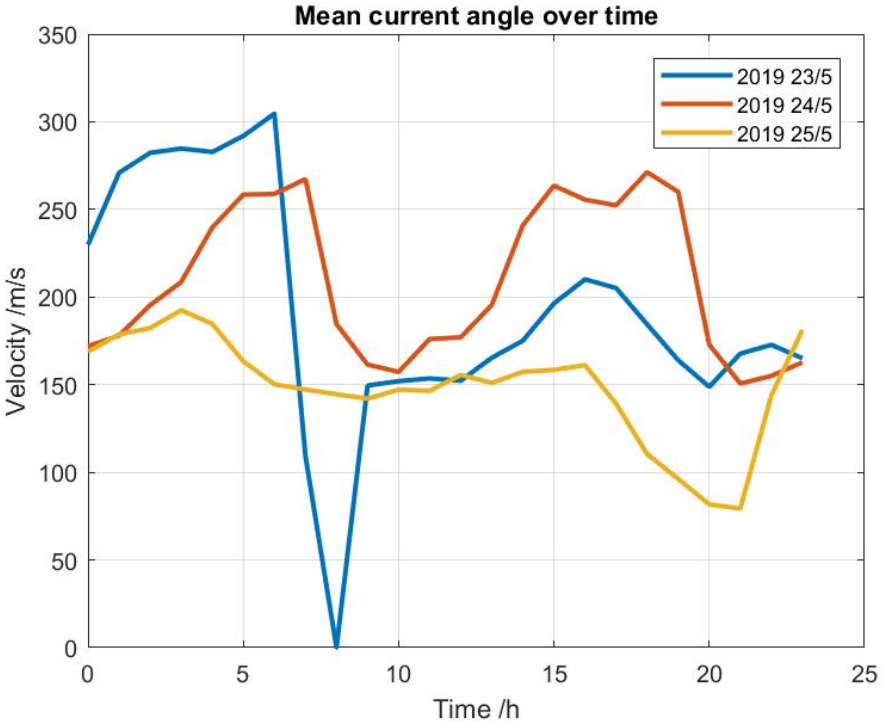

Figure 20: Mean value of the current angle from the buoy VINGABS [20].

4 Control Strategy

4.1 Basic Control Strategy

The basic idea is to follow the lead boat at a certain distance. This is done by the lead boat sending out its coordinates for the PWC to follow.

By setting the velocity reference to a fixed value and using the reference position and current position to find the heading angle, these can then be controlled individually.

In order to achieve the set velocity and heading, PID-controllers for each control problem was used as:

$$u(t) = K_p \cdot \big(e + \frac{1}{T_i}\int_0^t e dt + T_d \frac{de}{dt}\big) = K_p e + K_i \int_0^t e dt + K_d \frac{de}{dt} \tag{82}$$

where e is the respective error e_u or e_ψ. Parameters K_p, K_i and K_d that result in a good response are to be found. The derivative part should have filter to avoid disturbances affecting the controller but in this case the control parameters are calculated without the filter part

The parameters of the heading-controller can be found by placing the poles of the Nomoto model according to [21]:

$$K_p = \frac{\omega_n^2 T}{K} \tag{83}$$

$$K_d = \frac{2\zeta\omega_n T - 1}{K} \tag{84}$$

$$K_i = \frac{\omega_n^3 T}{10K} \tag{85}$$

where ω_n is the natural frequency, ζ is the relative damping. The parameters K and T refers to the static gain and time constant of the Nomoto model. The tunable parameters are now ζ and ω_n. The relative damping ζ is set to 1 as to have no overshoot. The natural frequency w_n is determined by the desired closed loop bandwidth as given by:

$$w_n = \frac{1}{\sqrt{1 - 2\zeta^2 + \sqrt{4\zeta^4 - 4\zeta^2 + 2}}} \cdot \omega_b \tag{86}$$

The control parameters for the surge motion can be found by similar pole placement for the surge motion with a PI-controller, again depending on the desired bandwidth and damping.

$$K_p = \frac{2\zeta\omega_n T - 1}{K} \tag{87}$$

$$K_i = \frac{\omega_n^2 T}{K} \tag{88}$$

Both controllers were designed to operate around 6 m/s (12 knots) using the first order models for surge and heading, which appear to be linear at these velocities.

The damping ζ was set to 1 in both controllers. The bandwidth was harder to choose. A few simulations were performed with bandwidths which did not saturate the input signal. A better solution would be to implement anti-windup

To use pole placement methods, simple linear models are required. The models used to identify the damping coefficient for the heading motion were used to design the heading-controller

$$G_{\text{steeryaw}} = \frac{K_{\text{nom}}}{sT_{\text{nom}} + 1} \cdot \frac{1}{s} \tag{89}$$

As the nonlinear model was matched with the Nomoto models found in [12], this Nomoto Model was also used to base the controller on

Steer	Surge u	K_{nom}	T_{nom}
± 15 deg	2.5 m/s (5 knots)	2	1
± 15 deg	4 m/s (8 knots)	2.33	0.67
± 15 deg	6 m/s (12 knots)	2.4	0.4

Table 4: Nomoto model parameters

To achieve a model for the surge motion, simple step input tests (Fig. 21) were made on the nonlinear model resulting in

$$G_{\text{thrustsurge}} = \frac{K}{sT_{\text{d}} + 1} \tag{90}$$

Throttle	Surge u	K	T_d
11%	2.5 m/s (5 knots)	22.72	1.92
22%	4 m/s (8 knots)	18.18	1.73
32%	6 m/s (12 knots)	18.75	1.7

Table 5: First order surge model

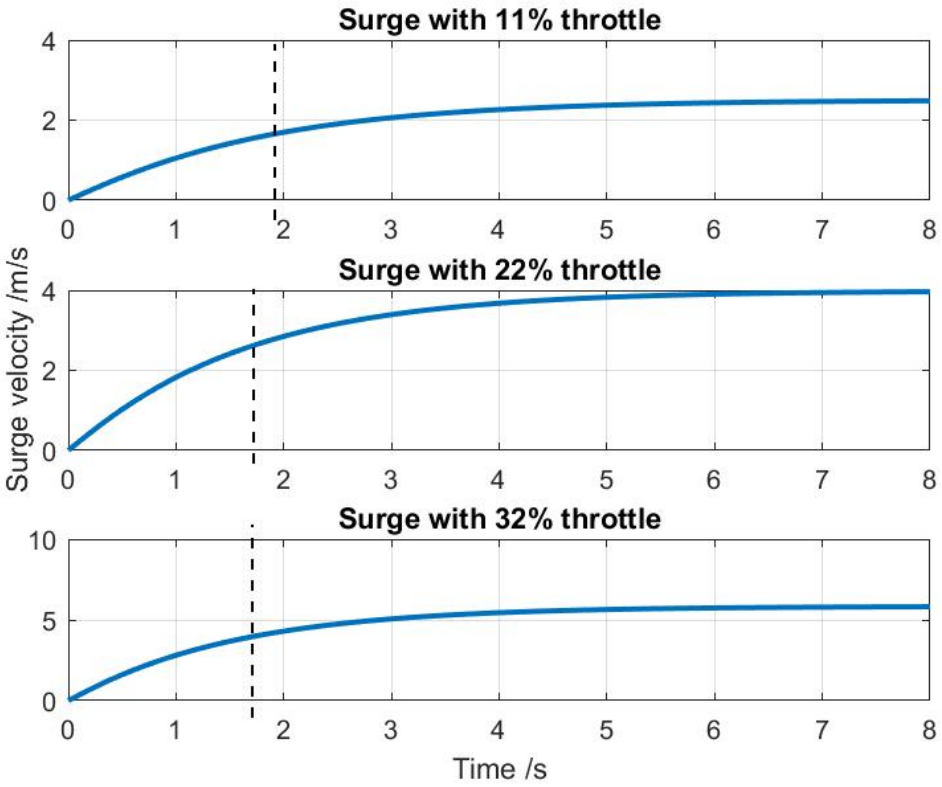

Figure 21: Linear first order model of the surge motion acquired by a step input in the nonlinear model.

The surge-controller was expected to only need to follow step inputs. By choosing a bandwidth which never used more than 50% the throttle seemed sensible.

The parameters of the controllers are found in Table 6. The heading-controller had to be tuned in order to function properly seen in the second row. Both controllers were designed around the surge velocity 6 m/s (12 knots).

K_p	K_i	K_d	ζ	w_b
1.13	3.62	0	1	3
K_p	K_i	K_d	ζ	w_b
3.62	1.68	1.13	1	3
15	0.5	5.0	-	-

Table 6: Controller Parameters Upper = Surge Controller, Middle = Heading Controller, Lower = Heading Controller (tuned)

4.2 Control Strategy for Disturbances

The bulk of this section deals with waves, which is deemed to be the major challenge facing the PWC. As mentioned in Section 3.2, waves are generated by winds and will largely have the same direction as winds. However, waves affect a tiny craft, such as PWC, to a much larger extent than winds. For that reason, the impact of winds are neglected going forward and control strategies will be devised for waves specifically.

Ocean currents will be treated as a drift, which is dealt with by the integrator in the controllers mentioned above. Ocean currents are assumed to be constant or at most varying slowly and lightly, both in magnitude and direction. It is also assumed that the wind- and thus wave-direction is constant in the inertial frame. These assumptions are based on the fact that a PWC involved in a rescue operation operates in a small local area for a short period of time (at most hours). According to the plots in Section 3.5, no major changes to the disturbances occurs in such a short period of time.

4.2.1 Challenges

One of the most significant challenges to keeping the autonomous PWC stable is the lack of a human aboard. A human aboard adds more weight to the very light craft, which means it would not be "thrown around" by the waves to the same extent. More crucially, a human aboard can use his body-movement to counteract forces that would push the craft off-balance. For example, if a wave hits from the side causing roll-motion to one side, shifting the body-weight to the other side can counter that motion in order to stabilize and prevent the craft from capsizing.

Since the role of a human as stabilizer is not replaced, certain precautions are taken:

- It is imperative that any clash between craft and wave occur head-on, since the craft is far more vulnerable to capsizing in rolling than pitching.
- Since the craft is meeting the wave head-on and since the weight of the human is gone, the craft should slow down as a precaution to prevent it from slamming into the wave too violently.

The waves will likely cause movements in heave (jumping) and nose-diving which lifts the stern, leaving the nozzle of the jet exposed to air. A problem this creates is that the output from the speed-controller suddenly does not create a thrust, i.e., there is no acceleration. While in the air, the error fed into the controller will not decline, resulting in a growing output from the integrator (Fig. 22).

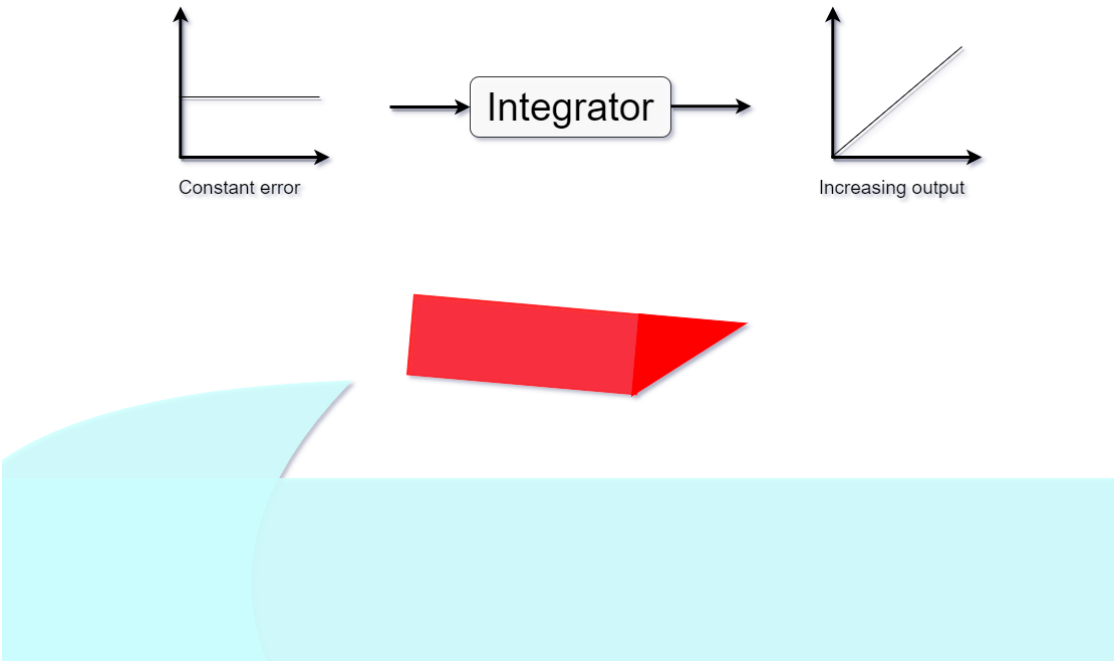

Figure 22: The controller whilst the craft is in the air.

The implication is that the PWC will have a larger than desired thrust when the stern (and nozzle) lands on water again, causing it to slam into the next wave with a potentially huge velocity. This project will not delve into this issue deeper and leaves it to future works.

4.2.2 Control Approach For Waves

The initial approach for dealing with waves was finding ways to stabilize the PWC by minimizing the oscillations, particularly in roll where it is most vulnerable to capsizing. A 6 DoF model of the PWC and a wave-model were deemed necessary to derive strategies that achieves that goal. Whilst the wave-model developed in Section 3.3 can still be useful in terms of determining if the PWC can be maneuvered fast enough to meet it in a certain way (for example head-on), it became clear after studying footage in rough waters that the control-strategies devised from the model would not be viable in real-life applications.

As mentioned in Section 3.2, the sea-state contains a spectrum of waves. This is not captured in our simplified disturbance model (Section 3.3), which only contains an ideal wave with a certain period and amplitude. Whilst this works for a larger watercraft that barely feels the smaller waves and is at the same time more robust when hit by larger waves, the situation is different for something as tiny as a PWC. Although the sea-state can be described by the significant wave amplitude H_s (mean height of the one third largest waves) [16], a lot of waves can still be be significantly larger or smaller than that. This creates the difficult situation in which a controller is adjusted for a certain wave-height and period, only to be randomly hit by a larger wave with a different period. Since it is not possible to

build a controller that accounts for all this irregularity uncertainty in the sea-state, the approach taken here is finding guidelines/behaviour/paths that minimizes the risk of capsizing whilst at the same time inching towards the desired position. These are largely based on the actions that an experienced PWC-driver would take. Even then, a PWC at its current design and size will still be vulnerable, but the idea is that these strategies provide a simple and viable chance for it to move towards its desired position without capsizing.

In this project, it is assumed that the craft will operate in one of these three conditions:

- **Calm waters**, i.e., little to no waves and disturbances.

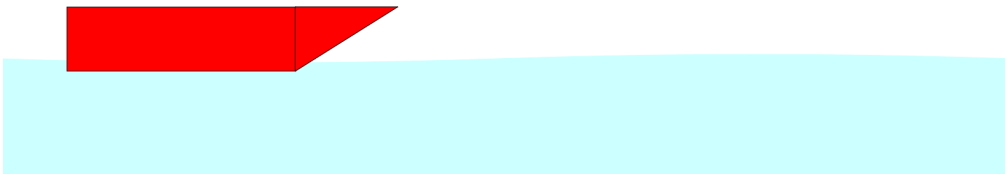

Figure 23: Calm waters, in which the craft maneuvers with ease. View from the side.

- **Choppy waters**, i.e., smaller waves/disturbances from random directions with a mean wave amplitude of 0-0.6 m that can still contribute to significant instability [22].

Figure 24: Choppy waters which can cause significant jolts. View from the side.

- **Rough waters**, i.e., with large waves with a mean wave amplitude above 0.9 m [22]. Vastly different and more difficult than the earlier two conditions.

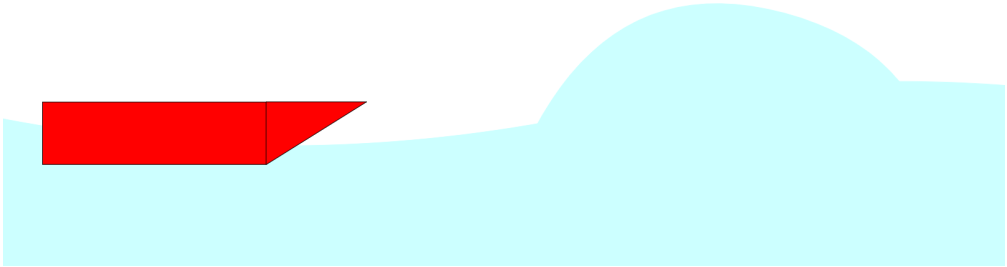

Figure 25: Rough waters, which can cause major instability. View from the side.

Two kind of approaches are taken:

1. For ***calm or choppy waters***, the PWC drives is situated in the wake of the lead boat (Fig. 26).
2. For ***rough waters***, a set of actions are taken depending on the encounter angle, as will be detailed in the upcoming section.

In the first approach, the craft is kept in the wake since the water there is smoother and disturbances are attenuated.

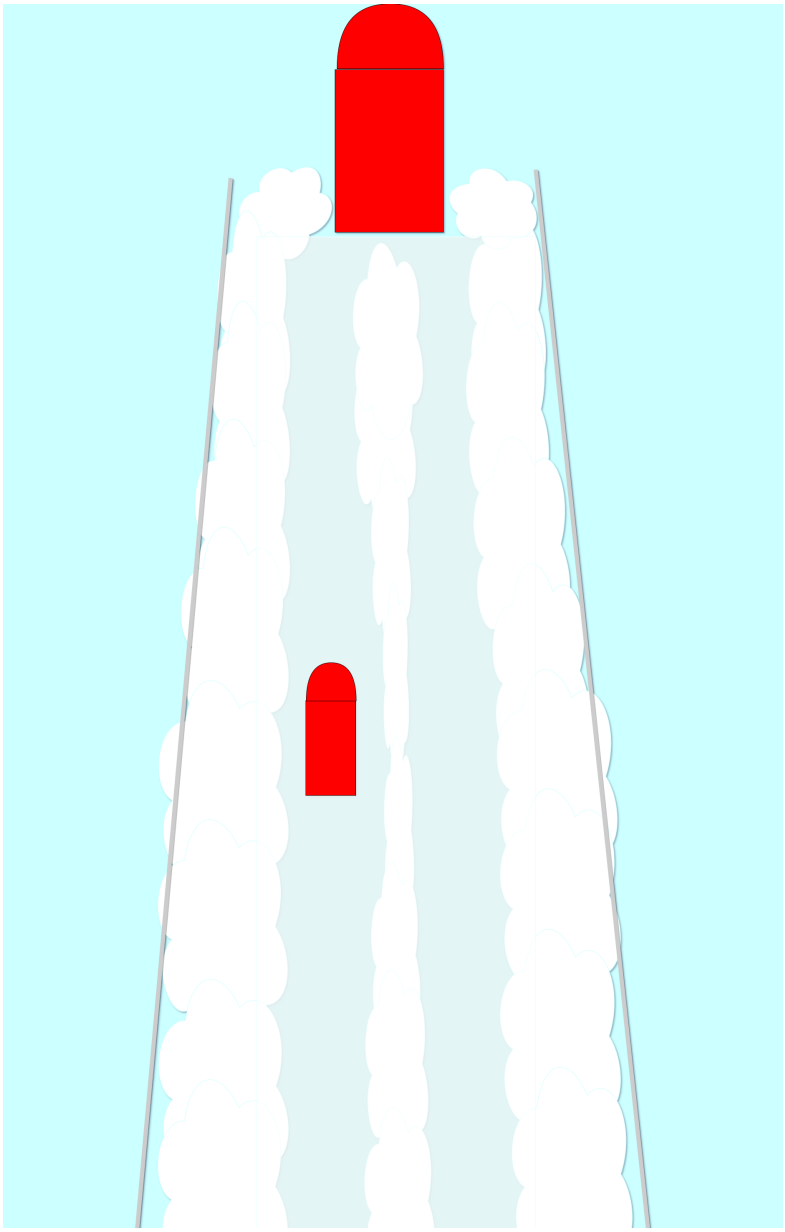

Figure 26: The RescueRunner is placed in the wake created by the lead boat.

Ideally, the PWC should make sure to stay behind the advancing waves (utmost wave lines in Fig. 26) associated with the wake. Crossing them in high speed

could cause a significant jump. It is also well advised to stay clear from the wash created by the jet, which is turbulent close to its source (nozzle).

For the second approach (rough waters), the nature of the challenge depend on the direction of the wave relative to the heading of the craft, i.e., AoA. The encounter angle can be grouped, according to [23], as:

- $0 \leq \gamma < 15$ Following Sea
- $15 \leq \gamma < 75$ Quartering Sea
- $75 \leq \gamma < 120$ Beam Sea
- $120 \leq \gamma < 150$ Bow Sea
- $150 \leq \gamma < 160$ Head Sea

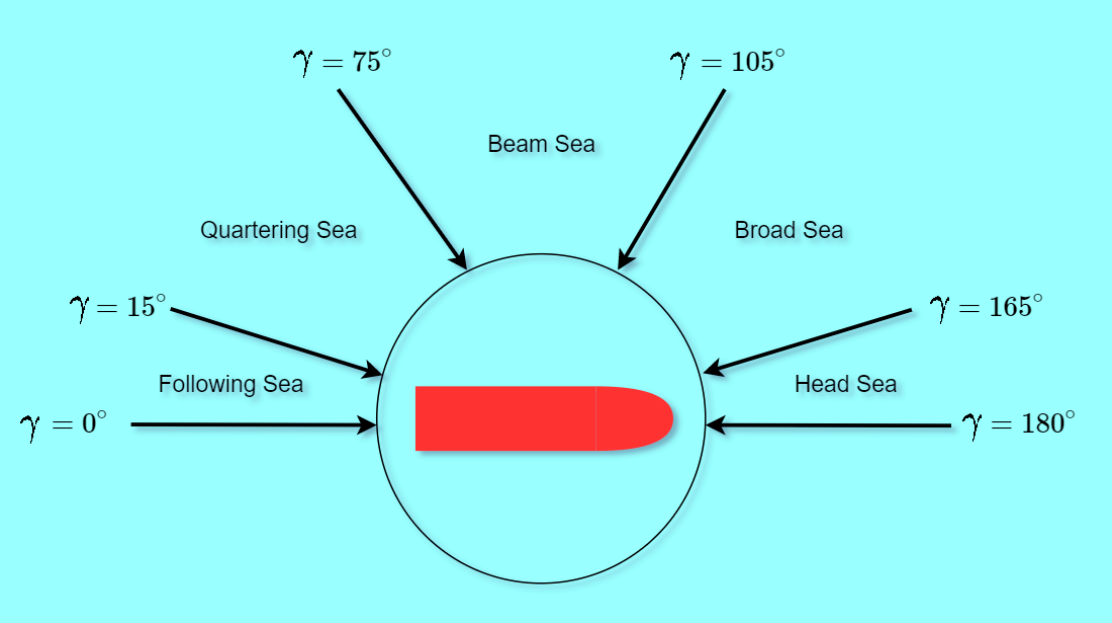

Figure 27: Sea definitions. The same applies symmetrically for the opposite side of the PWC.

The control-strategy for each five of these cases will be detailed in the upcoming sections.

4.2.3 Head Sea

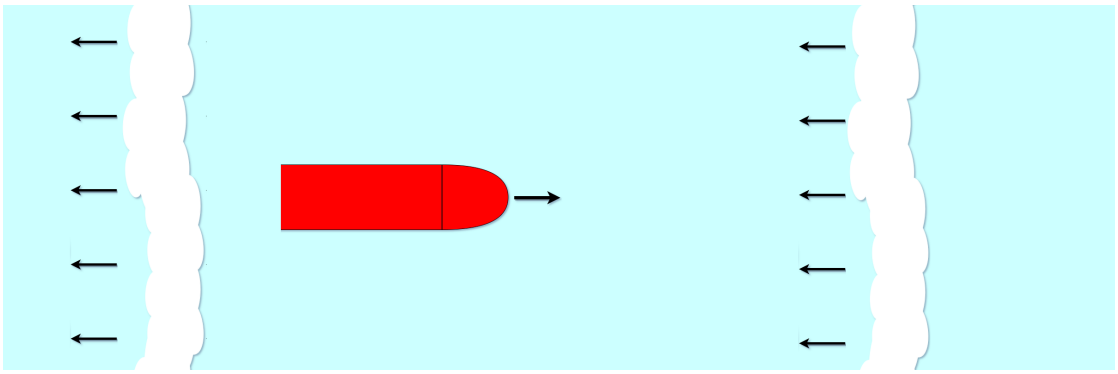

Figure 28: The waves hit the craft head on. View from above.

Due to the geometry of the craft – which is more susceptible to capsizing in roll than pitch – and due to the lack of human input, our highest priority should be to meet the waves head on.

When meeting a wave head-on, the craft should drive slowly and accelerate in between the waves, i.e., as soon it lands on water and before it hits the next wave. This is done in order to avoid a powerful slam between the craft and wave that could result in a big pitch disturbance (raised bow), which could cause the craft to capsize.

Since this is a situation where the craft and waves are moving towards each other, the encounter frequency will be substantial (i.e., low encounter period). The craft thus has very limited time to accelerate, since it meets the waves in rapid succession. Thrust will thus be exerted as a short pulse in every period.

4.2.4 Following Sea

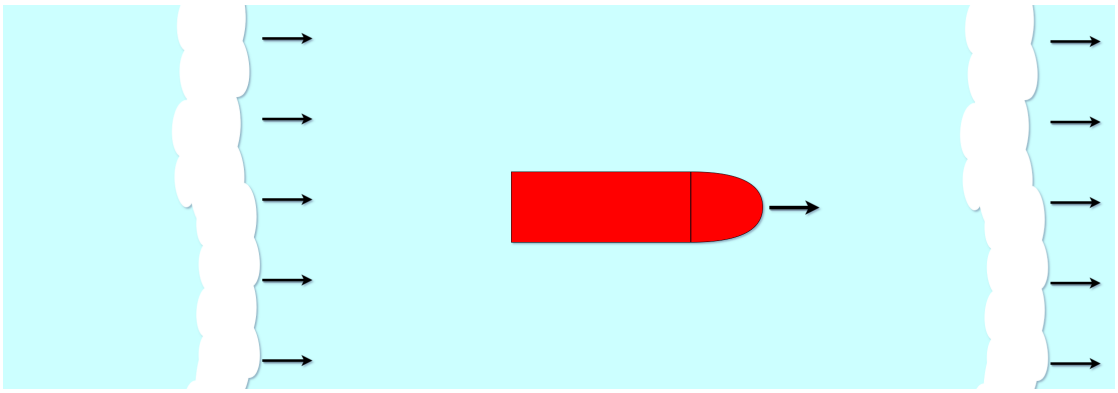

Figure 29: The craft is moving along with the waves.

When the wave moves in the same direction as the craft, three approaches can be taken:

1. If the craft drives with a higher speed than the waves, eventually it will catch the wave crest in front of it.
2. If the craft drives with a slower speed than wave, the wave crest behind will catch up and hit the craft from behind.
3. The craft never crosses a wave, i.e., a relative speed of roughly 0, and should position itself slightly behind the wave at all times.

The first case presents significant dangers. As the craft passes the wave crest, it will experience a steep drop in a manner which causes the bow to nose-dive right into the backside of the next wave, resulting in a loss of control. As the bow is down, the following wave tends to push the elevated stern sideways, leaving the craft vulnerable to capsizing [24, 25].

The second case represents a similar form of risk. The following wave will lift the and consequently sink the bow. As the bow digs in into the water, the wave force from behind will push the stern sideways, once again leaving the craft vulnerable to capsizing [26].

The safest approach in following seas is to ride on the back of a wave, i.e., the third case [25]. To maintain the position, the velocity of the craft must match the velocity of the wave, see Eq. (71)

$$0 = \omega_0 - \frac{\omega_0^2}{g} U \cos 0 \quad \Rightarrow \quad U = \frac{g}{\omega_0} \tag{91}$$

4.2.5 Beam Sea

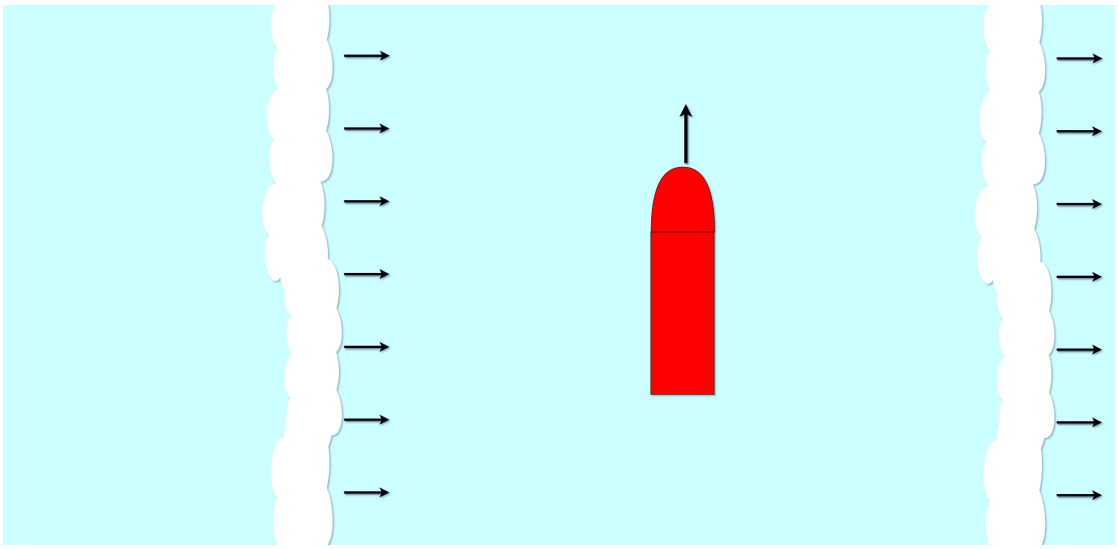

Figure 30: Waves from the side hitting the craft on its beam.

By far the most dangerous situation for the PWC is waves slamming straight on the beam, since it is far more susceptible to rolling than pitching. For larger boats,

waves on beams are not as dangerous and a zig-zig maneuver – where the waves are met at a 45 degrees angle – usually gets the job done safely. This is not the case with something as small (and unmanned) as a PWC and it is crucial to meet the waves head-on. Three options to this problem are being considered:

1. Turn towards the waves and hit them head-on.

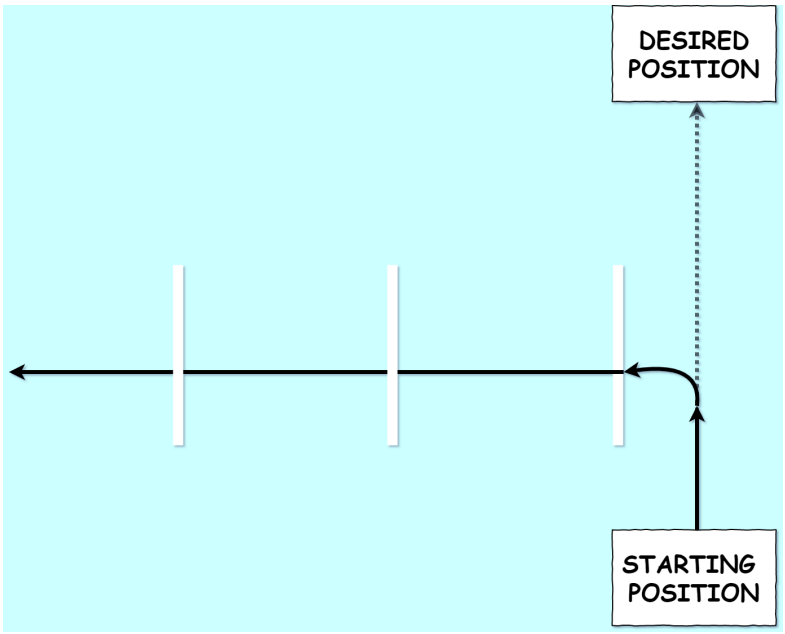

Figure 31: Seen from above. The craft turns towards the waves and drives head-on indefinitely.

2. Drive towards the desired position and only turn towards the wave when they are about to hit (Fig. 32).

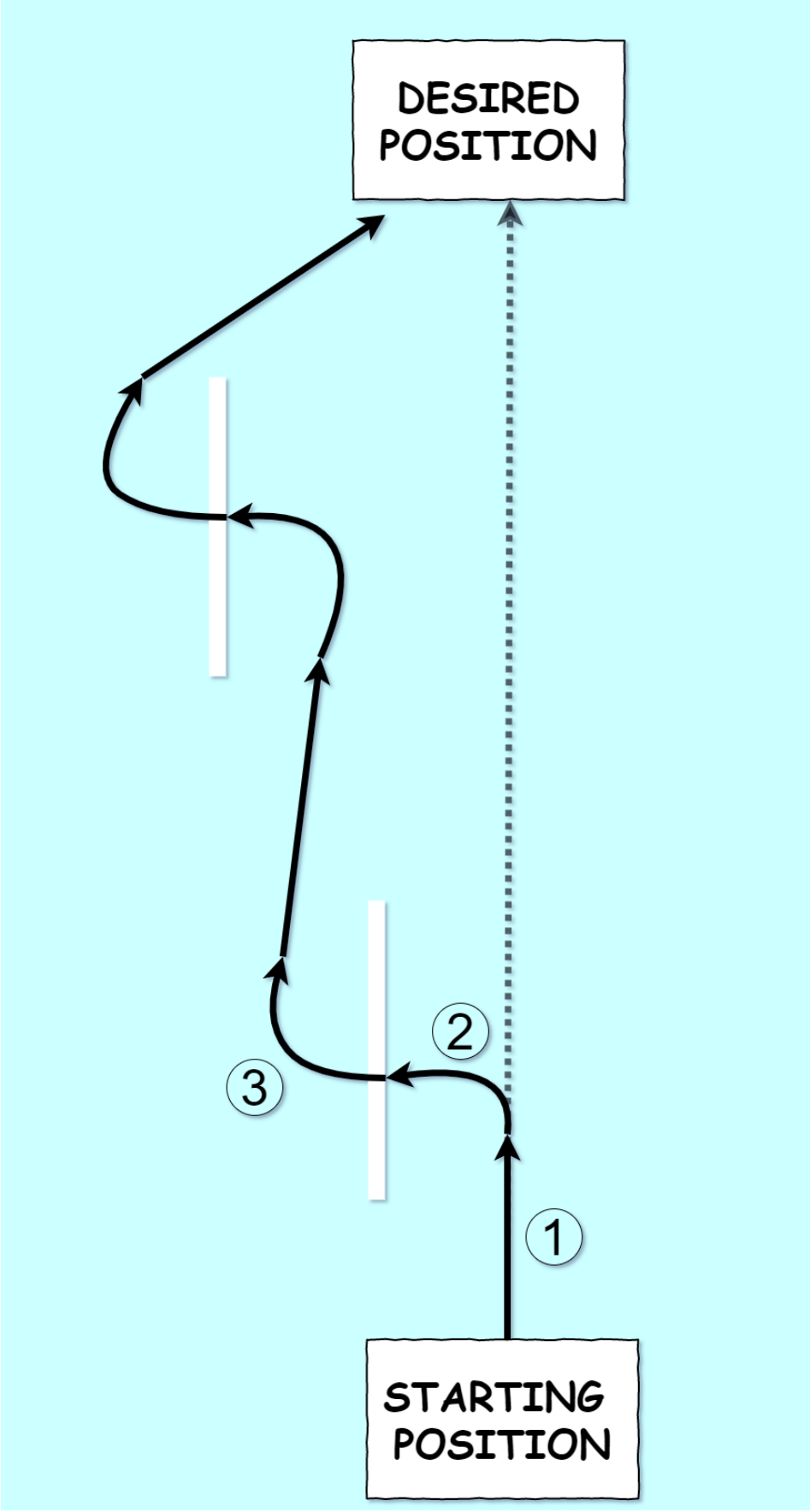

Figure 32: The craft turns towards the waves just when they are about to hit.

3. Drive in between two waves with a direction and velocity such that the craft never interact with the wave. The horizontal component of the craft's velocity V_{craft} should be equal to the wave velocity V_{wave}.

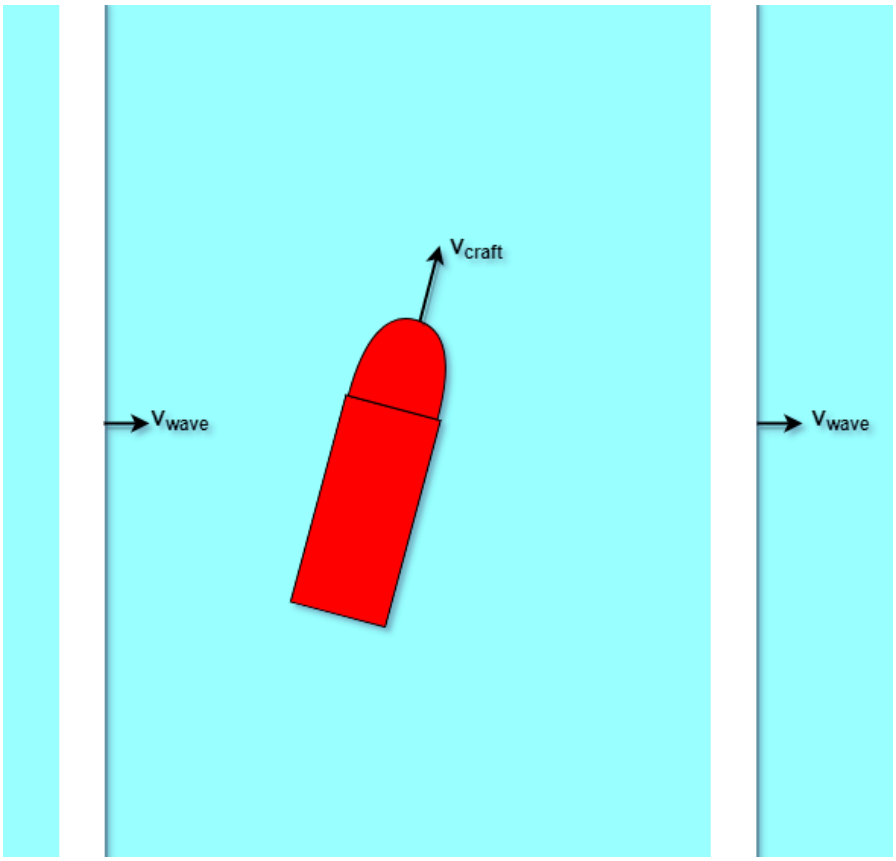

Figure 33: The craft drives in between waves with a direction and velocity such that it never hits the waves.

The issue with the first option, as seen in Fig. 31, is that the craft will drive away perpendicularly from its intended straight path and will thus never reach its desired position. This is thus an option that should only be used in emergency situations when it is simply a matter of trying to keep the craft afloat.

The idea behind the second option is that the craft deals with the waves without drifting off too much from its intended path. The viability of this option hinges on whether the craft is capable of turning fast enough. This will obviously also depend on how broadly spaced the waves are, i.e., it might be fast enough for longer waves since it will have more time to turn. The following steps are taken each loop:

1. Drive towards the desired position.
2. Turn towards the wave when they are about to hit.
3. After hitting the wave, turn towards the desired position.

A change that can be made to this option is to turn away from the wave (i.e., following sea) instead of towards it (head-on). That would give the PWC significantly more time to make the turn without hitting the wave, since it will be running away from it. The main drawback with this is that the waves will be hitting the craft from behind which, as mentioned above, can be significantly more risky than meeting it head-on [24]. Additionally, the drift from the intended path would be much larger since the encounter frequency is lower.

The third option is achieved by adjusting the velocity and the AoA (with the waves) such that the encounter frequency in Eq. (71) is as close to zero as possible. If the craft for instance has a fixed forward speed U, the AoA it needs is:

$$\omega_e = \left| \omega_0 - \frac{\omega_0^2}{g} U \cos\gamma \right| = 0 \quad \Rightarrow \quad \gamma = \arccos \frac{g}{\omega_0 U} \tag{92}$$

The faster the PWC moves, the smaller the AoA has to be which minimizes the drift. That the craft can travel at higher velocities is one of the main advantages of this option [26]. Moving at high speed also introduces risks, since even the slightest steering-error can cause a clash with the wave.

4.2.6 Quartering Sea

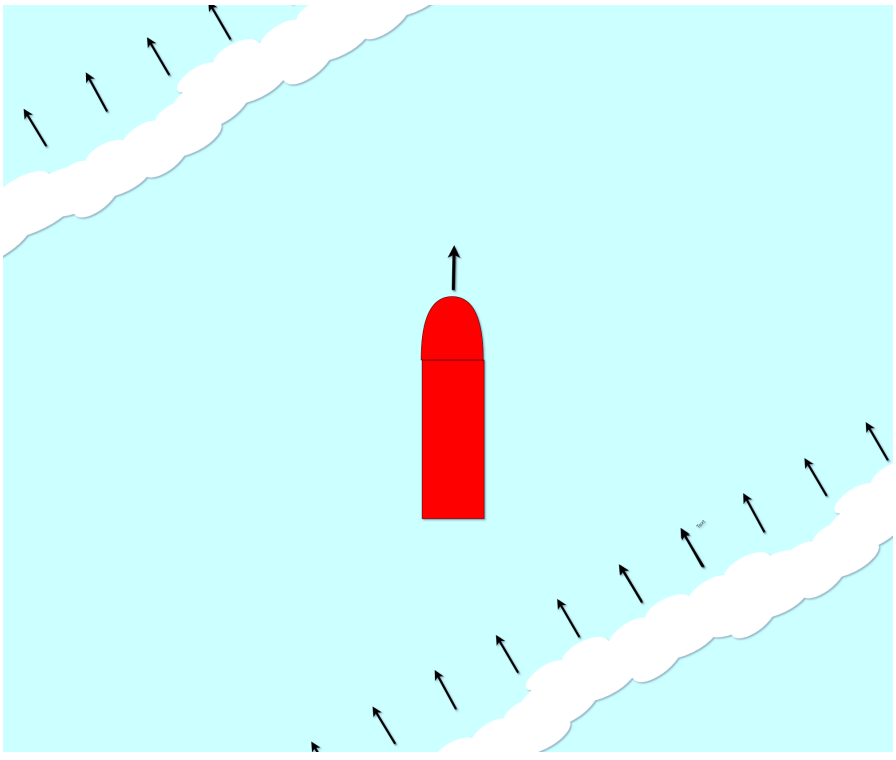

Figure 34: The waves hits the craft at an angle from behind.

This situation is analogous to following seas and should be treated in the same manner, i.e., staying in between two waves. Since the waves are angled (non-zero

AoA), the $\cos\gamma$ term in Eq. (71) will be less than unity and result in a larger velocity:

$$0 = \omega_0 - \frac{\omega_0^2}{g} U \cos\gamma \quad \Rightarrow \quad U = \frac{g}{\omega_0 \cos\gamma} \tag{93}$$

The PWC is thus able to drive faster towards its desired position without crossing waves than in the case of following sea.

4.2.7 Broad Sea

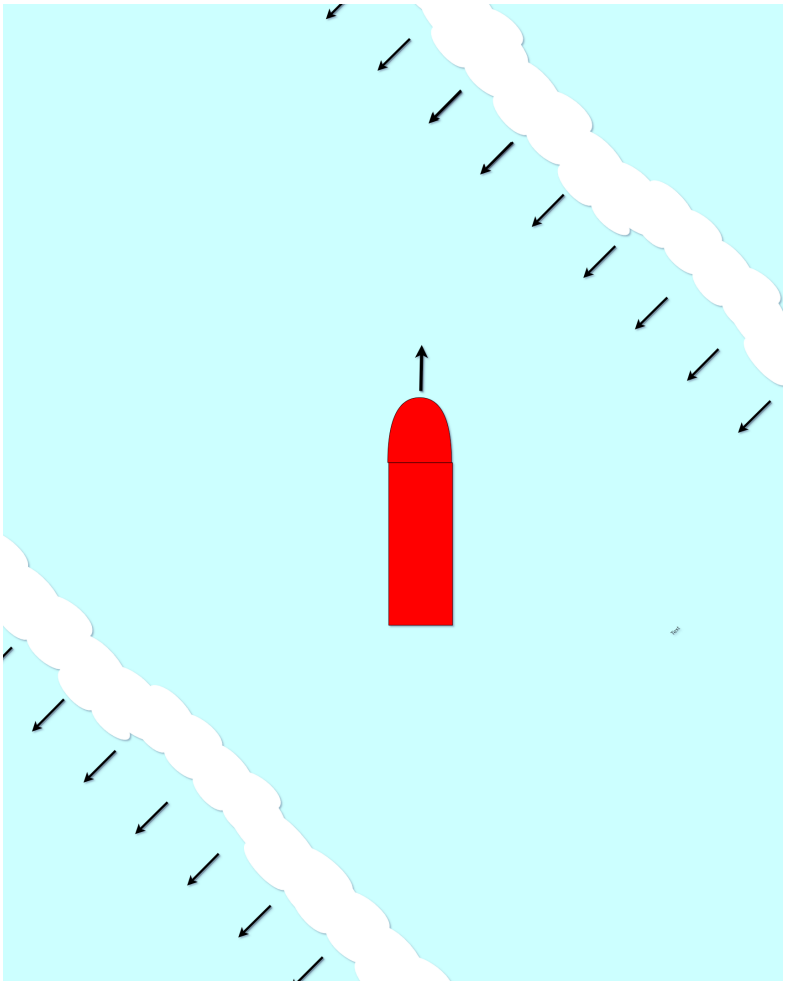

Figure 35: Viewed from above. The waves hit the craft at an angle head on.

This is a combination of head sea and beam sea. Since the PWC is most susceptible to capsizing in its roll-angle, the craft should prioritize meeting the waves head on. There are two main options:

1. Turn and meet the waves head-on. Eventually it will have to account for the drift away from the intended path.

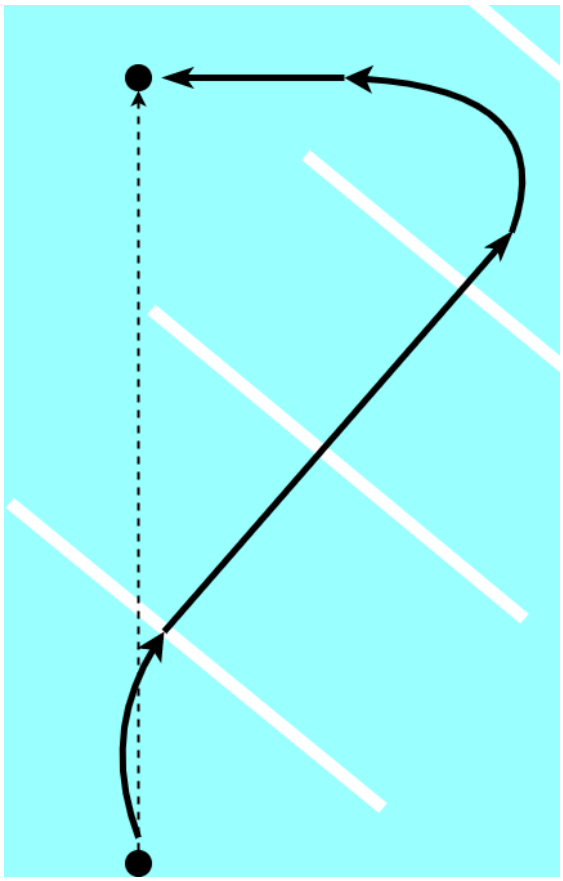

Figure 36: The path in option 1. The PWC turns and meets the waves head on, but it drifts away from its intended path and compensates for that in order to reach its desired endpoint.

2. Drive straight towards the desired position and turn towards the waves only when they are about to hit, similar to the second option in Fig. 36, except the turn is less than 90°.

There are two main phases in option one. When the PWC has turned towards the waves, it will experience head sea and should be controlled as mentioned in the head sea section. When it has drifted away too much, it suddenly experiences quartering sea.

The viability of the second option hinges on the encounter frequency. If the frequency is too large, the PWC might not be fast enough to turn towards the wave.

5 Implementation

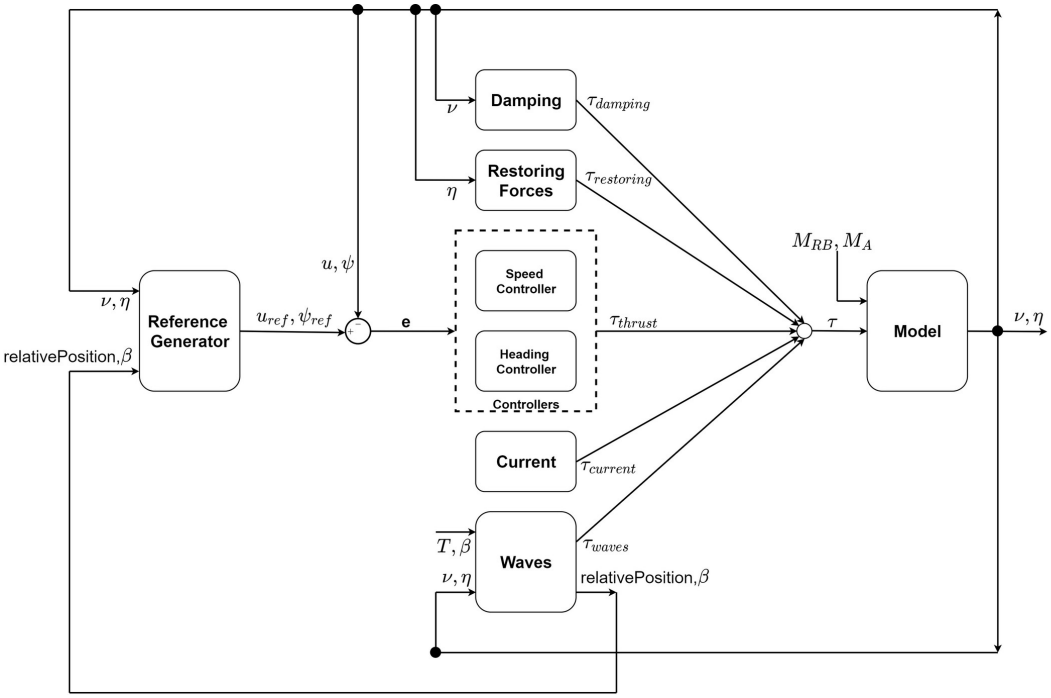

Figure 37: Schematic of the implementation in Simulink

Before running simulations, an overview of how the simulation is implemented is given. The system was implemented in Simulink and the schematics of how it was built can be seen in Fig. 37, which contains:

- **Reference Generator** to the left, which sends reference values to the controller.
- **Controllers** in the center, which sends out a thrust corresponds to the reference values.
- **Model** to the right, which contains the dynamics of the PWC.
- **Hydrostatic and hydrodynamic-forces** above, like restoring forces and damping.
- **Disturbances** below, such as current and waves.

Since the program will only be tested on simulation, the stream of data (coordinates and velocity) that would have come from lead boat is replaced with predefined waypoints and a constant speed of 5 m/s (10 knots). The reason 5 m/s is chosen is because we could not extract damping parameters above that speed.

5.1 Model

This block contains the kinetics and kinematics of the PWC. As mentioned in the modelling chapter, the implementation of the PWC model is largely done with a

already implemented block diagram that was provided by the *MSS Toolbox* [13] that is based on Eq. (94):

$$(M_{RB} + M_A)\dot{\nu} + (C_{RB}(\nu) + C_A(\nu))\nu = \tau \tag{94}$$

where τ contains all forces. Since the Coriolis-centripetal matricies C_{RB} and C_A are derived from the inertia matricies, only M_{RB} and M_A have to be fed into the diagram from the left hand side of Eq. (94). A modification is made to the term:

$$C_A(\nu)\nu = \begin{bmatrix} -qZ_{\dot{w}}w + rY_{\dot{v}}v \\ pZ_{\dot{w}}w - rX_{\dot{u}}u \\ -pY_{\dot{v}}v + qX_{\dot{u}}u \\ vw(Y_{\dot{v}} - Z_{\dot{w}}) + qr(M_{\dot{q}} - N_{\dot{r}}) \\ uw(Z_{\dot{w}} - X_{\dot{u}}) + pr(N_{\dot{r}} - K_{\dot{p}}) \\ uv(X_{\dot{u}} - Y_{\dot{v}}) + pq(K_{\dot{p}} - M_{\dot{q}}) \end{bmatrix} \tag{95}$$

In the last row which corresponds to the yaw moment, the term $uv(X_{\dot{u}} - Y_{\dot{v}})$ is known as the **Munk moment** and can be very destabilizing [27]. In a perfect non-linear model, there would be drag and damping terms that counteracts it [28]. But due to all the simplifications and assumptions that were made, it will overwhelm all the other yaw terms. The Munk moment will therefore be omitted from Eq. (95) going forward.

On the right hand side of the equation, τ encompasses the following forces and disturbances:

- Force from the propulsion engine τ_{thrust},
- Damping forces τ_{damping},
- Restoring forces $\tau_{\text{restoring}}$,
- Forces from waves τ_{waves},
- Forces from currents τ_{current}.

These are all summed before sent into the subsystem, as seen from Fig. 37. The Model block calculates and outputs the velocity vector ν and the position vector η.

5.2 Reference Generator

This block is responsible for sending out speed and heading references to their respective controller.

As mentioned earlier, in calm or choppy waters the PWC should stay in the wake of the lead boat. For the sake of simplification, this will only mean that the PWC drives straight behind the lead boat. The PWC should not be closer than 20 m away from the leadboat in order to minimize the risk of collision, but also for the

sake of not being too close to the destabilizing jet stream from the lead boat. The PWC should also not be further than 50 m from the lead boat, as the affect of the wake gradually diminishes. This is something to take into consideration and studied more carefully when implementing it for a real system with a lead boat. In this case, only simulations with pre-defined waypoints will take place. The heading reference is obtained through:

$$\psi_{ref} = \text{atan2}(y_{\text{wp}} - y, x_{\text{wp}} - x) \tag{96}$$

where (x_{wp}, y_{wp}) is the coordinates of the waypoint and (x,y) the position of PWC. And as mentioned earlier, the speed reference is constants at $u_{ref} = 5$ m/s (10 knots). Each waypoint has a radius of 5 m associated with it, such that the waypoint has been reached when:

$$\sqrt{(y_{\text{wp}} - y)^2 + (x_{\text{wp}} - x)^2} < 5 \text{ m} \tag{97}$$

The Reference Generator proceeds by turning its attention on the next waypoint.

In rough waters, the Reference Generator is more advanced. The references sent out corresponds to the chosen algorithm given for each of the five sea conditions given in Section 4.2.2. In addition to the earlier mentioned inputs, it is also fed the wave direction. This controller has five modes, one for each sea-condition given in Fig. 27. Depending on mode (or sea-state), the heading references are calculated in a manner that corresponds to the control strategies for each condition. To figure out which sea-condition the PWC is dealing with and how to react, the following steps are taken:

1. Obtain the direction of the wave β and as well as the heading ψ_{SL} of a straight line from the current position of the PWC to the waypoint, see Eq. (96).
2. Obtain the AoA of that straight line through $\gamma_{\text{SL}} = \beta - \psi_{SL}$ and feed it into the function *CheckMode*, which determines what sea-condition that corresponds to according to the angles given in Fig. 27.
3. When the desired waypoint is reached, repeat the same steps for the next waypoint.

When deciding how to calculate the references for that specific sea-condition, knowing position of the PWC relative to the waves is critical. That is why *relativePosition* from the wave-block is fed into the Reference Generator, as seen from Fig. 37. Thus, it will be able to determine what reference-values should be sent at what time. For instance, if the PWC is dealing with head sea, the Reference Generator wants to only accelerate (i.e. $u_{ref} > 0$) when the PWC is in between the waves (i.e., $relativePosition = 0.5$).

5.3 Controllers

There exists two controller, one for the speed of the PWC and one for the heading and their respective parameters where obtained in Section 5.1. The speed error $e_{speed} = (u_{ref} - u)$ is fed into the speed-controller and the heading-error $e_{heading} = (\psi_{ref} - \psi)$ into the heading-controller. Whilst the speed-controller has no problems interpreting its error e_{speed}, the heading-controller can have more difficulties with its own error $e_{heading}$.

When ψ_{ref} is calculated in Eq. (96), it returns an angle in the interval $[\pm\pi]$. It will thus have a jump discontinuity point, which results in difficulties for the controller in deciding the "shortest route" (or smallest angle) to reach the reference heading if the shortest route passes over this point.

This problem shares its solution with the current estimate of heading-angle. If multiple laps have been performed, the estimated heading-angle will be outside of the interval. These two problems can both on their own, or together create situations where the craft will have to turn the wrong way and literally unwind itself.

To keep the angle estimate in the right interval for fair comparison and error calculation, the following modulation is used:

$$\text{angle} = \text{mod}(\text{angle} + \pi, 2\pi) - \pi \tag{98}$$

This angle conversion should also be used on the control error to avoid the controller making an unnecessary turning motion to reach its destination.

As an example, imagine having the heading angle 0°. Then the reference changes to 135° which initiates a right turn. The next change is to -135°. The error becomes -270° which which means a turn in the opposite direction despite the fact that its obviously closer to make the 90° turn and keep the same turning direction. By applying the modulation on the error, the angle value gets the magnitude (in this case 90°) but also the proper sign (corresponding to turning direction).

To illustrate the problem, look at Table 7 and Fig. 38. The first set of rows shows the example in the figure while the two other shows the opposite problem as well as one scenario with no problem. These are only the initial values. As soon as the angles pass the jump point, the modulation makes no difference as seen in the third set of rows

Step	Heading(°)	Reference (°)	error(°)	Direction	mod (°)	Direction
1	0	135	135	Right	135	Right
2	135	-135	-270	Left	90	Right
1	0	-135	-135	Left	-135	Left
2	-135	+135	270	Right	-90	Left
1	0	+35	+35	Right	+35	Right
2	+35	+135	+100	Right	+100	Right

Table 7: Heading angle problem measured in degrees (°) for simplicity

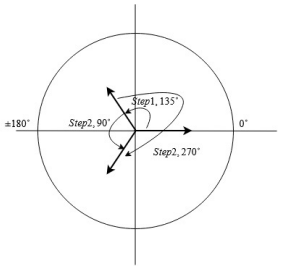

Figure 38: Heading angle problem

5.4 Forces And Disturbances

5.4.1 Hydrostatic And Hydrodynamic Forces

The implementation of damping and restoring forces given in Section 2.7 are straight forward and is only a matter of setting up the vectors as given earlier.

5.4.2 Currents

As mentioned in Section 3.4 , the currents will be implemented as a regular input disturbance. Knowing the direction relative to the PWC that the currents are acting on i.e., AoA, is critical to determine the how magnitude of the force and moment components in τ_c. The first step is therefore to calculate the AoA γ_c for a given current-direction ζ and PWC-heading ψ.

The scaling factors in Eq. (81) are only given for the range $[0, \pi]$. Thus, the AoA γ_c is converted from $[-\infty, \infty]$ to $[-\pi, \pi]$. In addition, if γ_c is in the range of $[-\pi, 0)$, the vector components in Eq. (78) are multiplied with -1. Calculation of the sway force Y is seen in Fig. 39.

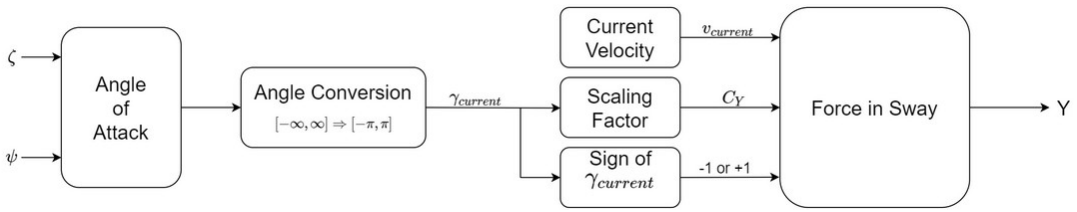

Figure 39: Calculation of the force in sway due to current.

5.4.3 Waves

A wave-period T and direction β is inserted into the wave-block, as well as the surge u and heading ψ of the PWC. The AoA $\gamma = \beta - \psi$ is calculated immediately. The AOA γ, surge u and wave-period T are inserted into Eq. (71) to derive the encounter period T_e. If T_e has changed more than 1% the earlier encounter period, the parameters t_c and r_c in Eq. (73) are updated.

An if-condition is available that outputs constant wave-forces only when the relative position r is between 0 and 1/10.

The wave-forces vary with the amplitude of the waves as well as the relative velocity between the PWC and wave. For the sake of simplicity, the wave-forces are assumed to be purely vertical and are given the constant value $V = 5000$ N. The levers to these are set to $l = 0.5$m. Depending on the AoA, γ, the output sent out will be:

$$\tau_{waves} = \begin{bmatrix} 0 \\ 0 \\ V \\ Vl\cos(\gamma - \pi) \\ Vl\sin(\gamma - \pi) \\ 0 \end{bmatrix} \tag{99}$$

The term $-\pi$ is added to ensure that if the waves are hitting the PWC from the front (i.e., $\gamma = \pi$), the response would be a positive pitch moment. The same applies for roll.

6 Simulations

This section contains simulations of our model and controllers in scenarios with and without disturbances.

6.1 Surge Controller

The surge PI-controller performed feasibly, without saturating the input. This means that faster acceleration is available, but was kept low as intended.

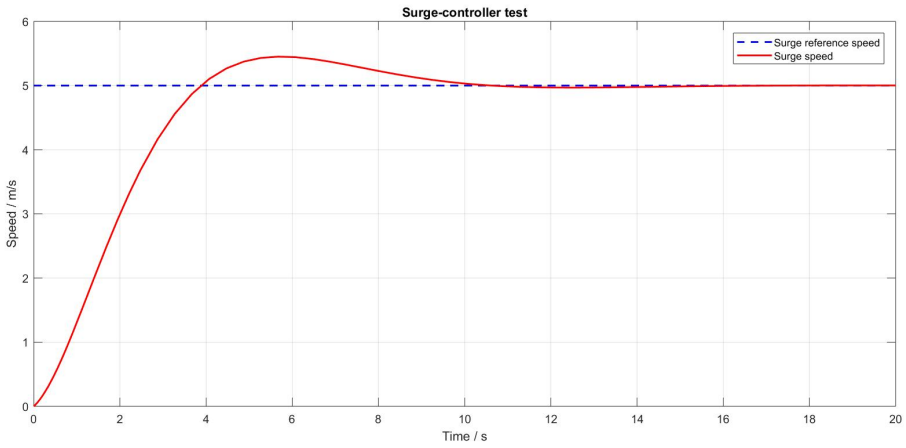

Figure 40: Surge motion during step input.

6.2 Heading Controller

The heading controller was based on the Nomoto model linearized around 6 m/s (12 knots). The initial controller did not give satisfactory results and the controller had to be tuned further. This may be due to the fact the attempt to find a suitable damping constant by comparing to the Nomoto models (Section 2.5.2) did not yield entirely accurate matches. After tuning, the controller produced more suitable results although not perfect, as it can be seen that a 90° turn would require at least 3 seconds.

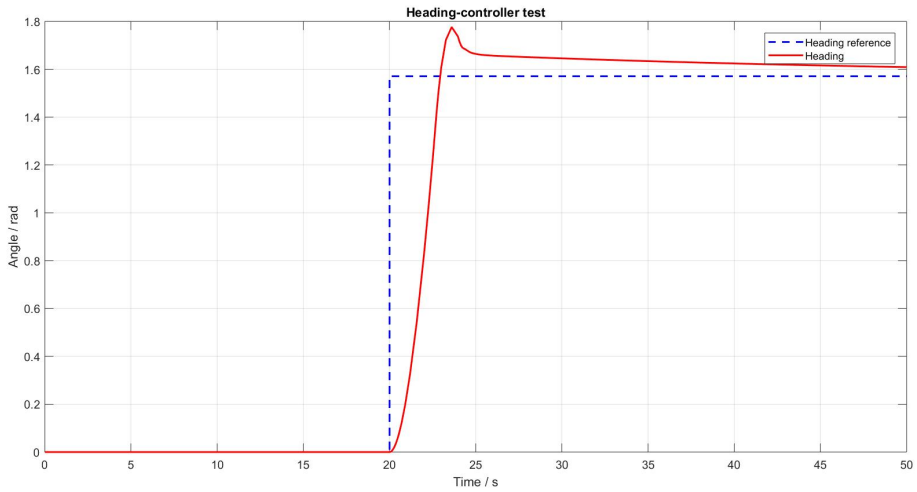

Figure 41: Yaw motion during step input (90°) and constant surge-velocity (5 m/s).

6.3 Turning evaluation

This section contains simulations where 90° turns are made when the PWC is moving at a constant surge-velocity of 5 m/s (10 knots).

6.3.1 Untuned Controllers

The Figs. 42 and 43 illustrate the poor performance of the initial heading-controller during a 90° turn. The overshoot is well above 90° despite the damping being set to 1 (critical damping). The surge controller shows somewhat unstable behaviour at the turn which is to be expected since when the steering angle is set to non-zero, part of the thrust is redirected to rotation.

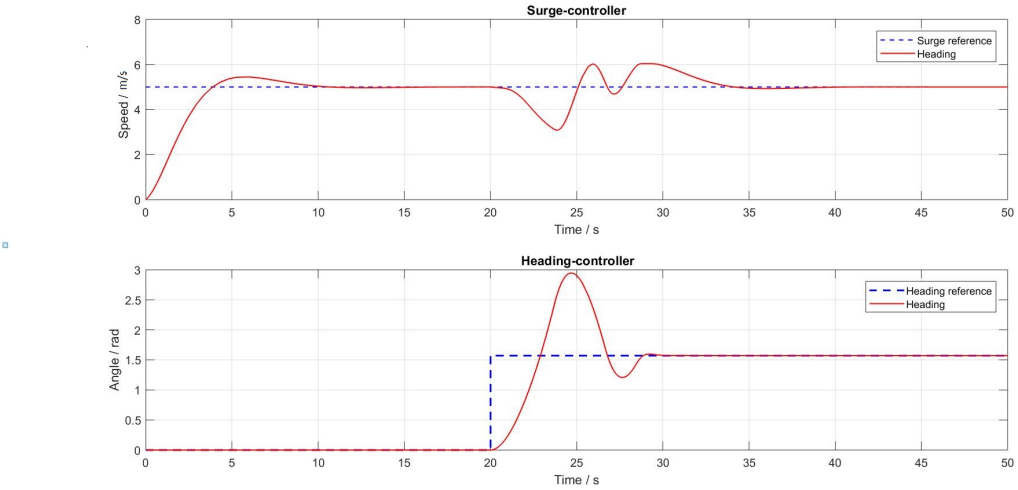

Figure 42: Untuned controllers

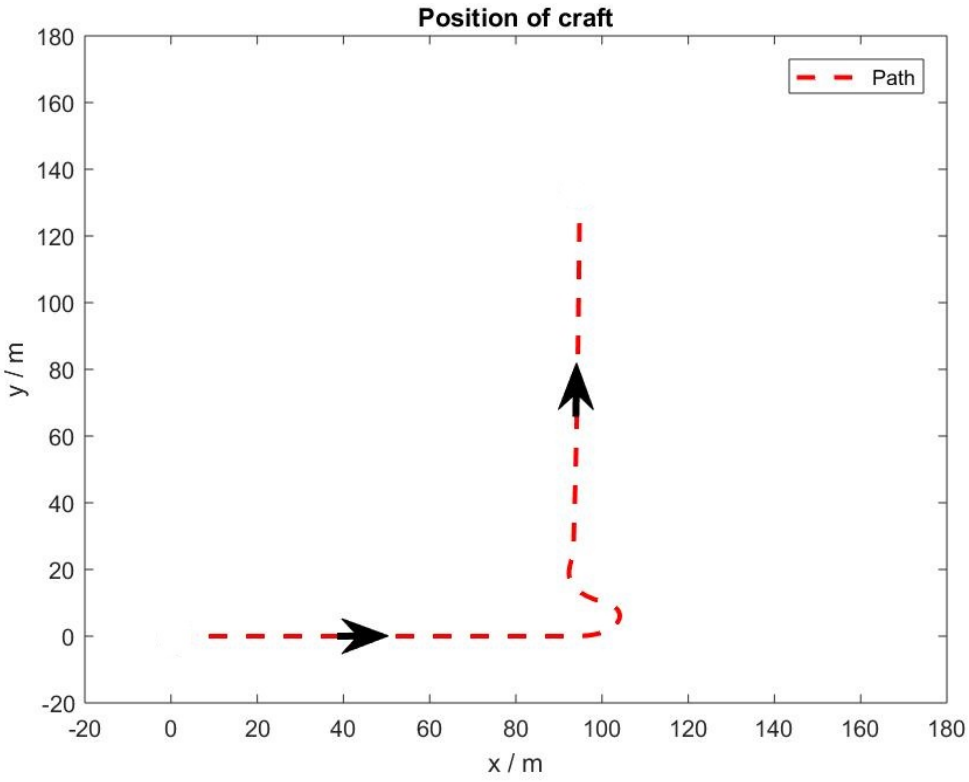

Figure 43: Path of PWC during turning motion with no disturbances and untuned controllers.

6.3.2 Tuned Controllers Without Disturbances

The tuned controllers in Figs. 44 and 45 performed much better. As the heading-controller is more stable, the impact on the surge-controller is also reduced.

Although the performance of the heading-controller has improved, it can be seen that a 90° turn would require at least 3 seconds.

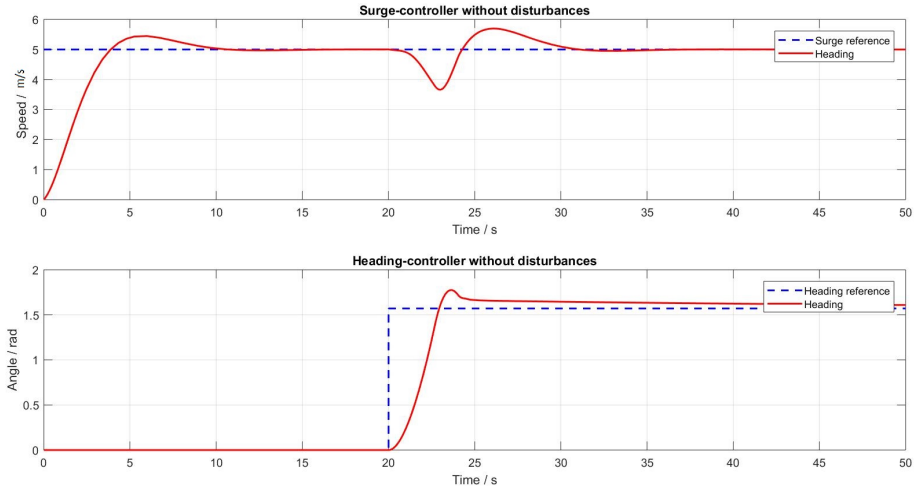

Figure 44: Tuned controllers without disturbances

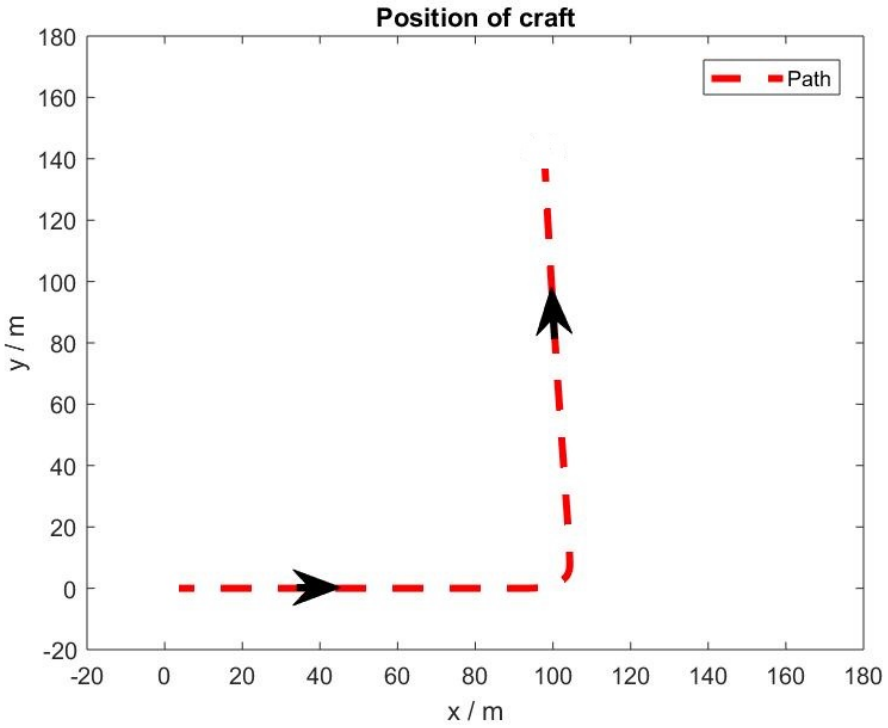

Figure 45: Path of PWC during turn motion with no disturbances.

6.3.3 Tuned Controllers With Disturbances

The disturbance present in this simulation is current. Using a current with a velocity of 1 m/s (2 knots), the heading-controller was evaluated during such a scenario.

The turning movement in Figs. 46 and 47 only showed a slightly smaller overshoot. After the turn is completed the craft drift sideways .

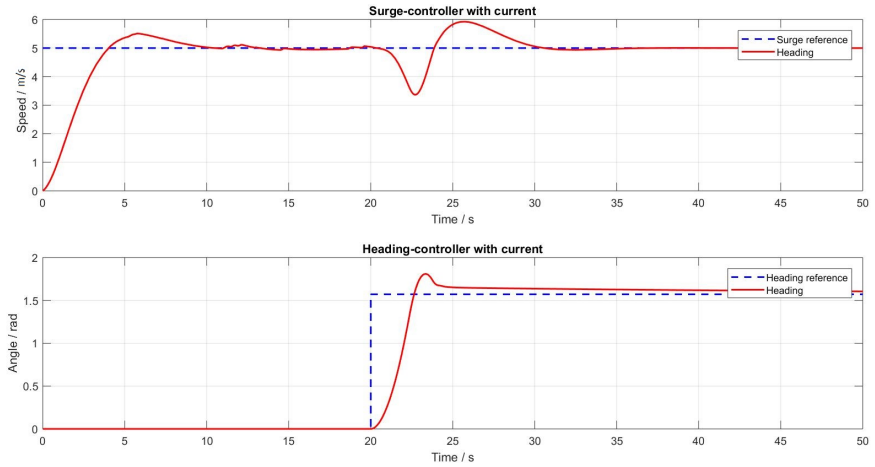

Figure 46: Tuned controllers with currents. Current velocity was 1 m/s (2 knots) and directed from left to right.

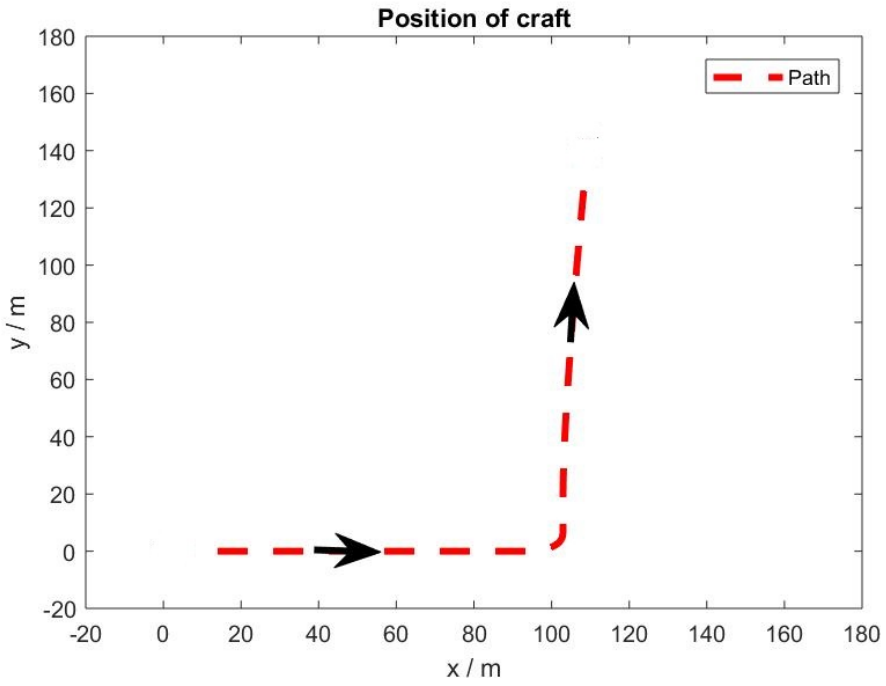

Figure 47: Path of the PWC with currents. Current velocity was 1 m/s (2 knots) and directed from left to right.

6.3.4 Tuned Controllers With Beam Waves

The second approach from the Beam Sea in Section 4.2.5 is being tested, i.e., if the heading controller is capable of turning the PWC fast enough towards the waves (head-on) before they hit. In these simulations, the PWC will begin to turn towards the wave when 70% of the encounter period T_e has passed. Two simulations take place. The first simulation where the PWC runs with a speed of $u = 5$ m/s (10 knots) and a wave period of $T = 6$ s:

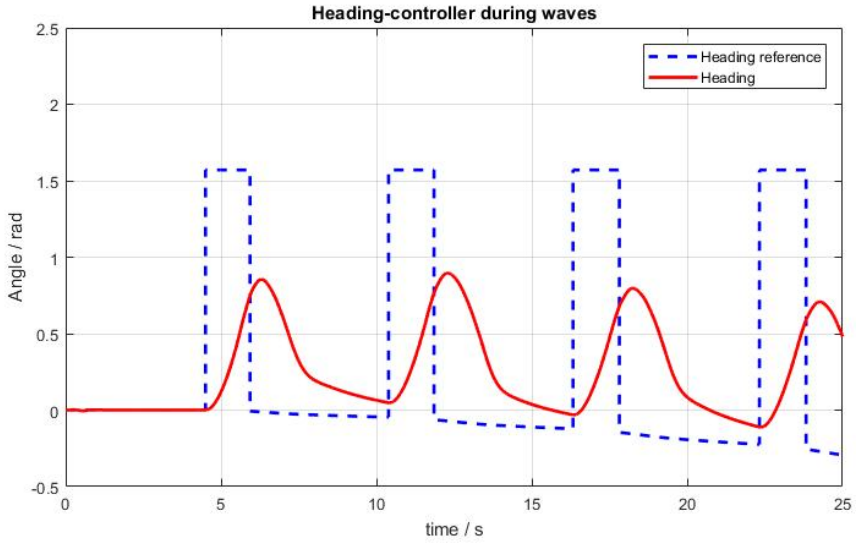

Figure 48: Heading controller with beam waves present. The wave period is 6 seconds.

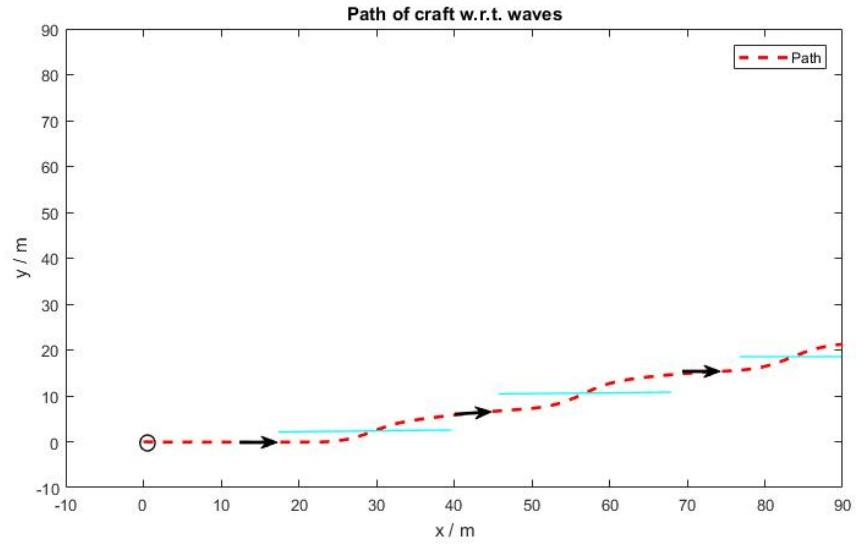

Figure 49: Path of PWC with respect to beam waves. The wave period is 6 seconds. The blue lines represents the wave front at the point of contact with the wave.

Second simulation where the PWC runs with a speed of $u = 5$ m/s (10 knots) and a wave period of $T = 8$ s:

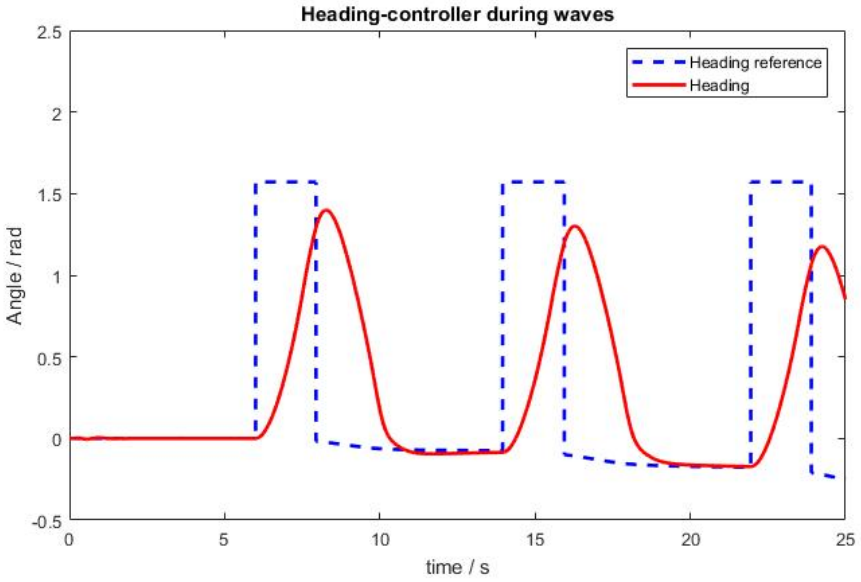

Figure 50: Heading controller with beam waves present. The wave period is 8 seconds.

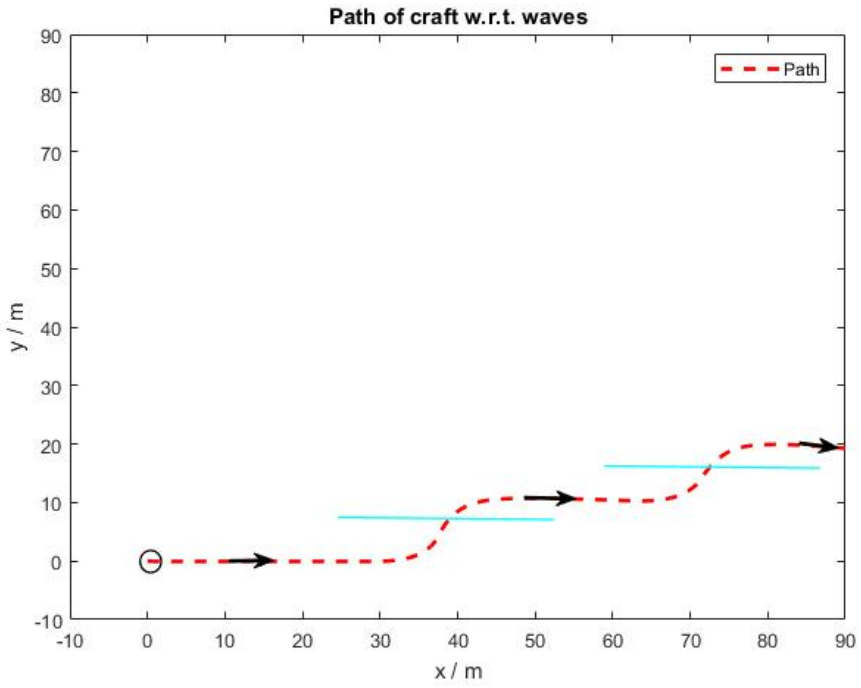

Figure 51: Path of PWC with respect to beam waves. The wave period is 8 seconds. The blue lines represents the wave-front at the point of contact with the craft.

6.3.5 Tuned Controllers With Increased Throttle

In an attempt to increase the rotational velocity, the surge velocity reference was increased during the turn resulting in a larger throttle output. This is seen in Figs. 52 and 53. Notice that the throttle amount is never saturated.

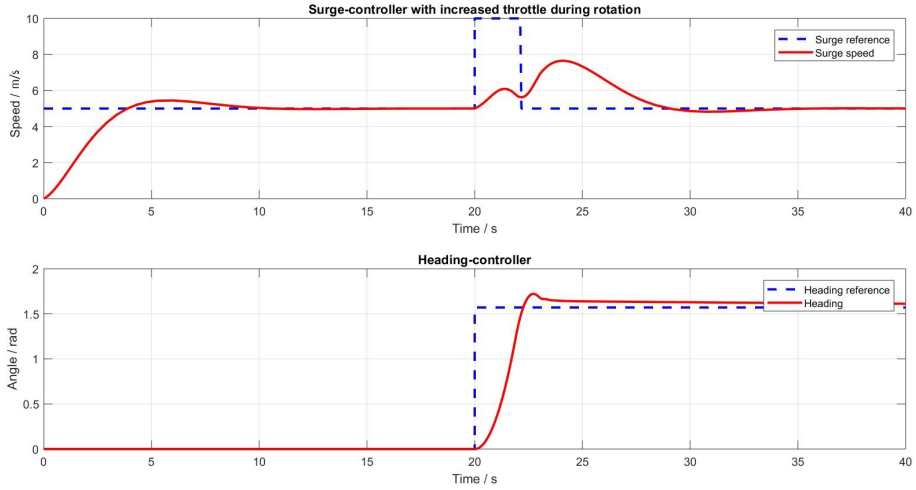

Figure 52: The surge and heading controllers when the throttle increases during turning motion.

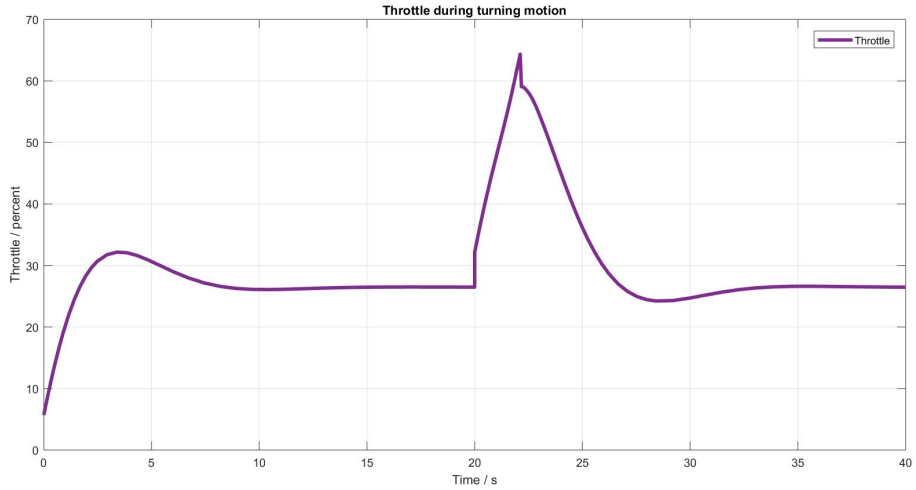

Figure 53: The throttle amount during a 90° turn at 5 m/s (10 knots) where the throttle is increased during the turn.

6.4 Path Following With No Disturbances

In this simulation, the PWC travels between waypoints that make up the corners of a hexagon, as is illustrated in Figs. 54 and 55. At first this test was done

without any disturbances. The large step shows when the angle slips over the gap between $\pm\pi$.

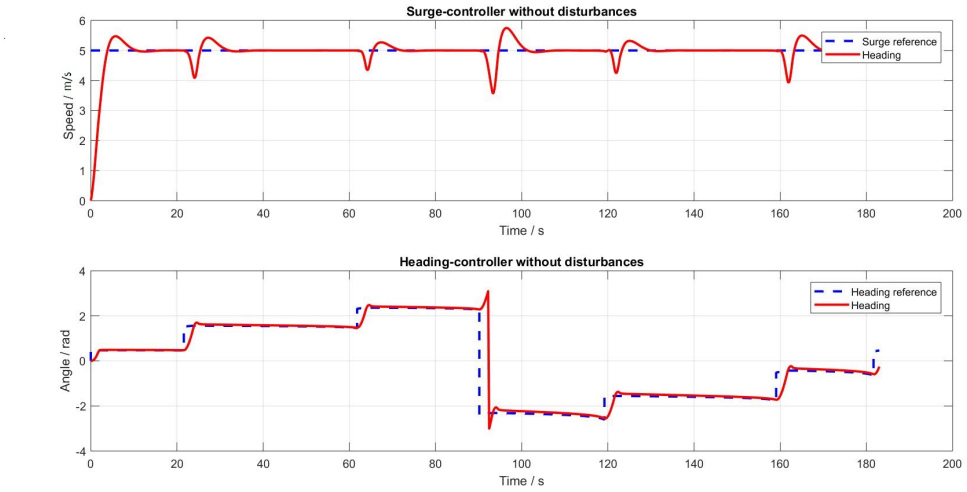

Figure 54: Controller outputs for a PWC during a hexagon movement without disturbances.

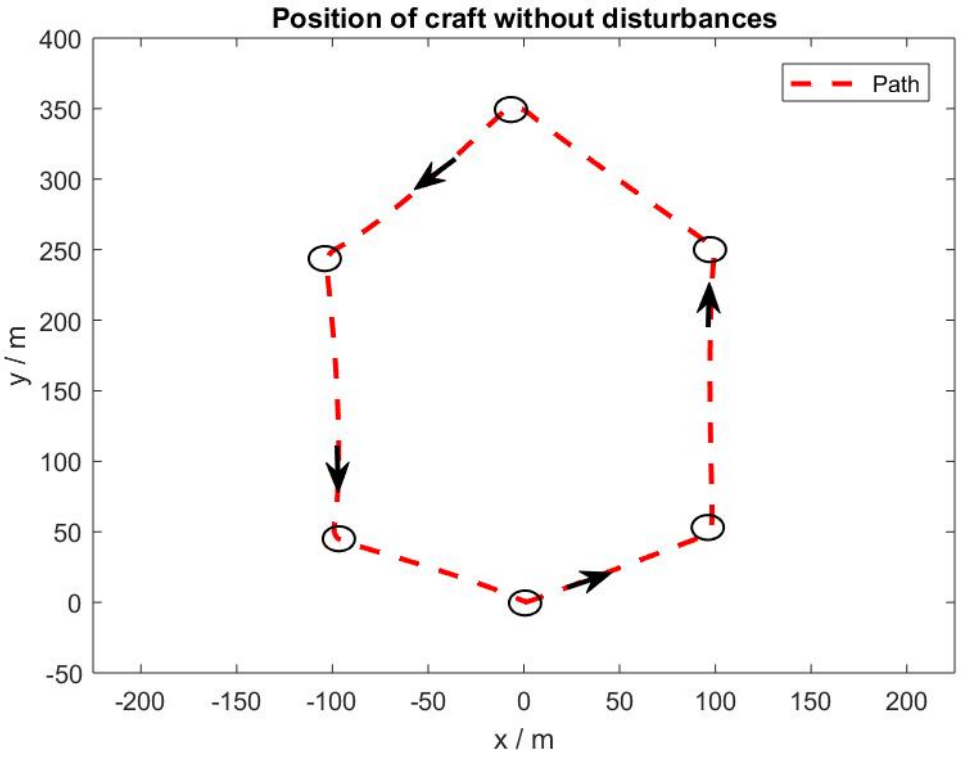

Figure 55: Path of a PWC during a hexagon movement without disturbances.

6.5 Path Following With Currents

Moving between the same previous waypoints but with currents (Figs. 56 and 57) shows that the drift does not cause too much trouble as long as a new heading angle is constantly calculated.

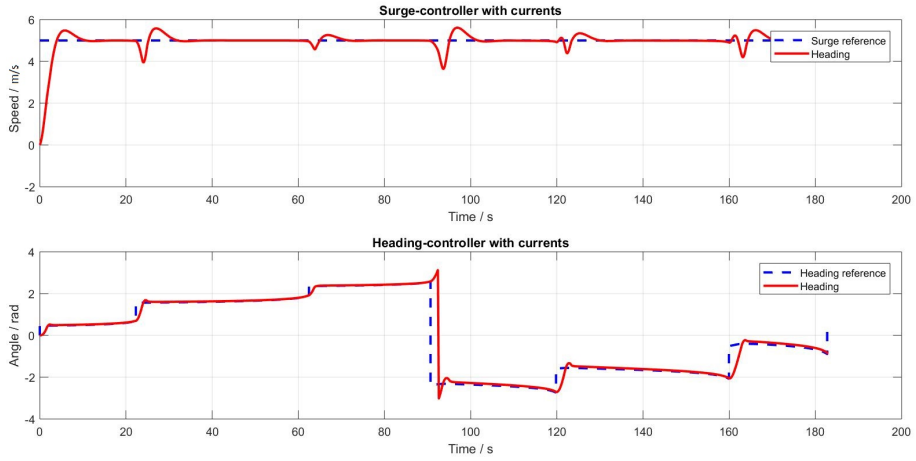

Figure 56: Path of a PWC during a hexagon movement with currents.

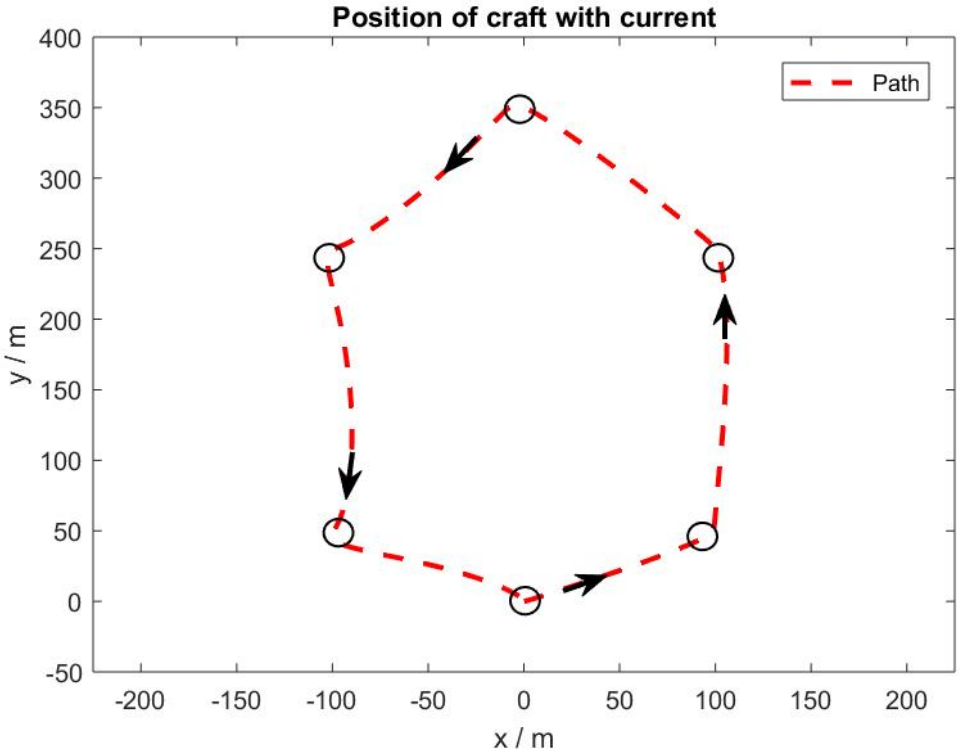

Figure 57: Path of a PWC during a hexagon movement with currents.

7 Discussion

7.1 Autopilot

In order to mitigate the risk of capsizing, it is crucial for the unmanned craft in this project is to meet the waves head-on. In Section 4.2.5 about beam sea, one of the three approaches given was heading towards the desired position and only turning towards the waves when they are about to hit. This is to ensure that the craft moves towards its desired position and deals with beam waves at simultaneously, without drifting away too much from the intended path. Above in the simulation section, this approach was tested. In the first simulation with a wave period of 6 seconds, the craft was way too slow and unable to meet the wave head-on. Although this improved in the second simulation with a wave period of 8 second where the craft came closer to meeting the waves head-on, the craft still did not manage to meet it head-on.

It is important to keep in mind that in both simulations the craft only ran with a speed of 5 m/s (10 knots). From the turning simulation in Section 6.3.3, it is seen that the craft with constant speed of 5 m/s would need roughly 3 seconds to complete a 90° turn. Since the desired speed is 5 m/s, the speed controller outputs a throttle/thrust that is below of what it is capable. Since the heading controller only affects the steering and not throttle, the turning motion is caused by a rotational moment that corresponds to roughly the same thrust level. Given that the throttle sent out from the speed controller is below its max value at a the speed reference 5 m/s, larger thrust is available. The idea is to increase the throttle from its steady-state value when turning, causing a larger thrust and thus rotational moment. This can be seen in the simulations conducted in Section 6.3.5, in which the heading reached its reference value roughly 1 second faster.

Another important factor is the fact that the steering angle is limited to 15° in the simulations, since the damping constants was obtained from data with a steering angle of 15°. The automated PWC, for which this project was originally intended for, is expected to have a maximum of 24° [5] which would increase the rotational acceleration at the expense of a surge acceleration.

Given the fact that most waves have a period in the range of 3-5 seconds – as seen in the Fig. 17 – this approach (turning towards the wave) lacks viability and the third option is to be preferred (Fig. 33).

7.2 Modelling

The model was based on either simple approximations of the ship hull, or previous work done on the RR. As discussed, in the end extra data was acquired from another report based on a third jetski. The previous work in [3] provided the theoretical estimations of the damping values of surge and heading. Unfortunately, attempts at applying the model for damping in heading motion with the rest of the model was unsuccessful.

Instead, data was used from [12] who had estimations of the parameters for Nomoto Models for different velocities. These models were used to find a suitable value for the damping coefficient in the heading motion.

This merging of data from multiple PWC was originally hoped to be enough to perform simulations and make conclusions on the autopilot. The adding of a third without any validation was a risk which was only done out of necessity. Attempts to be able to perform test for validation was made but due to time and other reasons this was unfeasible. These tests are described in Appendix B.

At the very least it allowed for simulations to be performed and analysed to a small extent and allowing the project to form some conclusions.

The parameters used in the added mass concept, both M_A and C_A had been done in previous work using strip theory. During this project it was found that contribution to the yaw moment in the C_A matrix did not behave well, causing instabilities. If any of the parameters were found with too rough approximations (in relation to each other) this might be the cause. It was concluded that the entire contribution to the yaw moment in the Coriolis-Centripetal matrix for added mass, row six in C_A, was set to zero.

As a final note, the ship hull is often approximated as an square or rectangle when calculating areas. These approximations are crude but many references argued they would be good enough.

7.3 Disturbances

7.3.1 Waves

Initially, the purpose for creating a wave model was to develop stabilizing controllers the specific intent to minimizes the pitch and roll motions. Whilst the pitch and roll are not directly controllable, the hope was to manage them through the optimizing the heading and thrust to the wave conditions. This is achievable in our wave model where the waves are identical and perfectly spaced. But the controller would be detached from the real life applications, where vast irregularities of the waves in terms of period and amplitude would confuse the controller. For larger watercraft, such as ships or even boats, these random irregular waves could be weathered, since they tend to be smaller. But for something as tiny as the PWC, they can turn out to be very destabilizing. This became more evident the more video clips of PWCs in rough waters we watched. That is why we largely pivoted away from our idealized/simplified wave model when designing control strategies, and instead put forward a set of measures that should be taken to mitigate the risks of capsizing. The strategies are largely based on actions that experienced PWC riders would take in real life. But then there is the added difficulty of not having a human aboard, that takes away weight and stability. But as mentioned in the delimitations, this project will not suggest changes to the overall design of a PWC.

7.3.2 Currents

Rather than modelling the input from the currents as a force, the model could be altered to use relative velocity instead. This would affect the coriolis/centripetal matrix C and the damping matrix D. This would be an easy way to implement it but as this project already struggled with the fact that no validation was performed it was deemed easier to keep as many sections of the model, both PWC and disturbances, separate.

Although the current model required the use of a factor from an oiltanker model, it was argued to only provide scaling factor depending on the AoA and applying appropriate force on surge, sway and yaw. The magnitude of the force was built on the velocity of the ocean current and crude approximations of the ship hull shape. If one were to need exact values of the input disturbance, this might not be a good model. However when only needing an "example" disturbance, it should be sufficient.

7.4 Controller Choice

It was easiest to control heading and surge independently despite them being connected. The choice fell to PID (heading) and PI (surge) controllers due to their simplicity. These controllers are well documented with multiple methods of analysing and designing especially when only applied on one input on output. It might be better to try a controller on the heading which uses both throttle and steer angle to get the fastest possible turning motion. As the throttle also controls the surge motion, it would be necessary to control both states. A form of state feedback might be useful, perhaps an LQR where priority is placed on the heading angle over the surge velocity.

There is no way of controlling states as pitch and roll and therefore no way of handling input from waves and wind who mainly affect these states. The disturbance rejection is not something to want from the controllers but rather the autopilot attempting to face the waves head on.

The ocean currents are assumed to be only slowly varying. This is only for the global frame as locally the influence will change depending of its AoA relative to the PWC. When moving in a constant direction this angle would remain the same and the disturbance would be constant. This is expected when there are no waves present (and no frequent turning motion). For this the integrator should be sufficient to avoid steady state errors. Constantly updating the heading angle will account for drift.

When often changing heading which the autopilot is expected to do when waves are present, the integrator would have to be more aggressive to efficiently be able to compensate.

The integral part of the heading controller became very weak, almost nonexistent and it may be worth trying to increase it.

7.5 Lessons From The Project

Coming into this project, both of us had little to no prior experience with a PWC or other water craft. In order to develop our understanding of PWC, plans were drawn to try out a RescueRunner at one of SSRS's stations as well as interviewing the staff about the challenges they face in rough waters. The trip never materialized. Instead we tried to understand everything through the lens of theory (literature, studies, etc). The issue with this approach is that most of the studies in this field is for water craft significantly larger than a PWC, such as ships and boats. While a lot of the forces affecting larger crafts are also present for the smaller ones, the size difference means that there are vast differences in their dynamics and their response to disturbances such as waves. These things can be difficult to capture from only reading and too often we thought of the PWC as a tiny ship.

At the latter part of the project, after having major difficulties deciphering how PWC actually reacts to disturbances (like waves), watching video clips online of small boats and PWC in rough waters was very useful. This is obviously something that should have been done extensively at the beginning of the project.

Another thing that was enormously informative was asking around in jetski forums online about the challenges they face and how they handle different scenarios. We managed to get a wide variety of responses that gave us lots of additional insight and perspective. This unfortunately also took place at the latter stages of the project, when it is obviously something that should have also been done at the beginning and would have saved us a lot of time.

In conclusion, we should have made sure to get a feeling/understanding (practical experience, video clips) for how a system works in real-life before delving into the theory.

7.6 Future Works

The first step is clearly model testing and validation. This project would have focused on finding a suitable damping model if time had allowed. The damping in surge and sway are the most important as these are the only states to control. Secondly, finding damping models for the roll and pitch to complete the model. Sway and heave are states that seem less important to model.

Autopilot designs are often meant to resemble the way a human would pilot the craft. Attempts to corroborate this by for instance interviewing a veteran pilot, perhaps from SSRS, in how they would maneuver the craft could be useful.

Ascertain if it is possible to increase the rotational speed without moving too far away from the desired course or reaching too high velocities. High velocities in surge might be a bad idea when the water is rough, even when its only little. High rotational speed will come at the cost of increase velocity. Still, high rotational speed is key if one wishes to use some autopilot as described in this project. Perhaps by simply testing with a human pilot to get a very good estimation of the best value of the rotational velocity.

The project has made two very large assumptions. Wave angle and period are constant and can be estimated. The data available from weather buoys gives the impression that the estimation is possible. If the estimation would remain constant between consecutive waves and useful for predictions is not known and should be looked into.

There is no control signal with which to control the roll and pitch values for stability. This leaves only the choice of piloting the craft to avoid tipping over. A human pilot also has the benefit of being able to use body weight to control these states. Perhaps examining the possibility to add such a control signal to the craft.

It must be remembered that even with precautions the PWC might still tip over. For a human driver a jetski's size often makes it possible to turn it back on its own without to much trouble. Perhaps this could also be solved in the same way as when trying to implement a method of controlling the states roll and pitch, i.e., using the same system to get it back up.

8 Conclusion

With the model achieved the key features were present allowing for simulations in 6 degrees of freedom. Since the model was compiled using data from multiple PWC's, the need for validation is great. The difficulty in modelling states as the angles pitch and roll lie with modelling the input of the disturbances and not their own dynamics. When designing an autopilot with the intent of avoiding waves it might be unnecessary to model the states of roll and pitch. Still, being able to at least have a crude model of them allows one to monitor them to some small extent, how the angles are behaving and evaluating if the autopilot succeeds in avoiding the waves.

Simple models for ocean currents were found and used to approximate the influence of currents on the PWC for use in simulations. Wind models were also described but not implemented, since their influence is negligible relative to the other disturbances. The largest focus was placed on models for wave behaviour but was a very difficult concept, as both the nature of the wave itself as well as the influence on the ship. A simple wave-model consisting of periodic square waves was constructed. It did not turn out to be very useful in this case, since the waves in real waters contain a lot of noise in terms of amplitude and period, and is not perfectly periodic as the model. That noise can have a significant impact on something as tiny as a PWC. It is plausible that this square wave model would be more useful for larger vessels.

Simple control structures such as PID controllers for heading and surge independently can control a PWC well enough in simulation without disturbances. When disturbances are present it becomes more difficult and might require more advanced control schemes. Ocean currents producing drift are easily countered if the heading angle is constantly updated. Ocean currents affecting the surge velocity are countered by the use of integral action in the surge controller.

The disturbances are dealt with through a set of strategies that depends on the direction of the waves. These strategies are largely based on actions taken by experienced riders. They provide a viable chance of moving towards the desired position without capsizing in rough waters.

To turn and face waves is difficult as it requires both knowledge of when the wave hits and time to complete the turn in time. The project assumed that wave period and angle could be estimated and be used for predicting when the next wave occurs. It is not certain this is possible. If the level of uncertainty and irregularities in disturbances (waves in particular) is large, designing a controller that would be viable in real life applications would be difficult.

References

[1] SSRS. *YearBook*. URL: https://www.sjoraddning.se/sites/default/files/ssrs_arsbok_2019.pdf. (accessed: 2020-02-20).

[2] Safe At Sea. *Our Procducs - Rescuerunner*. URL: https://www.safeatsea.se/rescuerunner/. (accessed: 2020-02-20).

[3] A. Bergholtz and C.-A. Hernvall. "Waypoint-based path following system for a jetski". MSc Thesis EX024/2015. Chalmers University of Technology, Gothenburg, Sweden, 2015.

[4] E. Ingemarrson, F. Kerstis, P. Lindessonand, M. Löfgren, H. Male, and F. Millqvist. "Autonomous WaveRunner Follow the Leader". BA Thesis EENX15-19-02. Chalmers University of Technology, Gothenburg, Sweden, 2019.

[5] A. Gunnarson, B. Lundgren, E. Alfredsson, J. Sjöberg, N. Danielsson, and V. Lindström. "Autonomous Waverunner – Drive By Wire Adapting a personal watercraft for remote controlled application". BA Thesis EENX15-19-01. Chalmers University of Technology, Gothenburg, Sweden, 2019, p. 19.

[6] T. I. Fossen. *Handbook of Marine Craft Hydrodynamics and Motion Control*. Chichester, West Sussex, United Kingdom: John Wiley Sons Ltd, 2011. Chap. 3, p. 45.

[7] T. I. Fossen. *Handbook of Marine Craft Hydrodynamics and Motion Control*. Chichester, West Sussex, United Kingdom: John Wiley Sons Ltd, 2011. Chap. 2.

[8] T. I. Fossen. *Handbook of Marine Craft Hydrodynamics and Motion Control*. Chichester, West Sussex, United Kingdom: John Wiley Sons Ltd, 2011. Chap. 3, pp. 45–56.

[9] T. I. Fossen. *Handbook of Marine Craft Hydrodynamics and Motion Control*. Chichester, West Sussex, United Kingdom: John Wiley Sons Ltd, 2011. Chap. 4, pp. 62–66.

[10] T. I. Fossen. *Handbook of Marine Craft Hydrodynamics and Motion Control*. Chichester, West Sussex, United Kingdom: John Wiley Sons Ltd, 2011. Chap. 6, pp. 118–120.

[11] T. I. Fossen. *Handbook of Marine Craft Hydrodynamics and Motion Control*. Chichester, West Sussex, United Kingdom: John Wiley Sons Ltd, 2011. Chap. 5.

[12] C. H. Svendsen, N. O. Holck, R. Galeazzi, and M. Blanke. "$\mathcal{L}_1$ Adaptive Manoeuvring Control of Unmanned High-speed Water Craft". In: (2019), p. 5.

[13] T. Perez and T. I. Fossen. *A Matlab Tool for Parametric Identification of Radiation-Force Models of Ships and Offshore Structures. Modelling, Identification and Control, MIC-30(1):1-15.* https://github.com/cybergalactic/MSS. 2009.

[14] T. I. Fossen. *Handbook of Marine Craft Hydrodynamics and Motion Control*. Chichester, West Sussex, United Kingdom: John Wiley Sons Ltd, 2011. Chap. 8, pp. 188–199.

[15] SMHI. *Wind Waves*. URL: https://www.smhi.se/en/theme/wind-waves-1.11275. (accessed: 2020-04-09).

[16] T. I. Fossen. *Handbook of Marine Craft Hydrodynamics and Motion Control*. Chichester, West Sussex, United Kingdom: John Wiley Sons Ltd, 2011. Chap. 8, pp. 199–221.

[17] A. W. Browning. "A Mathematical Model to Simulate Small Boat Behaviour". ID Code: 9631. PhD thesis. Bournemouth University, Dorset, United Kingdom, 1990. Chap. 6, pp. 210–231.

[18] T. I. Fossen. *Handbook of Marine Craft Hydrodynamics and Motion Control*. Chichester, West Sussex, United Kingdom: John Wiley Sons Ltd, 2011. Chap. 8, pp. 187–188.

[19] T. I. Fossen. *Handbook of Marine Craft Hydrodynamics and Motion Control*. Chichester, West Sussex, United Kingdom: John Wiley Sons Ltd, 2011. Chap. 7, pp. 154–156.

[20] SMHI. *Data och Analyser för väder samt Sveriges klimat och miljö*. Observationsdata - Oceanografi. Station = VINGA BS, Parameter = Strömriktning och hastighet. URL: https://www.smhi.se/data. (accessed: 2020-03-01).

[21] T. I. Fossen. *Handbook of Marine Craft Hydrodynamics and Motion Control*. Chichester, West Sussex, United Kingdom: John Wiley Sons Ltd, 2011. Chap. 12, p. 375.

[22] Jetdrift. *How to ride a jet ski in rough water*. URL: https://www.jetdrift.com/how-to-ride-a-jet-ski-in-rough-water/. (accessed: 2020-03-09).

[23] T. I. Fossen. *Handbook of Marine Craft Hydrodynamics and Motion Control*. Chichester, West Sussex, United Kingdom: John Wiley Sons Ltd, 2011. Chap. 8, p. 209.

[24] T. Neale. *Small-Boat Handling*. URL: https://www.boatus.com/magazine/trailering/2015/april/small-boat-handling.asp. (accessed: 2020-03-11).

[25] United States Power Squadrons. *Reading the waves*. URL: http://www.theensign.org/uspscompass/compassarchive/compassv5n8/v5n8_waves.htm. (accessed: 2020-03-12).

[26] M. Kosnik. *Vessel Handling*. URL: https://wiki.mq.edu.au/display/dbsag/Vessel+handling. (accessed: 2020-03-12).

[27] T. I. Fossen. *Handbook of Marine Craft Hydrodynamics and Motion Control*. Chichester, West Sussex, United Kingdom: John Wiley Sons Ltd, 2011. Chap. 6, p. 121.

[28] B. Ferreira, M. Pinto, A. Matos, and N. Cruz. *Modeling and motion analysis of the MARES autonomous underwater vehicle*. Porto, Portugal: University of Porto, 2009.

[29] S. Staacks, H. Heinke, D. Dorsel, T. Gnacke, C. Stampfer, S. Hütz, J. Held, and A. Krampe. *Phyphox*. URL: https://phyphox.org/. (accessed: 2020-03-01).

[30] Android. *GNSSLoggerAnalyser*. URL: https://developer.android.com/guide/topics/sensors/gnss. (accessed: 2020-03-01).

[31] L. Moreira, T. I. Fossen, and C. G. Soares. "Modeling, Guidance and Control of Esso Osaka Model". In: (2005), pp. 14–16.

A Appendix

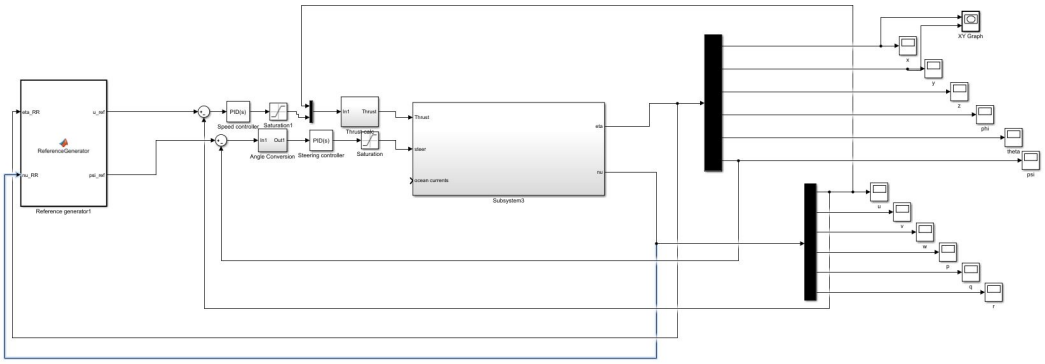

Figure 58: Simulink Model of the damping forces.

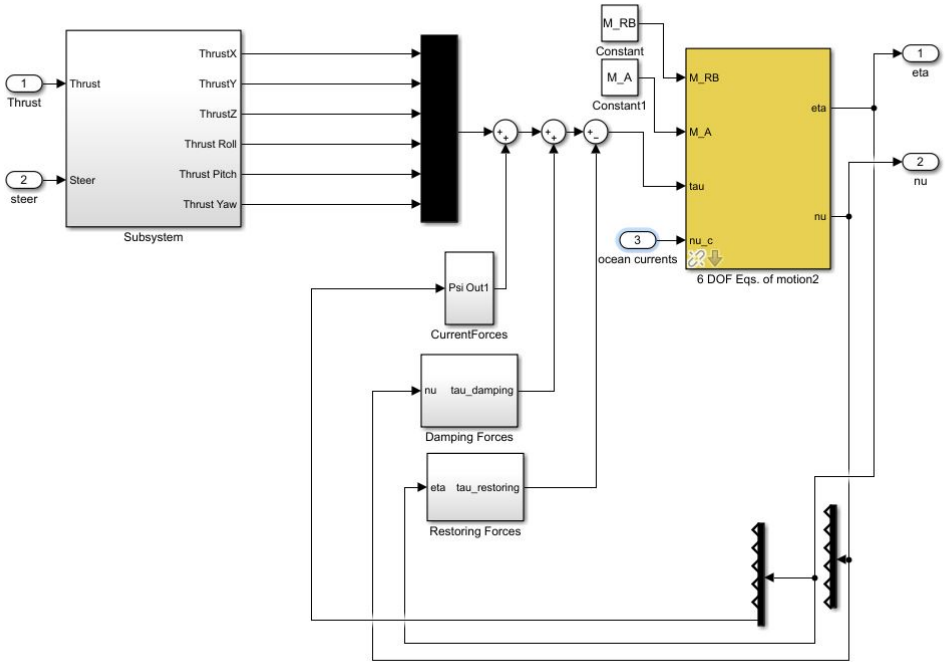

Figure 59: Simulink Model of the damping forces.

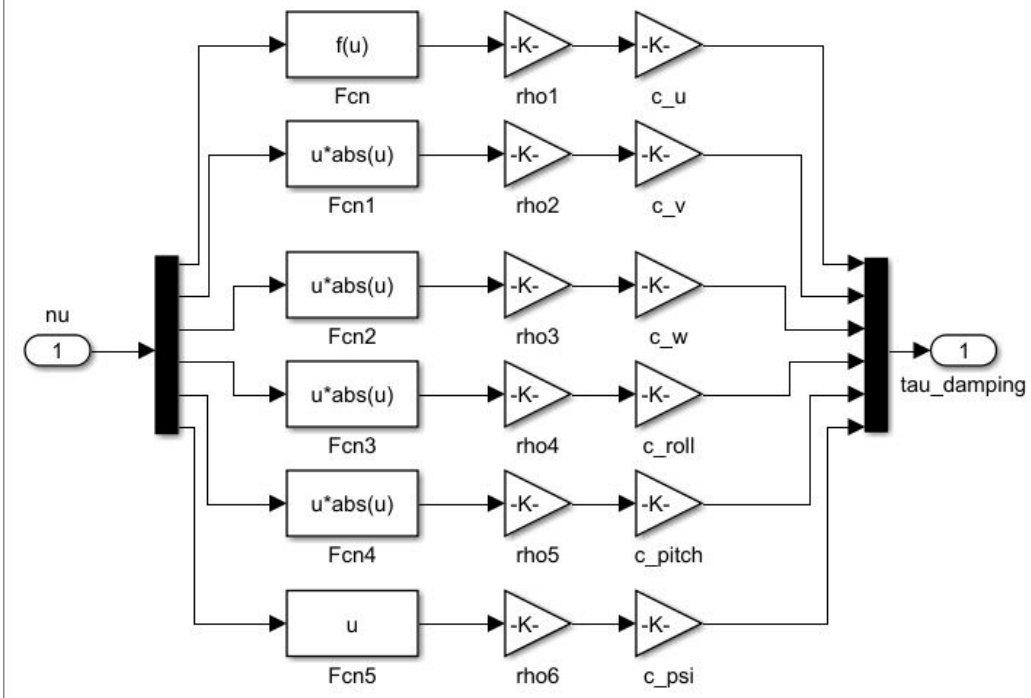

Figure 60: Simulink Model of the damping forces.

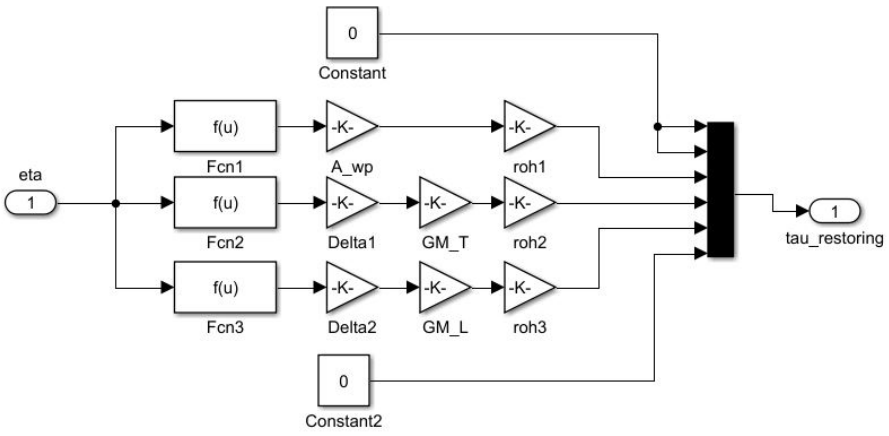

Figure 61: Simulink Model of the damping forces.

B Appendix

With a few troubles on the parameters for the damping a series of tests were designed to be performed quickly to adjust the model. These tests were designed to be performed with the Rescuerunner with a manual pilot. However with the lack of time these test where never performed. The thesis supplemented the damping parameters with data from another project, described in that section.

B.1 Measurement

To validate the model, the following data is needed

- Velocity and position - Found using Mobile phone GPS + Accelerometer
- Yaw angular velocity - Mobile phone Gyroscope
- Pitch and roll angular velocity - Mobile phone Gyroscope.
- Throttle and steer angle - Harder to measure unless during maxed values

All accelerometer and gyroscope values could be collected using the app `phyphox` [29]. The GPS position was expected to be both noisy and have a low update frequency. The frequency inadequacy was hoped to be compensated by accelerometer readings. To improve improve GPS measurement readings a method `RTK` (Realtime Kinetics) could be used. In a short summary it requires, other than the standard GPS feature, information from a base node within some proximity that allows for a correction calculation of the position. For Android phones, the `GNSSLogger` allows logging of these measurements and the PC application `GNSS Analysis` allows for computation. Do note that the phone requires an internet connection for the correcting values from the base nodes and not all phones are capable of receive the raw GNSS values. In these tests a `Samsung S8` was used. A list of other compatible phones and instructions can be found at [30].

The throttle and steer angle were hard to measure and to keep constant through out the tests.

Although the main parameters M and C are estimated using approximations and could use verification the project focused on the damping forces as these are hard to estimate theoretically. This could be done using graph matching.

B.2 Surge Motion

To identify the c_u parameter of the damping force in surge motion a step input test (and the removal of input) could be performed. An example is giving in Fig. 63.

Data to register:

- Velocity - Preferably a combination of GPS and accelerometer
- (Bonus) Input - Thrust or throttle level

Performance:

- Accelerate the PWC until constant velocity is achieved
- Steer is zero.
- Reduce the throttle input to zero.
- Perform this for velocities [1, 2, 4, 5] m/s ([2, 4, 8, 10] knots). Note: For velocities planing occurs the resistance will change dramatically when the passing over this edge.
- For each test match the curves from a simulation (which is set to start at the same velocity) using the parameter c_x .
- (Bonus) If the throttle input was measured. The curve matching could also be performed for the rise period.

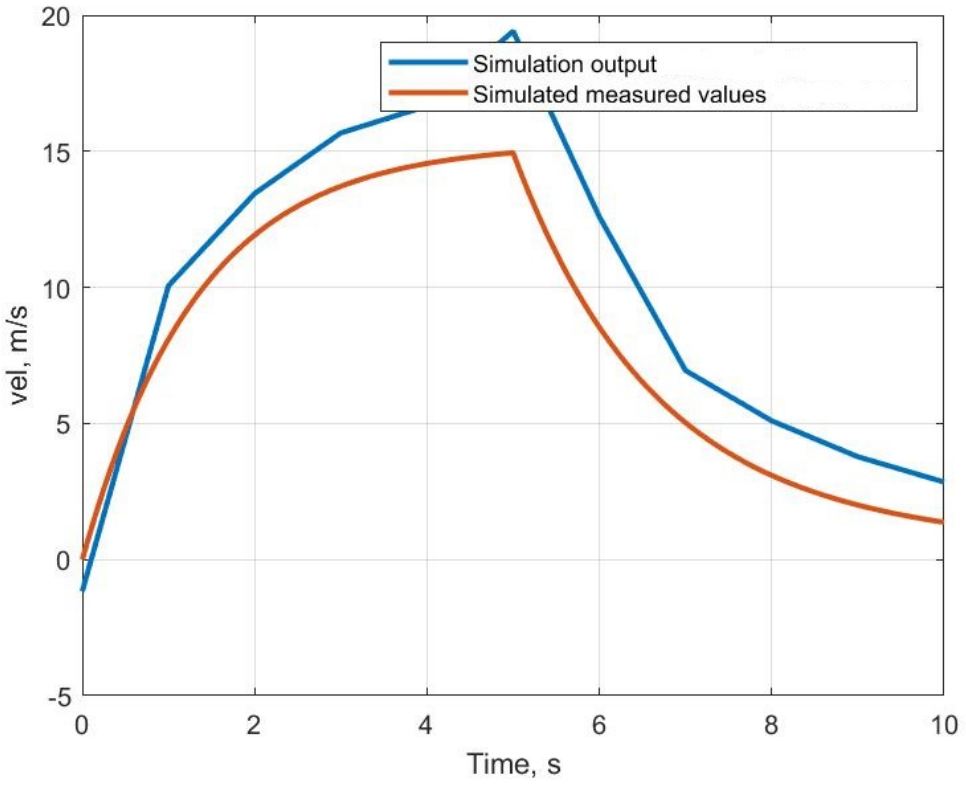

Figure 62: Expected results of a parameter estimation attempt.

For low velocities the estimation should remain similar but due to planning there should be an edge where the resistance changes dramatically. The previous thesis [4] performed such a test with good results.

B.3 Yaw Motion

The damping in the rotational motion could be estimated in the same way as for surge and is expected to give similar results as seen in Fig. 63.

Data to register:

- Velocity - Preferably a combination of GPS and accelerometer
- Angular velocity (yaw) - Gyroscope
- Steer Angle - Use max steer angle or place a set of markers on the handlebar and a set of references on the fixated part of the PWC to allow for a decent angle estimation.
- (Bonus) Thrust input

Performance:

- Accelerate the PWC to a constant velocity, [2, 5] m/s ([4, 10] knots).
- Steer is kept zero
- While at constant speed, turn the handlebar to the angles [5, 10, 25] degrees. - Maintain the angle until a constant angular velocity is reached. (should only be a few seconds)
- Return the handlebar to zero degrees and keep measuring until the angular velocity is zero.
- For each test match the curves from a simulation (which is set to start at the same angular velocity) using the parameter c_ψ
- (Bonus) If the throttle input was measured the curve matching could be performed on the rise period as well.

The parameter should, if possible, be estimated for multiple speeds and multiple steer angles as it is expected to be nonlinear. If needed gain scheduling could be applied for a more accurate model.

B.4 Roll and Pitch

These measurements will be performed in stationary mode. The dynamics might change for nonzero velocities but the test will be difficult to perform under such circumstances.

Again, the main objective is to find suitable values for the damping constant c_{roll} and c_{pitch} which could be done by matching curves.

Measurements:

- Angular velocities in Roll and Pitch

Performance:

- Keep the PWC stationary. By manual force, tilt it to a small angle [5, 10, 15] degrees
- Release the PWC and wait until the oscillations have receded.
- For each test match the curves from a simulation using the parameters c_ϕ and c_θ

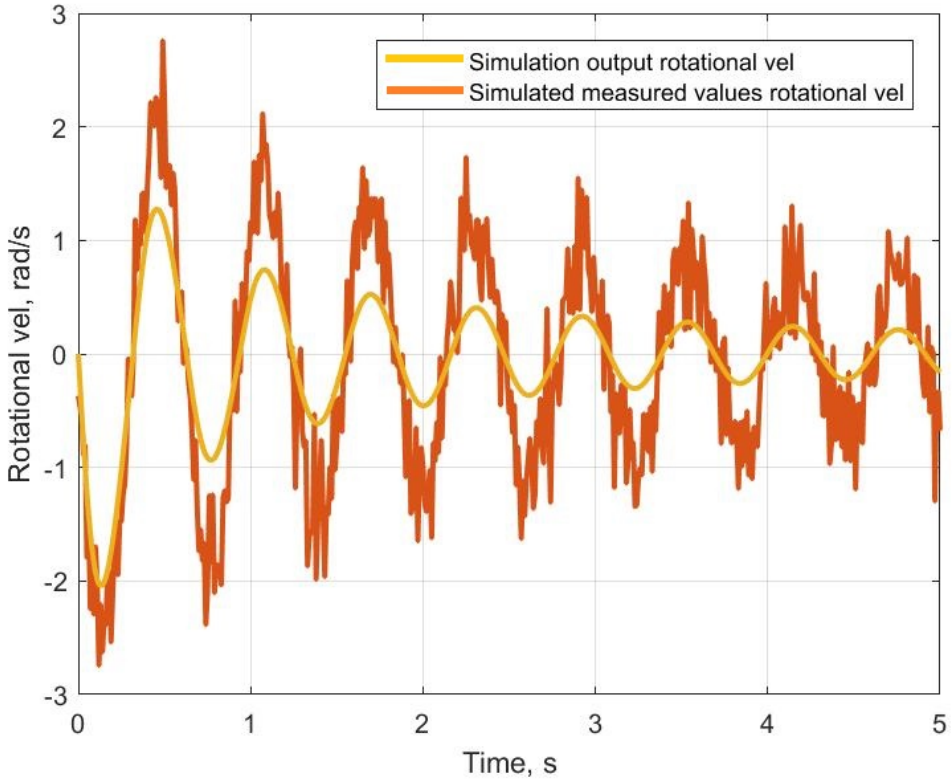

Figure 63: Expected results of a parameter estimation attempt.

As a way of both estimating the parameters for a Nomoto model (first order system) for use in controller design but also a way of validating the model, as a whole one could perform a zig-zag test. This means by driving the PWC in a zig-zag, motion with constant velocity (or near constant) and changing the steering angle between two set values when the heading angle has reached a certain value. In [31] describes how to use this to find the parameters the Nomoto Model.

$$K_{nom} = -\frac{\psi_1 - \psi_2}{\int_{t_1}^{t_2} \delta dt} \tag{100}$$

and

$$\frac{K_{nom}}{T_{nom}} = -\frac{r_1 - r_2}{\int_{t_1}^{t_2} \delta dt} \tag{101}$$

An example of what the results would look like is seen in Figs. 64-66.

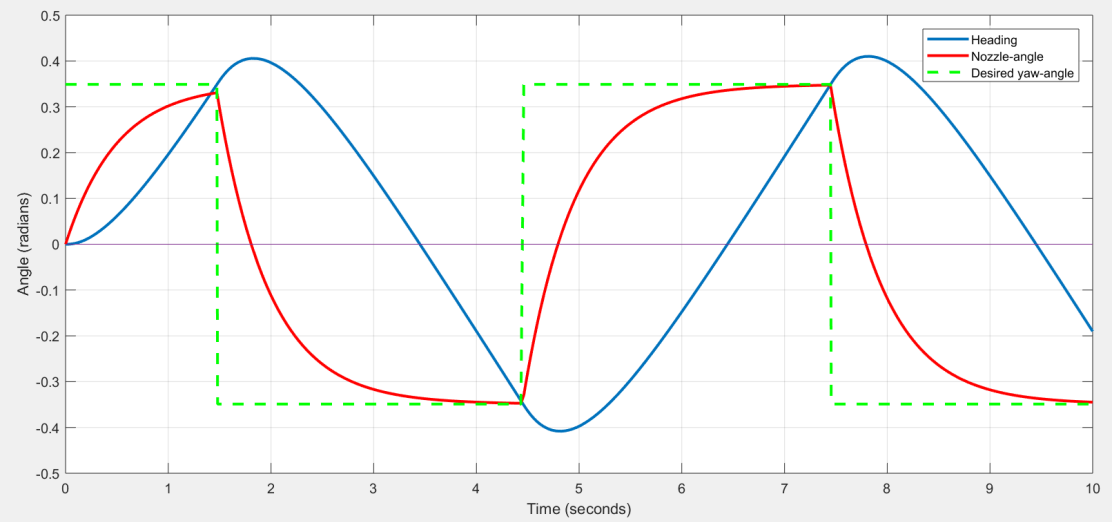

Figure 64: Example of results from a zig-zag test.

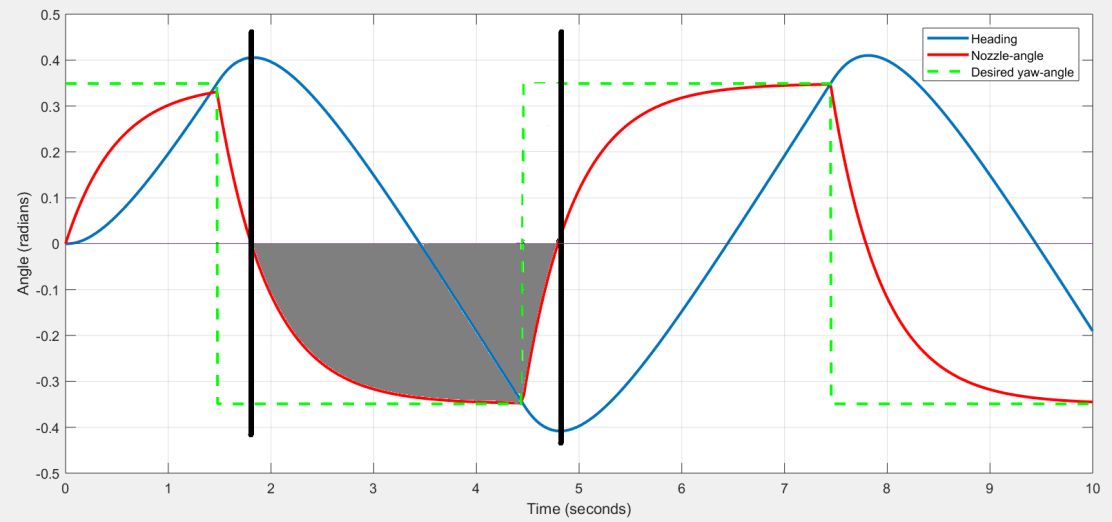

Figure 65: Example of what parts to use to calculate the nomoto parameters.

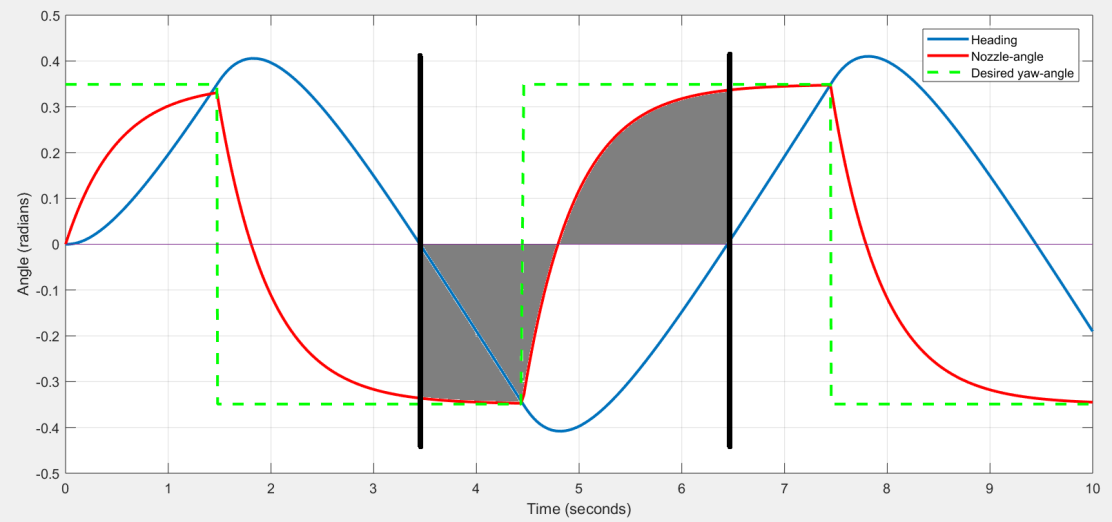

Figure 66: Example of what parts to use to calculate the nomoto parameters.

Lund University
Department of Automatic Control
Box 118
SE-221 00 Lund Sweden

Document name
MASTER'S THESIS

Date of issue
May 2020

Document Number
TFRT-6103

Author(s)
Jonas Voigt
Abdulah Alkaysi

Supervisor
Anders J Johansson, Department of Electrical and Information Technology, Lund University, Sweden
Anders Robertsson, Dept. of Automatic Control, Lund University, Sweden
Rolf Johansson, Dept. of Automatic Control, Lund University, Sweden (examiner)

Title and subtitle
Autopilot for a Personal Watercraft

Abstract

The objective in this thesis is to develop an autopilot for a personal watercraft (PWC) – popularly known as a jetski – that is capable of maneuvering in calm and rough waters alike. Maneuvering a PWC in calm waters is usually easy. It gets more challenging in rough waters, where environmental disturbances that can significantly destabilize the craft are present.

In this project, two control strategies are developed; one with the sole focus of positioning and one with regard to environmental disturbances. The positioning controller can be thought of as an autopilot in calm conditions, i.e., no significant disturbances are present. It is divided into a PI-controller that handles thrust and a PID-controller that handles steering. These are tuned through a series of simulations on our PWC-model.

To deal with the disturbances, simple models of these were constructed with the intention of crafting a control algorithm through simulations. However, after studying footage of PWC and other smaller craft in rough waters, it became clear that the sea-state is too unpredictable to rely on control algorithms devised from our simple and idealized wave-model. To obtain strategies that work in real life applications, strategies that are used by experienced (human) riders are brought up.
Thus, depending on the direction of the waves, the PWC moves towards its desired position in a certain specific way. Whilst these strategies do not guarantee stability, they are deemed to give the PWC a viable chance of moving towards its desired position without capsizing in rough waters.

Keywords

Classification system and/or index terms (if any)

Supplementary bibliographical information

ISSN and key title
0280-5316

ISBN

Language
English

Number of pages
1-82

Recipient's notes

Security classification